NASA/TP—2013–217477

Closeout Report for the Refractory Metal Accelerated Heat Pipe Life Test Activity

J. Martin, R. Reid, E. Stewart, R. Hickman, and O. Mireles
Marshall Space Flight Center, Huntsville, Alabama

January 2013

The NASA STI Program…in Profile

Since its founding, NASA has been dedicated to the advancement of aeronautics and space science. The NASA Scientific and Technical Information (STI) Program Office plays a key part in helping NASA maintain this important role.

The NASA STI Program Office is operated by Langley Research Center, the lead center for NASA's scientific and technical information. The NASA STI Program Office provides access to the NASA STI Database, the largest collection of aeronautical and space science STI in the world. The Program Office is also NASA's institutional mechanism for disseminating the results of its research and development activities. These results are published by NASA in the NASA STI Report Series, which includes the following report types:

- TECHNICAL PUBLICATION. Reports of completed research or a major significant phase of research that present the results of NASA programs and include extensive data or theoretical analysis. Includes compilations of significant scientific and technical data and information deemed to be of continuing reference value. NASA's counterpart of peer-reviewed formal professional papers but has less stringent limitations on manuscript length and extent of graphic presentations.

- TECHNICAL MEMORANDUM. Scientific and technical findings that are preliminary or of specialized interest, e.g., quick release reports, working papers, and bibliographies that contain minimal annotation. Does not contain extensive analysis.

- CONTRACTOR REPORT. Scientific and technical findings by NASA-sponsored contractors and grantees.

- CONFERENCE PUBLICATION. Collected papers from scientific and technical conferences, symposia, seminars, or other meetings sponsored or cosponsored by NASA.

- SPECIAL PUBLICATION. Scientific, technical, or historical information from NASA programs, projects, and mission, often concerned with subjects having substantial public interest.

- TECHNICAL TRANSLATION. English-language translations of foreign scientific and technical material pertinent to NASA's mission.

Specialized services that complement the STI Program Office's diverse offerings include creating custom thesauri, building customized databases, organizing and publishing research results…even providing videos.

For more information about the NASA STI Program Office, see the following:

- Access the NASA STI program home page at <http://www.sti.nasa.gov>

- E-mail your question via the Internet to <help@sti.nasa.gov>

- Fax your question to the NASA STI Help Desk at 443–757–5803

- Phone the NASA STI Help Desk at 443–757–5802

- Write to:
  NASA STI Help Desk
  NASA Center for AeroSpace Information
  7115 Standard Drive
  Hanover, MD 21076–1320

NASA/TP—2013–217477

Closeout Report for the Refractory Metal Accelerated Heat Pipe Life Test Activity

J. Martin, R. Reid, E. Stewart, R. Hickman, and O. Mireles
Marshall Space Flight Center, Huntsville, Alabama

National Aeronautics and
Space Administration

Marshall Space Flight Center • Huntsville, Alabama 35812

January 2013

TRADEMARKS

Available from:

NASA Center for AeroSpace Information
7115 Standard Drive
Hanover, MD 21076–1320
301–621–0390

This report is also available in electronic form at
<https://www2.sti.nasa.gov>

TABLE OF CONTENTS

TABLE OF CONTENTS (Continued)

LIST OF FIGURES

LIST OF FIGURES (Continued)

LIST OF FIGURES (Continued)

LIST OF FIGURES (Continued)

LIST OF TABLES

LIST OF TABLES (Continued)

LIST OF ACRONYMS AND SYMBOLS

AMM	Advanced Methods and Materials, Inc.
Ar	argon
ARO	after receipt of order
ASTM	American Society for Testing and Materials
CH_3CH_2OH	ethanol
CH_3OH	chilled methanol
DBTT	ductile-to-brittle transition temperature
EB	electron beam
Fe	iron
GDMS	glow discharge mass spectroscopy
GTA	gas tungsten arc
HCL	hydrogen chloride
HDPE	high-density polyethylene
He	helium
HIP	hot isostatic pressing
HNO_3	nitric acid
H_2O_2	hydrogen peroxide
H_2SO_4	sulfuric acid
ID	inner/inside diameter
LDPE	low-density polyethylene
Mo-Re	molybdenum-rhenium

LIST OF ACRONYMS AND SYMBOLS (Continued)

MSFC	Marshall Space Flight Center
N	nitrogen
Na	sodium
NaCL	sodium chloride
NaOH	sodium hydroxide
Nb	niobium
NH_3	ammonia
Ni	nickel
OD	outer/outside diameter
PM	powder metallurgy
PTFE	polytetrafluoroethylene
RF	radio frequency
RFP	radio frequency power
RT	room temperature
SS	stainless steel
TFE	tetrafluoroethylene
Ti	titanium
TIG	tungsten inert gas
TP	Technical Publication
UV	ultraviolet
V	vanadium
VAC	Vacuum Atmospheres Company

LIST OF ACRONYMS AND SYMBOLS (Continued)

VHN	Vickers hardness number
Zr	zirconium

NOMENCLATURE

A	area
C_o(v)	oxygen concentration in vanadium
C_p	specific heat
$C_{p,h2o}$	specific heat of water (J/kg·K)
$C_{p,hp}$	specific heat of heat pipe (J/kg·K)
$C_{p,j}$	specific heat of element *j* (J/kg·K)
D	diameter
D_i	diameter of inner wall
D_o	diameter of outer wall
d	density
f	function
h_{cond}	effective conduction heat transfer coefficient (W/K)
h_{rad}	effective radiation heat transfer coefficient (W/K)
h_{tot}	effective total heat transfer coefficient (W/K) (h_{eff}=h_{cond}+h_{rad})
j	element number
k	thermal conductivity
k_{gas}	thermal conductivity of He-Ar gas (W/m·K)
k_j	thermal conductivity of element *j* (W/m·K)
L	axial length (m)
$\dot{m}$	flow rate

NOMENCLATURE (Continued)

m_{h2o}	mass of water (kg) ($m_{h2o}=\rho_{h2o}V_{h2o}$)
m_{hp}	mass of heat pipe (kg)
Q	power
q_{cond}	conduction heat transfer rate (W)
q_{rad}	radiation heat transfer rate (W)
q_{tot}	total heat transfer rate (W) ($q_{tot}=q_{cond}+q_{rad}$)
r_i	inner radius (m)
r_o	outer radius (m)
s	gap thickness (m) ($s=r_o-r_i$)
T	temperature
$T_{i,}$	initial temperature (K)
$T_{i,h2o}$	initial temperature of water (K)
$T_{i,hp}$	initial temperature of heat pipe (K)
$T_{i,j}$	initial temperature of element j (K)
T_o	outside temperature (K)
T_{sink}	sink temperature or temperature of vacuum chamber inner wall (K)
T_{ss}	steady-state temperature (K)
$T_{ss,h2o}$	steady-state temperature of water (K)
$T_{ss,hp}$	steady-state temperature of heat pipe (K)
t	thickness
V	volume; velocity

NOMENCLATURE (Continued)

V_{h2o}	volume of water (m^3) ($V_{h2o}=m_{h2o}/\rho_{h2o}$)
V_j	volume of element j (m^3)
ΔT	temperature difference (K) ($\Delta T=T_i-T_o$)
ΔT_{h2o}	temperature difference of water (K) ($\Delta T_{h2o}=T_{ss,h2o}-T_{i,h2o}$)
ΔT_{hp}	temperature difference of heat pipe (K) ($\Delta T_{hp}=T_{ss,hp}-T_{i,hp}$)
Δt	time step (s)
ε	emissivity
ε_i	emissivity of inner wall
ε_o	emissivity of outer wall
ρ	density
ρ_{h2o}	density of water (kg/m^3)
ρ_j	density of element j (kg/m^3)
σ	Stefan-Boltzman constant (5.67×10^{-8} W/m^2K^4)

TECHNICAL PUBLICATION

CLOSEOUT REPORT FOR THE REFRACTORY METAL ACCELERATED HEAT PIPE LIFE TEST ACTIVITY

1. INTRODUCTION

The primary goal of the accelerated heat pipe life testing activity was to focus on an experimental investigation of aging effects, using a series of 16 molybdenum-rhenium (Mo-Re) alloy heat pipes. To accelerate the response rate of potential life-limiting factors, an increase in both temperature and mass flux was imposed. Specific test conditions for each of the heat pipes are summarized in table 1. The first set of seven tests, referred to as the G Series, is based on the American Society for Testing and Materials (ASTM) G68–80 and examines time-dependent corrosion by holding constant temperature and mass fluence boundary conditions over the operating interval.[1] The second set of nine tests, referred to as the F Series (Fisher central composite F(–4) to F(4)), imposes variations in both operating temperature and mass fluence, with the intent of providing insight into the cross correlation of these parameters with respect to corrosion rates. Detailed documentation covering the approach, design, and layout of the heat pipes and test support systems was previously reported.[2–4] Due to a change in program direction and funding, the heat pipe project was terminated prior to build and testing.

Table 1. Baseline heat pipe life test matrix conditions (water coolant).

Test Identifier	Power Level (W)	Heat Pipe Temp. (K)	Gas Gap Mixture	Gas Gap Width (in)	Coolant Flow (gpm)	Coolant Delta Temp. (K)	Number of Heat Pipes
G Series	3,000	1,273	He-32%Ar	0.025	0.61	18.8	7
F(–4)	5,000	1,273	He-6%Ar	0.025	0.77	24.6	1
F(–3)	1,000	1,273	He-32%Ar	0.103	0.11	35.2	1
F(–2)	3,000	1,373	He-32%Ar	0.031	0.56	21.1	1
F(–1)	3,000	1,173	He-32%Ar	0.021	0.65	17.6	1
F(0)	3,000	1,273	He-32%Ar	0.025	0.61	18.8	1
F(1)	2,000	1,223	He-32%Ar	0.037	0.54	13.9	1
F(2)	4,000	1,223	He-32%Ar	0.017	0.67	22.8	1
F(3)	2,000	1,323	He-32%Ar	0.046	0.50	15.2	1
F(4)	4,000	1,323	He-32%Ar	0.020	0.63	24.0	1

The 16 heat pipe envelopes were to be constructed of Mo–44.5%Re material, formed using the powder metallurgy (PM) process by Rhenium Alloys, Inc., and assembled by Advanced Methods and Materials, Inc. (AMM). The heat pipes were designed with an active length of ≈12 in (3-in evaporator and 9-in condenser) and an outer diameter (OD) of 0.625 in. The proposed wick structure was an annular crescent design fabricated from seven layers of Mo-5%Re 400 × 400-mesh cloth (average 0.001-in-diameter wire). The final cylindrical wick structure had an OD of ≈0.48 in and a wall thickness of 0.014 in, resulting in an annular flow gap of ≈0.022 in. The wick tube was equipped with a bonded plug at the evaporator end while the condenser end remained open, sealed by the excess liquid sodium (Na) that pools at the end of the condenser section. The evaporator end plug was fitted with a zirconium- (Zr-) based getter pack to irreversibly trap impurities collected in the evaporator pool during normal operation. Power transfer into and out of the heat pipe would be provided by noncontact methods to minimize the potential for introducing impurities. Power was to be supplied using a radio frequency (RF) induction coil on the evaporator section and removed from the condenser using a low-pressure static gas (helium (He) and argon (Ar) mixture) gap coupled water calorimeter. Each heat pipe temperature was to be monitored with a single, noncontact optical pyrometer, sighted at the evaporator exit just upstream of the calorimeter assembly. Figure 1 illustrates the basic layout of the heat pipe with attached support hardware.

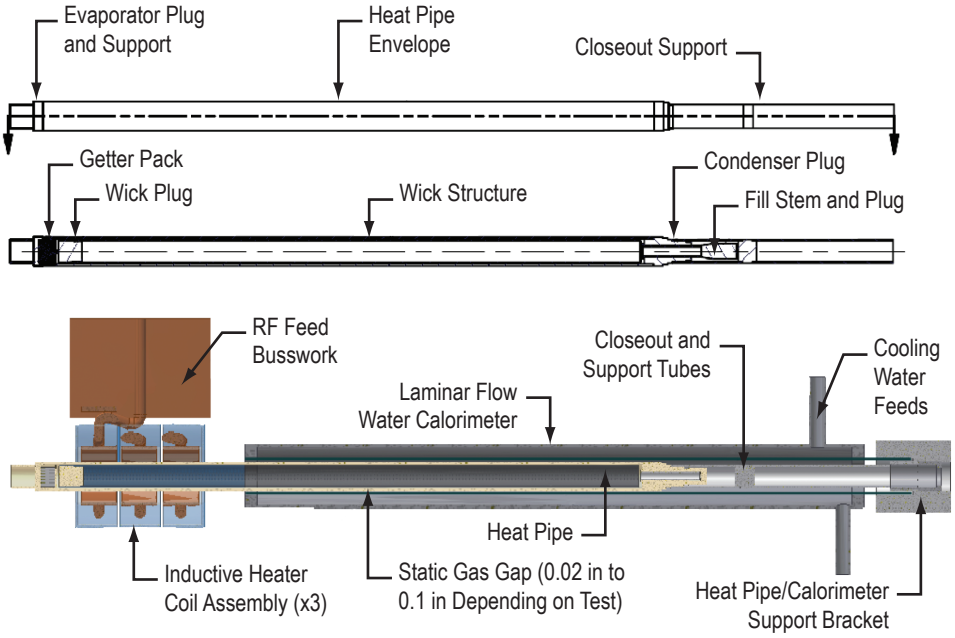

Figure 1. Heat pipe cross section with ancillary test systems.

The planned evaluation activity would require around-the-clock operation of the heat pipes with a goal of accumulating up to 3 years of test time. During this test time, at approximately 6-mo intervals, the heat pipes would be removed and examined by a combination of nondestructive and destructive methods to assess the accelerated effects of aging on both the wick and heat pipe envelope.

1.1 Laboratory Layout

To accomplish the outline testing, a portion of the floor space within the NASA Marshall Space Flight Center (MSFC) Building 4655 high-bay area was designated to house the setup and operation. This location is in close proximity to both facility water and power interfaces, while minimizing interference with normal day-to-day operations. Geometric constraints were developed for each of the primary test support systems, such that an approximate laboratory layout could be generated.

Figure 2(a) illustrates the proposed laboratory setup and figure 2(b) is a photograph of the floor space prior to hardware setup. The illustration does not include two 19-in instrumentation racks and the table to house the data acquisition/control hardware and computers. Also omitted are tubing runs for the water cooling and gas systems, power wiring runs for all equipment, and the RF distribution busswork.

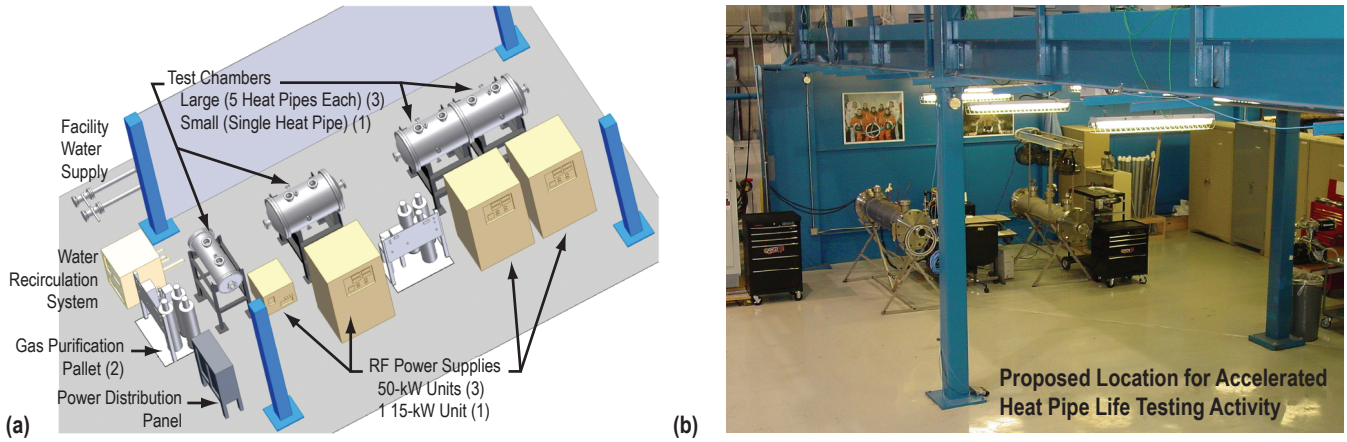

Figure 2. General laboratory layout for accelerated heat pipe life testing: (a) Proposed laboratory setup and (b) photograph of floor space prior to hardware setup.

Although this project was terminated prior to setting up the hardware support systems within the laboratory, the environmental test chambers and the inert gas purification pallets, two of the basic support systems, were already in fabrication and have been completed.

1.2 Hardware Procurements

A majority of the test support systems have been detailed and the specifications developed to support the procurement process. Once final vendor submissions were received, selection was based on combined cost and technical evaluation criteria. Several of the large hardware components were detailed in previous reports that covered the heat pipe material and fabrication specifications and the RF inductive coil fabrication and performance specifications. Since that time, specifications for many of the remaining hardware components have been developed and procurements initiated. Appendices A–G provide details for many of the larger components that were procured.

Many smaller purchases for items such as tubing, relief valves, fittings, raw materials, vacuum system components, etc. have also been made and are not listed individually. With termination of the project, all procurements underway were cancelled using the most logical approach, which was finishing those that were nearing completion while descoping others that were at suitable break points. Many of the early hardware orders for off-the-shelf items had already been completed and material goods received. A number of procurements that were underway and were adjusted included the following:

- Heat pipe wick structure fabrication—Development activity for the wick structure was completed and successfully demonstrated. This activity was then terminated to recoup remaining funds. Since the screen mesh material is an extremely limited and expensive commodity, to complete the fabrication of the wicks would be an unnecessary waste of material.

- Heat pipe envelope/assembly fabrication—Material for the heat pipe envelopes has been procured, rod stock completed, and tubing stock nearing completion. It was elected to complete the material fabrication and accept delivery of the raw stock. Weld development activity and component fabrication such as getter packs was also terminated.

- RF power system—Modeling analysis of the inductive coil assemblies and RF busswork for the required test geometries was completed. No material procurement or hardware fabrication had been initiated on the inductive coils, making this a logical break point to terminate the contract.

- Environmental test chambers—A contract was in place, materials had been acquired, and fabrication in process, therefore cancellation would have resulted in a significant loss. The chambers were completed.

- Laminar flow water calorimeters—The procurement process had been initiated with specification posted and potential vendors contacted. The solicitation was canceled prior to closure of the procurement posting cycle and no vendor quotes were received.

- Inert gas purifier units—A contract award had been made and fabrication initiated. The contract was descoped to a single unit with a minor price impact.

- Two-band optical pyrometers—A contract award had been made and fabrication was underway. The contract was descoped from 17 to 8 units.

- Water circulation pump pallet—The initial procurement cycle had been completed with vendor quotes received and evaluated. The solicitation was canceled prior to making an award with no penalty.

- Magnetic flow meters—The procurement had been posted and potential vendors contacted. The solicitation was canceled prior to receiving final vendor quotes.

2. WATER-COOLING SYSTEM CONSIDERATIONS

During specification and layout of the calorimeter cooling system, concerns regarding loss of coolant conditions were identified. This situation appeared especially relevant due to the nature of the proposed testing, operating around the clock for up to 6 months at a time. Undoubtedly unexpected power outages, hardware failure, and computer software errors would occur, resulting in system shutdowns. To examine potential effects, thermal analyses were performed to assess the potential temperature rise within the heat pipe calorimeters due to two failure scenarios. The first case examined was where facility water was lost but the recirculation loop water continued to circulate (power was not lost). The assumption was made that RF input power to the heat pipes would be turned off immediately, and as a worst case, all of the heat contained within the heat pipes at operational temperature would be absorbed by the water. Results indicate that sufficient water volume exists within the system to safely absorb the energy without boiling. The second failure scenario case examined was where power was lost, resulting in a loss of recirculation coolant flow. This analysis required an unsteady assessment of the transient temperature rise within the stagnant calorimeter. Results indicate that portions of the water will likely exceed its boiling temperature. The belief is that some localized dryout will occur but with no damage to the system (temperatures do not exceed copper melting point). Care should be taken to allow the calorimeters to cool down prior to restarting the system, minimizing the potential for water-hammer-like pressure spikes. Both of these analyses are low-order assessments; however, the results are believed to be conservative.

2.1 Thermal Analysis for Loss of Facility Coolant Flow Condition

The objective of this analysis was to estimate the temperature rise of the heat pipe calorimeter resulting from the loss of facility water, assuming that the RF input power is turned off simultaneously. Under this scenario, the recirculation water continues to flow but is no longer able to reject heat into the facility water. The issue becomes, what volume of water is required to absorb the heat contained within the heat pipes and maintain a water temperature below some allowable maximum temperature, e.g., the boiling temperature of water? More specifically, does the expansion tank need to be oversized to facilitate this heat soak-back? A low-order assessment was performed, which is simply a steady-state balance of thermal energy. The resulting temperature rise is given by the following equations:

$$m_{h2o}C_{p,h2o}\Delta T_{h2o} = m_{hp}C_{p,hp}\Delta T_{hp} \quad , \tag{1}$$

$$\rho_{h2o}V_{h2o}C_{p,h2o}\left(T_{ss,h2o} - T_{i,h2o}\right) = m_{hp}C_{p,hp}\left(T_{i,hp} - T_{ss,hp}\right) \quad , \tag{2}$$

and

$$V_{h2o} = \frac{m_{hp}C_{p,hp}\left(T_{i,hp} - T_{ss}\right)}{\rho_{h2o}C_{p,h2o}\left(T_{ss} - T_{i,h2o}\right)} \quad , \tag{3}$$

where at steady state, $T_{ss,h2o}=T_{ss,hp}=T_{ss}$, and $T_{i,hp} \geq T_{ss} \geq T_{i,h2o}$ (i.e., the heat pipe cools and the water warms to the same temperature). The analysis should overpredict the water temperature because there are additional masses that will absorb heat (e.g., calorimeter metal, support structures, piping, etc.) that are not taken into account. Equation (3) was assessed with a spreadsheet analysis, producing the results in figure 3 for required water volumes (V_{h2o}) as a function of steady-state temperature (T_{ss}). Water properties (ρ_{h2o}) and ($C_{p,h2o}$) are calculated at a pressure of 0.414 MPa and a temperature of $(T_{ss}+T_{i,h2o})/2$.[5] The Mo-44.5%Re heat pipe properties, m_{hp} and $C_{p,hp}$, are specified as 16 kg and 250 J/kg K, respectively, for the plotted results. The initial heat pipe temperature ($T_{i,hp}$) is set equal to 1,400 K (a maximum value).

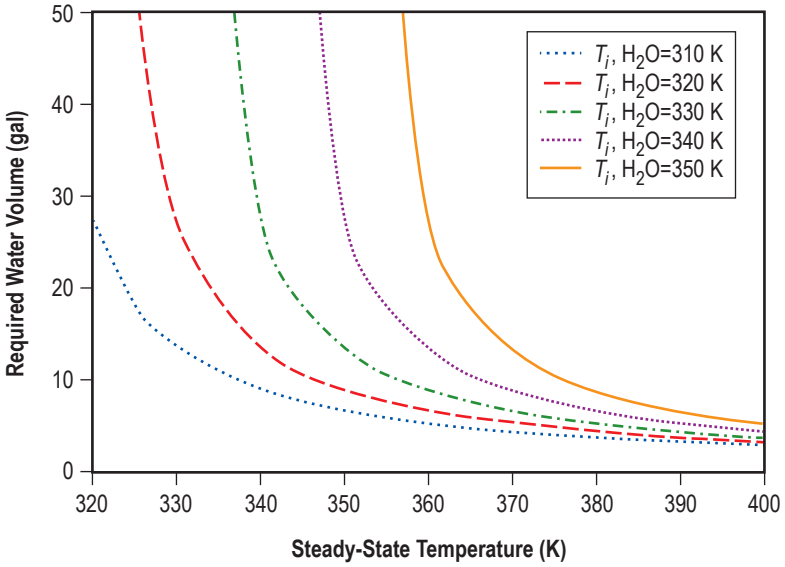

Figure 3. Equilibrium temperature and volume of water required to cool 16 kg of Mo-44.5%Re where initial temperature of Mo-44.5%Re is 1,400 K.

As stated, the final steady-state temperature (T_{ss}) will be greater than the initial water temperature ($T_{i,h2o}$), and as indicated by figure 3, as T_{ss} approaches $T_{i,h2o}$, the required water volume (V_{h2o}) approaches infinity. At the assumed operating pressure, 0.414 MPa, the boiling temperature of water is 418 K. Figure 3 illustrates that for an initial water temperature ($T_{i,h2o}$) as high as 350 K, 10 gal of water will absorb the thermal energy and produce a steady-state temperature (T_{ss}) of <380 K. For the planned system, over 15 gal of water are contained in the 50 ft of 0.5-in-diameter tubing, 20 ft of 4-in-diameter piping, and the water circulation pallet reservoir. Therefore, sizing the expansion tank to provide sufficient water for heat soak-back does not appear necessary.

Table 2 provides the design parameters calculated for the various heat pipe calorimeter test series. The maximum water outlet temperature is 335 K, which is the maximum bulk or average temperature of the recirculating water. Using this value as the initial water temperature ($T_{i,h2o}$) in these calculations is conservative, because the majority of the water in the recirculation loop will very likely be at or near the inlet temperature of 300 K. Table 2 also indicates that the calorimeter inner wall temperatures may be as

high as 396 K (for case F(– 4)), and as a result, the water temperature near the wall will approach this value. It is believed that in the transient, following shutdown of the RF power supplies, the wall temperature will drop rapidly as the heat flux decays across the calorimeter inner wall, even with the subsequent rise in the average water temperature.

Table 2. Heat pipe calorimeter parameters for a film gap width of 0.015 in.

Film Cooling Water Inlet Temperature	300 K									
Film Gap Width	0.015 in									
Calorimeter Heat Extraction Length	9.25 in									
Calorimeter Total Length	13 in									
Test Condition	**Units**	**G Series**	**F(–4)**	**F(–3)**	**F(–2)**	**F(–1)**	**F(1)**	**F(2)**	**F(3)**	**F(4)**	**F(0)**
Power	W	3,000	5,000	1,000	3,000	3,000	2,000	4,000	2,000	4,000	3,000
Heat Pipe to Calorimeter Gas Gap Width	in	0.025	0.025	0.103	0.031	0.021	0.037	0.017	0.046	0.02	0.025
Heat Pipe Temperature	K	1,273	1,273	1,273	1,373	1,173	1,223	1,223	1,323	1,323	1,273
Calorimeter Channel Wall Temperature	K	360	396	338	360	360	340	380	340	380	360
Log Mean Temp. Difference (Wall to Fluid)	K	502	83.3	13.8	49.5	50.9	32.7	68.2	32	67.5	50.2
Cooling Film Flow ΔT (Outlet-Inlet)	K	18.8	24.6	35.2	20.1	17.6	13.9	22.8	15.2	24	18.8
Cooling Flow Outlet Temperature	K	318.6	324.4	335	319.9	317.4	313.8	322.6	315	323.8	318.6
Cal. Film Flow ID	in	0.795	0.794	0.951	0.806	0.786	0.818	0.777	0.836	0.785	0.795
Cal. Film Flow OD	in	0.825	0.824	0.981	0.836	0.816	0.848	0.807	0.866	0.815	0.825
Water Film Flow Rate	Gal/min	0.6	0.77	0.11	0.56	0.65	0.54	0.67	0.5	0.63	0.6
Heat Transfer Coef k	W/m^2K	4,009.09	4,035.15	4,075.22	4,014.7	4,004.1	3,986.03	4,027.64	3,991.38	4,032.91	4,009.09
Reynolds No.		1,651.62	2,234.2	289.99	1,542.72	1,760.48	1,369.09	1,936.03	1,244.12	1,842.06	1,651.62
Calorimeter Pressure Drop	psi	3.7	4	0.5	3.3	4	3.5	3.8	3.1	3.5	3.7

2.2 Thermal Analysis for Loss of Recirculation Coolant Flow Condition

The objective of this analysis was to estimate the temperature rise of the calorimeter resulting from the loss of recirculating water flow, i.e., the water has no velocity but remains within the system and assumes that the RF input power is turned off simultaneously. While a first-look, steady-state assessment analogous to that performed in section 2.1 is useful, the issue is the transient temperature rise within the calorimeter. Following shutdown of the RF power supplies, the energy within the heat pipes dissipates into the calorimeter, producing a temporary rise in temperature due to the stagnate calorimeter's reduced ability to remove the heat. The low-order assessments performed here are based on the geometry given in figure 4, where the total calorimeter length (L) is equal to 0.33 m. The material parameters are listed in table 3.

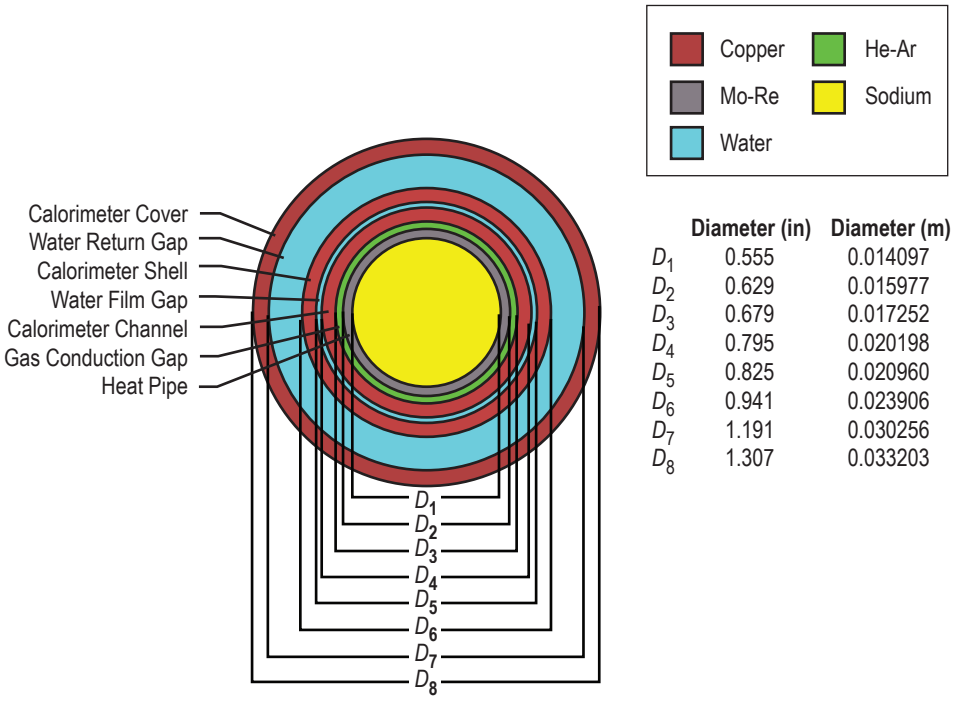

	Diameter (in)	Diameter (m)
D_1	0.555	0.014097
D_2	0.629	0.015977
D_3	0.679	0.017252
D_4	0.795	0.020198
D_5	0.825	0.020960
D_6	0.941	0.023906
D_7	1.191	0.030256
D_8	1.307	0.033203

Figure 4. Heat pipe calorimeter geometry.

Table 3. Average heat pipe and calorimeter model parameters.

Element	Material	ID (m)	OD (m)	ρ (kg/m^3)	C_p (J/kg-K)	k (W/m-K)	T_i (K)
1	Mo-Re	0.014097	0.015977	13,800	250	90	1,273
2	Copper	0.017252	0.020198	8,900	380	400	400
3	Water	0.020198	0.02096	985	4,200	0.65	325
4	Copper	0.02096	0.023906	8,900	380	400	325
5	Water	0.023906	0.030256	985	4,200	0.65	325
6	Copper	0.030256	0.033203	8,900	380	400	325

Using the parameters in table 3 to perform a steady-state energy balance analogous to that performed in section 2.1 yields a steady-state temperature equal to 392 K. The equation governing this is as follows:

$$T_{ss} = \frac{\sum_{j=1}^{6} \rho_j V_j C_{p,j} T_{i,j}}{\sum_{j=1}^{6} \rho_j V_j C_{p,j}} \quad , \tag{4}$$

where the subscript *j* corresponds to the element number in table 3. The steady-state temperature (392 K) is well below the melting point of copper (≈1,300 K) and even the boiling point of water (418 K) at the assumed pressure of 0.414 MPa. This is especially good since additional heat absorption masses and/or heat leak paths have been neglected in this assessment. However, the transient temperature response is the concern here, and ideally any temperature spike would not cause the water to boil, much less cause the copper to soften. The following equations[6] are used to perform the transient assessment:

$$\rho_j V_j C_{p,j} \frac{\partial T_j}{\partial t} = \int_0^{A_j} q_{cond,j} \partial A_j + \int_0^{A_j} q_{rad,j} \partial A_j \quad , \tag{5}$$

$$\int_0^{A_j} q_{cond,j} \partial A_j = \frac{2\pi L k_j}{\ln\left(D_{o,j}/D_{i,j}\right)} \left(T_{i,j} - T_{o,j}\right) \quad , \tag{6}$$

and

$$\int_0^{A_j} q_{rad,j} \partial A_j = \frac{\pi \, D_{i,j} L \sigma}{\frac{1}{\varepsilon_{i,j}} + \frac{1-\varepsilon_{o,j}}{\varepsilon_{o,j}} \left(\frac{D_{i,j}}{D_{o,j}}\right)} \left(T_{i,j}^4 - T_{o,j}^4\right) \; . \tag{7}$$

The equations are coded into the Fortran 90 program, listed in appendix H, which solves them numerically using an explicit time-stepping approach. The equations solved are as follows:

$$T_1^{t+\Delta t} = T_1^t - \left(\frac{\Delta t \pi L}{\rho_1 V_1 C_{p,1}}\right) \left[\frac{2k_{gas}}{\ln\left(D_3 / D_2\right)} \left(T_1 - T_2\right) + \frac{D_2 \sigma}{\frac{1}{\varepsilon_1} + \frac{1-\varepsilon_2}{\varepsilon_2} \left(\frac{D_2}{D_3}\right)} \left(T_1^4 - T_2^4\right) \right]^t \quad , \tag{8}$$

$$T_2^{t+\Delta t} = T_2^t - \left(\frac{\Delta t \pi L}{\rho_2 V_2 C_{p,2}}\right) \times$$

$$\left[\frac{2k_3}{\ln\left(D_4+D_5/2D_4\right)}\left(T_2-T_3\right)-\frac{2k_{gas}}{\ln\left(D_3/D_2\right)}\left(T_1-T_2\right)-\frac{D_2\sigma}{\frac{1}{\varepsilon_1}+\frac{1-\varepsilon_2}{\varepsilon_2}\left(\frac{D_2}{D_3}\right)}\left(T_1^4-T_2^4\right)\right]^t \quad , \tag{9}$$

$$T_3^{t+\Delta t}=T_3^t-\left(\frac{2\Delta t\pi L}{\rho_3 V_3 C_{p,3}}\right)\left[\frac{k_3}{\ln\left(2D_5/D_4+D_5\right)}\left(T_3-T_4\right)-\frac{k_3}{\ln\left(D_4+D_5/2D_4\right)}\left(T_2-T_3\right)\right]^t \quad , \tag{10}$$

$$T_4^{t+\Delta t}=T_4^t-\left(\frac{2\Delta t\pi L}{\rho_4 V_4 C_{p,4}}\right)\left[\frac{k_5}{\ln\left(D_6+D_7/2D_6\right)}\left(T_4-T_5\right)-\frac{k_3}{\ln\left(2D_5/D_4+D_5\right)}\left(T_3-T_4\right)\right]^t \quad , \tag{11}$$

$$T_5^{t+\Delta t}=T_5^t-\left(\frac{2\Delta t\pi L}{\rho_5 V_5 C_{p,5}}\right)\left[\frac{k_5}{\ln\left(2D_7/D_6+D_7\right)}\left(T_5-T_6\right)-\frac{k_5}{\ln\left(D_6+D_7/2D_6\right)}\left(T_4-T_5\right)\right]^t \quad , \tag{12}$$

and

$$T_6^{t+\Delta t}=T_6^t-\left(\frac{\Delta t\pi L}{\rho_6 V_6 C_{p,6}}\right)\left[D_8\sigma\varepsilon_3\left(T_6^4-T_{\sin k}^4\right)-\frac{2k_5}{\ln\left(2D_7/D_6+D_7\right)}\left(T_5-T_6\right)\right]^t \quad . \tag{13}$$

where the superscripts $t+\Delta t$ and t indicate that values are specified at the next time step and the current time step, respectively. The motivation for actually writing the software, rather than using existing thermal software programs (e.g., SINDA), was the desire to incorporate this type of analysis into a spreadsheet approach that is commonly used for preliminary design trades. It is emphasized here that the analysis is low order, and higher fidelity thermal software could be used to further assess the localized effects and/or potentially provide a higher degree of accuracy. Calculated results are illustrated in figures 5 and 6, and again may be seen as conservative from the perspective that additional heat-absorbing masses are neglected. Heat is allowed to escape the calorimeter via thermal radiation from the external surface, but not through the water piping or solid supports. Figure 6 differs from figure 5 in that the Mo-Re element's wall thickness was tripled to assess the sensitivity to the total heat stored in the heat pipe. The motivation is that the results of figure 5 only use the heat pipe Mo-Re shell layer and neglect the heat stored within the wick screen and Na. It is believed that increasing the Mo-Re wall thickness by a factor of 3 is conservative, in that more than the actual stored heat is added to the analyses.

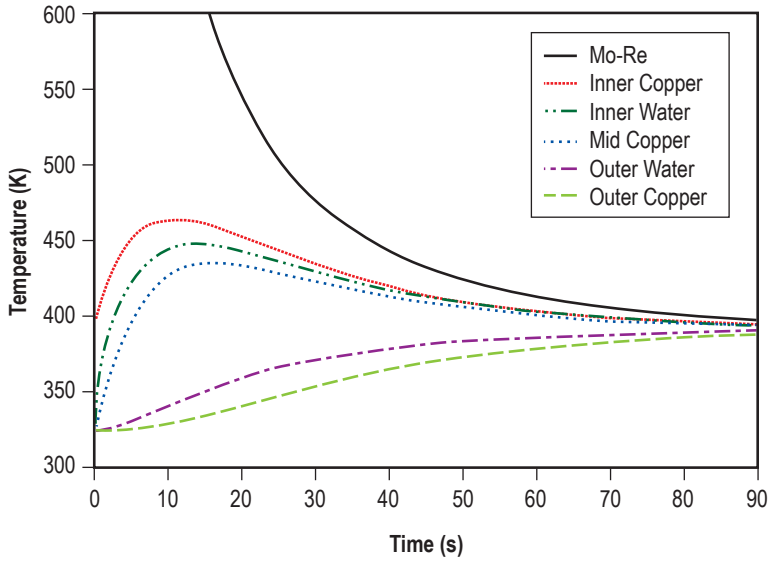

Figure 5. Calorimeter transient soak-back temperatures for the baseline heat pipe geometry.

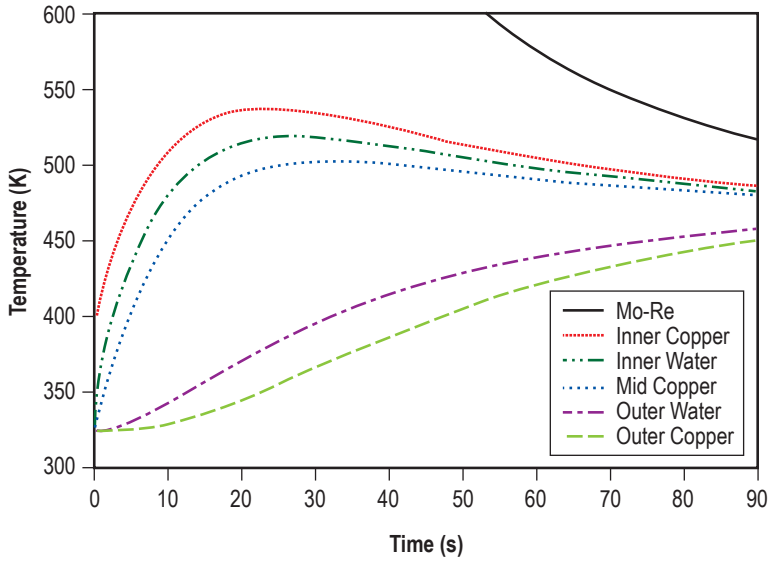

Figure 6. Calorimeter transient soak-back temperatures for three times the baseline heat pipe Mo-Re mass.

In all cases examined, the maximum temperature reached by the copper is below 550 K. Results indicate that portions of the water will likely exceed its boiling temperature of 418 K. However, the belief is that some localized dryout will occur, but with no damage to the system (i.e., copper temperatures do not exceed melting temperatures) as long as care is taken to allow the calorimeters to cool below the boiling point prior to restarting the system, the potential for water-hammer-like pressure spikes will be minimized.

3. CALORIMETER CONSIDERATIONS

During this project alternate calorimeter designs were identified to potentially reduce material cost and simplify fabrication requirements. In addition, to verify that the selected instrumentation could accurately assess the heat pipe power (calorimeter coolant flow and temperature rise) a simplified uncertainty assessment was performed.

3.1 Use of Standard Tube Sizes to Meet Calorimeter Performance

The original heat pipe calorimeter layout made use of drawn copper tube material to form the three coaxial tube elements (channel, shell, and cover) requiring unique tubing sizes for each of the proposed test setups. At that time, a company was identified that indicated it could provide the specified material; however, due to a combination of cost, availability, and minimum order requirements, the drawn tubing option was revisited with an eye on using readily available standard sizes. Table 4 lists the original drawn tubing dimensions that would be required to satisfy operational requirements. The basic assumption with the drawn stock approach was that the material could be drawn to any given ID and OD while holding a fixed tube wall thickness of 0.058 in. These values were used as a basis to begin the selection of standard tube sizes.

Table 4. Heat pipe calorimeter drawn tubing requirements (all dimensions are in inches).

Calorimeter Geometry (Elements)	G	F(–4)	F(–3)	F(–2)	F(–1)	F(1)	F(2)	F(3)	F(4)	F(0)
Quantity	7	1	1	1	1	1	1	1	1	1
Heat Pipe OD	0.625	0.625	0.625	0.625	0.625	0.625	0.625	0.625	0.625	0.625
Gas Conduction Gap Width	0.027	0.027	0.105	0.033	0.023	0.039	0.018	0.048	0.022	0.027
Calorimeter Channel Tube ID	0.679	0.678	0.835	0.69	0.67	0.702	0.661	0.72	0.669	0.679
Calorimeter Channel Tube OD	0.795	0.794	0.951	0.806	0.786	0.818	0.777	0.836	0.785	0.795
Calorimeter Channel Tube Wall Thickness	0.058	0.058	0.058	0.058	0.058	0.058	0.058	0.058	0.058	0.058
Calorimeter Shell Tube ID	0.825	0.824	0.981	0.836	0.816	0.848	0.807	0.866	0.815	0.825
Calorimeter Shell Tube OD	0.941	0.94	1.097	0.952	0.932	0.964	0.923	0.982	0.931	0.941
Calorimeter Shell Tube Wall Thickness	0.058	0.058	0.058	0.058	0.058	0.058	0.058	0.058	0.058	0.058
Water Film Flow Gap	0.015	0.015	0.015	0.015	0.015	0.015	0.015	0.015	0.015	0.015
Calorimeter Cover Tube ID	1.191	1.19	1.347	1.202	1.182	1.214	1.173	1.232	1.181	1.191
Calorimeter Cover Tube OD	1.307	1.306	1.463	1.318	1.298	1.33	1.289	1.348	1.297	1.307
Calorimeter Cover Tube Wall Thickness	0.058	0.058	0.058	0.058	0.058	0.058	0.058	0.058	0.058	0.058
Water Return Path Gap	0.125	0.125	0.125	0.125	0.125	0.125	0.125	0.125	0.125	0.125

The use of standard tubing was expected to simplify the overall design by minimizing the differences between each calorimeter, and reducing the number of unique tubes required. Using this approach, the width of the gas conduction gap between the heat pipe and channel tube would be controlled by selecting a sufficiently thick-walled calorimeter channel tube section to allow for internal boring. No machining was planned for either the shell or cover tube elements. The standard tubing sizes identified in the initial calorimeter assessment are listed in table 5 and were selected to roughly meet the gas gap, water film flow gap, and water return flow gap requirements.

Table 5. Standard tube sizes identified.

Calorimeter Element	Tube OD (in)	Tube Wall Thickness (in)
Channel Tube—Requires Three Sizes	0.875	by 0.109 by 0.095 by 0.083
Shell Tube—Requires Three Sizes	1.000 1.125	by 0.049 by 0.083 by 0.049
Cover Tube—Requires Two Sizes	1.500	by 0.083 by 0.065

The dimensions for each of the 16 calorimeters are provided in table 6, which was generated from a simple sizing spreadsheet (app. I) based on the initial gas conduction gaps set by the original drawn tubing analysis. The use of standard tubing requires that the water film flow gap be set to a width of 0.0135 in, slightly tighter than the 0.015 in width calculated in the original analysis. This is not expected to present any difficulties. In addition, the water return path is opened up slightly from 0.125 in to 0.167 in for all but the F(–3) case. The final weight of a completed calorimeter unit is estimated at 3.7 lb.

As a quick check, the selected standard tube sizes were used in the simplified calorimeter sizing spreadsheet developed at the beginning of this project. The results follow expected trends with an increase in coolant temperature rise and a corresponding drop in flow rate (the smaller film gap improves the heat transfer); pressure drop is approximately the same due to the lower flow rate. Table 7 provides tabulated values for each of the calorimeter configurations and appendix J contains the full spreadsheet used in the assessment.

Table 6. Calorimeter assembly layout with standard tube sizes—machining of channel tube only (all dimensions are in inches).

Calorimeter Geometry (Elements)	G	F(–4)	F(–3)	F(–2)	F(–1)	F(1)	F(2)	F(3)	F(4)	F(0)
Quantity	7	1	1	1	1	1	1	1	1	1
Heat Pipe OD	0.625	0.625	0.625	0.625	0.625	0.625	0.625	0.625	0.625	0.625
Gas Conduction Gap Width	0.027	0.027	0.105	0.033	0.023	0.039	0.018	0.048	0.022	0.027
Calorimeter Channel Standard Tube OD	0.875	0.875	1	0.875	0.875	0.875	0.875	0.875	0.875	0.875
Calorimeter Channel Tube Standard Wall Thickness	0.109	0.109	0.083	0.095	0.109	0.095	0.109	0.083	0.109	0.109
Wall Material to be Machined (From the Radius)	0.011	0.011	0.005	0.03	0.07	0.09	0.02	0.06	0.06	0.011
Calorimeter Channel Final Tube ID	0.679	0.679	0.835	0.691	0.671	0.703	0.661	0.721	0.669	0.679
Calorimeter Shell Standard Tube OD	1	1	1.125	1	1	1	1	1	1	1
Calorimeter Shell Tube Standard Wall Thickness	0.049	0.049	0.049	0.049	0.049	0.049	0.049	0.049	0.049	0.049
Calorimeter Shell Standard Tube ID	0.902	0.902	1.027	0.902	0.902	0.902	0.902	0.902	0.902	0.902
Final Water Film Flow Gap	0.013	0.013	0.013	0.013	0.013	0.013	0.013	0.013	0.013	0.013
Calorimeter Cover Tube Standard OD	1.5	1.5	1.5	1.5	1.5	1.5	1.5	1.5	1.5	1.5
Calorimeter Cover Standard Tube Wall Thickness	0.083	0.083	0.065	0.083	0.083	0.083	0.083	0.083	0.083	0.083
Calorimeter Cover Standard Tube ID	1.334	1.334	1.370	1.334	1.334	1.334	1.334	1.334	1.334	1.334
Final Water Return Path Gap	0.167	0.167	0.123	0.167	0.167	0.167	0.167	0.167	0.167	0.167

Table 7. Calorimeter parameters for a film gap width of 0.0135 in.

Film Cooling Water Inlet Temperature	300 K	Film Gap Width		0.0135 in	Calorimeter Heat Extraction Length		9.25 in	Calorimeter Total Length			13 in
Test Condition	**Units**	**G Series**	**F(–4)**	**F(–3)**	**F(–2)**	**F(–1)**	**F(1)**	**F(2)**	**F(3)**	**F(4)**	**F(0)**
Power	W	3,000	5,000	1,000	3,000	2,000	2,000	4,000	2,000	4,000	3,000
Heat Pipe to Calorimeter Gas Gap Width	in	0.025	0.025	0.104	0.031	0.037	0.037	0.017	0.046	0.02	0.025
Heat Pipe Temperature	K	1,273	1,273	1,273	1,373	1,223	1,223	1,223	1,323	1,323	1,273
Calorimeter Channel Wall Temperature	K	355	390	332	355	337	340	373	338	373	355
Log Mean Temperature Difference (Wall to Fluid)	K	40.8	66.9	11.9	40.8	27.5	32.7	53.9	27.4	53.9	40.8
Cooling Film Flow ΔT (Outlet-Inlet)	K	26	42.2	29.5	26	17.6	13.9	34.8	19.3	34.8	26
Cooling Flow Outlet Temp.	K	325.8	342	329.3	325.8	317.4	313.8	334.7	319.1	334.7	325.8
Cal Film Flow ID	in	0.875	0.875	1	0.875	0.875	0.818	0.875	0.875	0.875	0.875
Cal Film Flow OD	in	0.902	0.902	1.027	0.902	0.902	0.848	0.902	0.902	0.902	0.902
Water Film Flow Rate	gal/min	0.44	0.45	0.13	0.44	0.43	0.54	0.43	0.39	0.43	0.44
Heat Transfer Coef k	W/m^2K	4,484.26	4,558.33	4,497.51	4,484.27	4,442.6	3,986.03	4,525.64	4,451.28	4,525.64	4,484.27
Reynolds No.		1,171.24	1,403.8	312.43	1,171.17	1,058.46	1,369.09	1,271.02	981.78	1,271.02	1,171.17
Calorimeter Pressure Drop	psi	3.2	2.6	0.9	3.2	3.5	3.5	2.8	3.2	2.8	3.2

3.2 Alternate Calorimeter Design

Another calorimeter concept was developed to support electric resistance heater testing. This calorimeter layout also makes use of a static gas gap technique to provide a noncontact thermal transport boundary, and may offer a potential alternative to the heat pipe three-tube calorimeter assembly currently baselined. This alternate concept incorporates a central copper tube, sized to set the required gas conduction gap width, which is covered on its outer surface with a spiral-wrapped copper tube containing the coolant flow. This tightly wound cooling tube is brazed to the surface of the central tube. Figure 7 illustrates this concept for a six-coil arrangement (the layout for testing electric resistance heater elements) mounted in parallel to the inlet and outlet coolant manifolds. During coil brazing, sufficient braze material should be provided to fill a majority of the gaps between adjacent coils and the central tube. However, due to the high thermal conductivity of copper and the close packing of the cooling coils, complete filling of the gaps would not be necessary to achieve the required performance levels. Figure 8 illustrates a typical wound coil on a central tube section and a postbraze cross section showing partially filled braze gaps. Possible benefits include a potentially simpler fabrication process, fewer required materials, and the ability to place viewing holes along the condenser, between coolant coils, should additional temperature measurements be required. The use of several parallel cooling coils along the length of the heat pipe calorimeter would minimize variations in temperature.

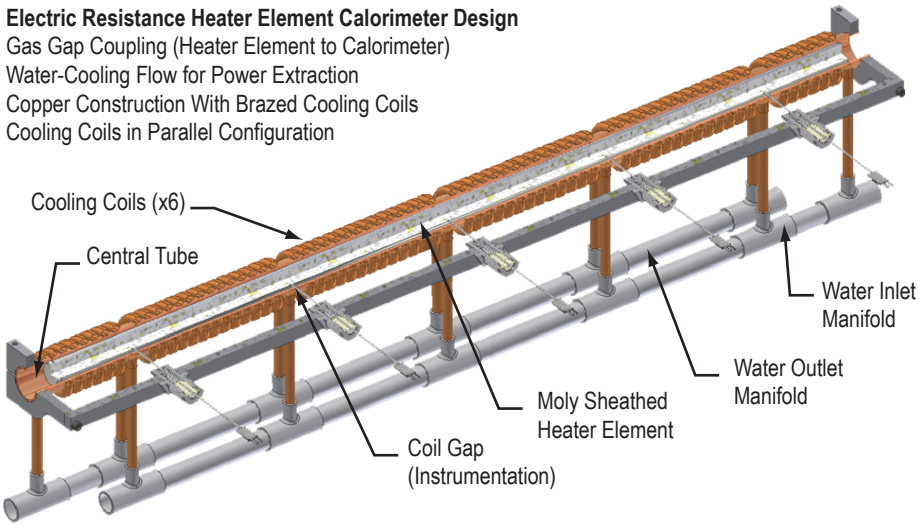

Figure 7. An alternate design—electric resistance heater element calorimeter design.

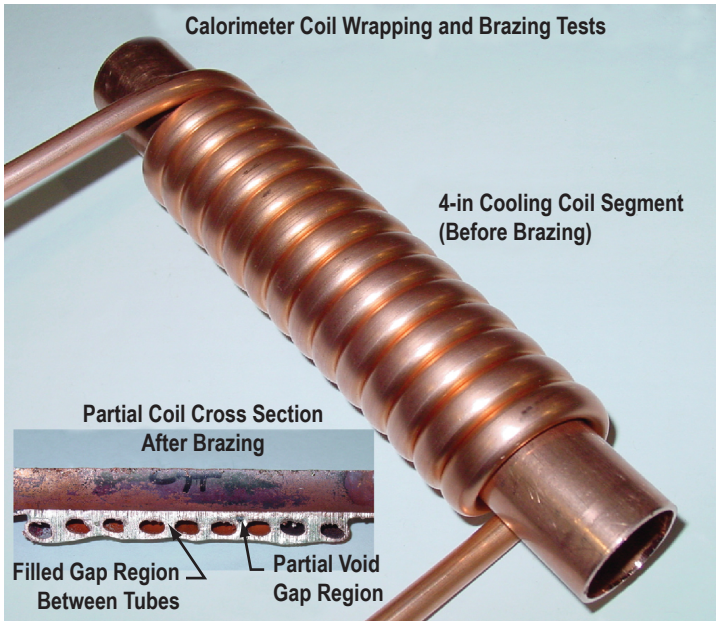

Figure 8. Brazing development testing for coil-type calorimeter design.

3.3 Calorimeter Power Measurement Uncertainty Estimate

To examine the uncertainty impacts of the flow meter and temperature instrumentation on measured heat pipe power, a rough uncertainty analysis was performed. The objective was to verify that readily available off-the-shelf hardware components could be used to obtain data with an uncertainty level of 5% or better. Details of this analysis are provided in appendix K, which compares various configurations including the use of paddle-wheel and magnetic-type meters for flow measurement, and single-point thermocouples and differential temperature meters for temperature measurement. The paddle-wheel/thermocouple configuration represents the cheapest approach, whereas the magnetic meter/differential temperature is the most expensive. Table 8 summarizes the results of this initial assessment, which indicates that an uncertainty of better then 5% is achieved for all instrumentation configurations examined.

Table 8. Summary of calorimeter power uncertainty with various instrumentation configurations.

Instrumentation Configuration	Uncertainty in Calorimeter Power (%)
Paddle Wheel With Thermocouples	4.2
Paddle Wheel With Differential Temperature	3.3
Magnetic Flow Meter With Thermocouples	2.9
Magnetic Flow Meter With Differential Temperature	1.3

The final selection of measurement devices was performed based on a combination of cost and durability (capable of lasting up to 3 years). Paddle-wheel-type flow meters cost approximately $1,400 each, magnetic meters cost up to $2,400 each. Differential temperature measurement units can range from $1,000 to $2,000 each, depending on range and accuracy. The paddle-wheel-type flow meters also offer an integrated temperature and pressure measurement in a single package. The final decision was to use magnetic flow meters with thermocouples to determine the calorimeter coolant temperature rise. This approach provides a low uncertainty without undue cost impact and good long-term reliability (no moving parts).

4. RADIO FREQUENCY HEATING SYSTEM

A contract was awarded to Fluxtrol, Inc. for the RF design, engineering details, and fabrication of both the inductive coil assemblies and interconnecting busswork. The contract was terminated at the completion of the inductive coil RF design and just prior to starting the detailed engineering; no hardware components were procured. A closeout summary detailing the RF design for each of the four coil assemblies is provided in appendix L. The RF inductive coil assemblies were required to provide the heat pipe evaporator nominal power levels, specified in table 9, while operating in a reduced pressure (75 torr) ultra-high-purity He/Ar environment for a period exceeding 3 years.

Table 9. Baseline heat pipe life test matrix.

Test Identifier	Power Level (W)	Heat Pipe Temp (K)	Gas Gap Mixture	Gas Gap Width (in)	Number of Heat Pipe Units	RF Coil Cluster Assembly
G-Series	3,000	1,273	He-32%Ar	0.025	7	1 and 2
F(–4)	5,000	1,273	He-6%Ar	0.025	1	4
F(–3)	1,000	1,273	He-32%Ar	0.103	1	3
F(–2)	3,000	1,373	He-32%Ar	0.031	1	2
F(–1)	3,000	1,173	He-32%Ar	0.021	1	2
F(0)	3,000	1,273	He-32%Ar	0.025	1	2
F(1)	2,000	1,223	He-32%Ar	0.037	1	3
F(2)	4,000	1,223	He-32%Ar	0.017	1	3
F(3)	2,000	1,323	He-32%Ar	0.046	1	3
F(4)	4,000	1,323	He-32%Ar	0.02	1	3

It was noted that three of the four assemblies were comprised of five inductive coil elements, forming a cluster arranged in a pentagonal series configuration. The interaction between these coils and neighboring components was modeled with Flux 2D software (marketed by CEDRAT Technologies). As a baseline, all coils are equipped with flux concentrators (Fluxtrol 50 material) to minimize coupling between neighboring coils and components, such as the calorimeter. The flux concentrator also provides a more symmetric and uniform power profile in the heat pipe evaporator, both axially and circumferentially. While the RF inductive coils provide the heat pipe evaporator power input, the final heat pipe operating temperature is set by the water calorimeter unit, which regulates the temperature using a static gas gap and coolant flow to maintain a specific power balance. An additional parameter affecting the power balance of RF cluster assemblies 2 and 3 is a variation in thermal loss due to different heat pipe operating temperatures. However, this loss is estimated to be approximately 2% of the total power load and not worth complicating the design of the inductive coils to compensate. A summary of the operational conditions for each of the RF assemblies is listed in table 10.

Table 10. Summary of RF inductive coil assembly layouts.

Configuration	Number of Heat Pipes	Total Heat Pipe Power (W)	Required RF Power With Estimated Loss (W)	Maximum Voltage (V)	Heat Pipe Power and Inductor Turns
Assembly 1	5	15,000	26,476	180	3,000 W—three turns
Assembly 2	5	15,000	26,476	180	3,000 W—three turns
Assembly 3	5	13,000	23,713	212	1,000 W—three turns 2,000 W—four turns 4,000 W—five turns
Assembly 4	1	5,000	8,190	60.6	5,000 W—five turns

To simplify both fabrication and setup of the inductive coils, the layout was standardized to three baseline coil geometries that included designs for three-, four-, and five-turn configurations. The number of inductor turns was minimized to reduce the required voltage to drive the RF coils; cluster assembly 3 had a maximum voltage drop of 212 V due to the mixture of three-, four-, and five-turn coils. The design gap width between the inductive coil and the heat pipe was set to 6.4 mm for all assemblies, providing a factor of 2 against the breakdown voltage estimated at ≈450 V (discussed in app. L). Powering each of the three five-coil RF assemblies would be a 50-kW Inductoheat SP16 solid-state RF power supply. The single-coil RF assembly would be powered by a Flexitune 15-kW RF power supply. A closed-loop water circulation system provided waste heat removal for the power supplies, busswork, and inductive coils.

5. HEAT PIPE DEVELOPMENT ACTIVITY

The development process for the Mo-Re refractory metal heat pipes was a two-step process: (1) Selection of a vendor for fabrication of heat pipe wicks and envelopes, and (2) final assembly of the complete units. The second step would involve heat pipe filling and closeout operations to be conducted at MSFC.

As part of this process, tube, rod, and plate stock material was procured to both develop welding procedures and fabricate the final components. As expected, the Mo-44.5%Re material baselined for this project has a long lead time with plate and rod stock requiring 8 to 12 weeks for delivery and drawn tube stock (formed with tube shells) requiring up to 20 weeks.

5.1 Mo-44.5%Re Material General Welding Development

To perform the final heat pipe closeout activity at MSFC, it was necessary to establish reliable and repeatable electron beam (EB) welds using in-house equipment. There are a total of three circumferential welds identified in the planned heat pipe closeout approach. The most critical of these is a single weld pass used to cap the severed heat pipe fill stem, sealing the internal heat pipe volume after Na is added. The remaining two welds attach the secondary containment cap and support tube. A general EB welding development plan was assembled to address relevant equipment settings using bead-on-plate type weld samples, formed from PM Mo-44.5%Re material.

Welding characteristics are a key concern for the fabrication of refractory metal components. Molybdenum and its alloys tend to be significantly less ductile in the as-welded condition.[7] This phenomenon is generally attributed to interstitial impurity segregation to the grain boundaries (higher Re content alloy) and to the large recrystallized grain structure (low Re content Mo). Ductility improvements have been demonstrated for high Re content Mo-Re alloys (>41%Re) but very little property data exist for welded material.

Electron beam welding has received considerable attention for the joining of Mo alloys. Electron beam welding is performed in a consistently controlled high-vacuum chamber, so there is less opportunity for interstitial contamination. Tungsten inert gas (TIG) welding in an inert atmosphere represents a considerably more complex monitoring problem. Electron beam welding also inputs significantly lower amounts of heat into the base metal, which minimizes thermal stress and grain growth. Fine control of the EB diameter and the focused high power allows much smaller heat-affected zones and weld metal, as compared to gas tungsten arc (GTA) welding. Ammon and Buckman reported a ductile-to-brittle transition temperature (DBTT) of 180 K for GTA welded Mo-50%Re, as compared to 80 K for the base metal material.[8] The difference between the base metal and welded material in DBTT was thought to be controlled predominantly by the large grain size. Morito reported considerable bend properties at 77 K for EB welded Mo-50%Re.[9] Kramer and Moore both reported successful EB welding of Mo-41% to 44.5%Re for space-based power systems.[10,11]

The initial weld development was to examine microstructure, chemistry, and bend testing to determine the DBTT. Data on refractory metal alloys have shown that welding has a pronounced effect on the DBTT and that bend testing is an excellent criterion for assessing the low-temperature ductility. Tests were to be performed on Mo-44.5%Re plate material (0.04-in thick) fabricated by Rhenium Alloys, Inc. using the PM processes. Table 11 lists the chemical composition of the Mo-44.5%Re plate. The plate material average grain size of 6 was determined in accordance with ASTM E3–95 and E112–96, shown in the figure 9 micrographs. Microhardness was performed in accordance with ASTM E3–84 using a Vickers diamond indentor with a 500-g load for 15 s. The average microhardness was 282.3 ± 3.8 Vickers hardness number (VHN). This material information was supplied by Rhenium Alloys, Inc., and the full description is provided in appendix M.

Table 11. Chemical composition of the Mo-44.5%Re plate.

Element	Impurity	Element	Impurity	Element	Impurity
H*	2.53	Zn	<0.1	Pr	<0.01
Li	<0.005	Ga	<0.05	Nd	<0.01
Be	<0.005	Ge	<0.05	Sm	<0.01
B	<0.005	As	<0.05	Eu	<0.01
C**	17	Se	<0.05	Gd	<0.01
N*	4	Br	<0.05	Tb	<0.01
O**	12.5	Rb	0.05	Dy	<0.01
F	<0.05	Sr	<0.1	Ho	<0.01
Na	1.1	Y	<0.1	Er	<0.01
Mg	<0.01	Zr	<0.1	Tm	<0.01
Al	2.1	Nb	<0.1	Yb	<0.01
Si	0.43	Mo	55.85 wt%	Lu	<0.01
P	0.11	Ru	<0.01	Hf	<0.01
S	0.13	Rh	<0.01	Ta	<50
Cl	0.05	Pd	<0.01	W	80
K	15	Ag	<1	Re	Balance
Ca	0.63	Cd	<1	Os	<0.01
Sc	<0.005	In	<0.1	Ir	<0.01
Ti	<10	Sn	0.17	Pt	<0.05
V	0.09	Sb	0.05	Au	<0.5
Cr	10	Te	<0.01	Hg	<0.05
Mn	0.89	I	<0.01	Tl	<0.01
Fe	9.5	Cs	<0.01	Pb	<0.01
Co	0.25	Ba	<0.5	Bi	<0.01
Ni	6.7	La	<0.01	Th	0.007
Cu	0.65	Ce	<0.01	U	0.13

* Determined by inert gas fusion-thermal conductivity.
** Determined by combustion-infrared absorbance.
Unless otherwise indicated, elements were analyzed by glow discharge mass spectroscopy (GDMS).
Results in ppm (ppm = parts per million = mg/Kg); 0.1000% by wt = 1,000 ppm unless otherwise indicated.
Methods: ASTM E 1937-04, ASTM E 1409-97, ASTM E 1447-01, ASTM E 1941-98, and GDMS.

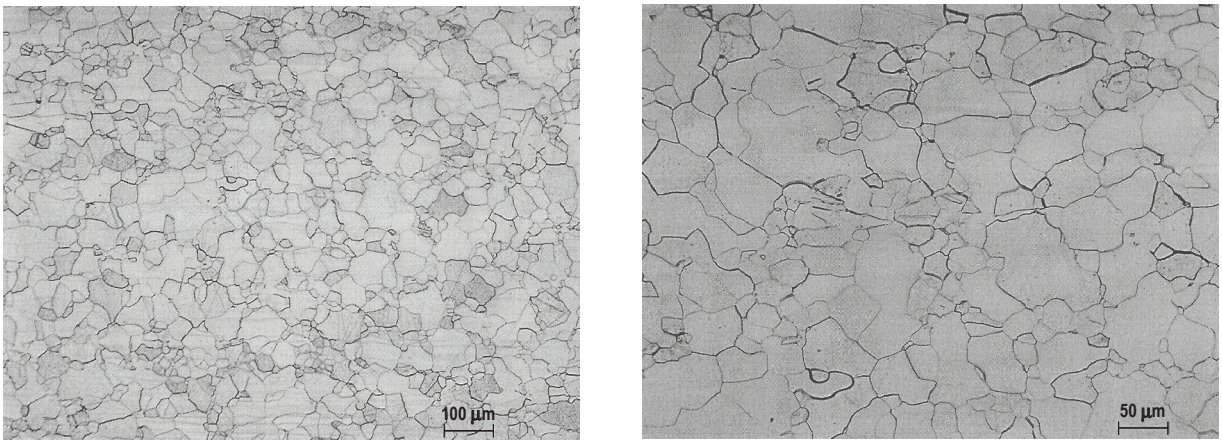

Figure 9. Micrographs of PM Mo-44.5%Re plate.

To perform EB welding evaluations, a series of bead-on-plates trials were planned, followed by bend testing of the samples. The weld fixture was ≈1.5 in long and consisted of a base block and two clamps, as illustrated in figure 10. The Mo-44.5%Re test samples were prepared by electrodischarge machining into blanks, measuring 0.5 in wide by 1 in long, followed by a chemical cleaning process as described in appendix N. The approach was to evaluate welding parameters over a range of values (such as current, voltage, spot size, and speed) by adjusting them with respect to as-welded ductility, microstructure, hardness, and chemistry. The effect on ductility will be measured by the maximum bend angle (up to 90 deg) at 77 K until failure occurs. Chemistry and microstructure results, such as grain size of the weld metal and heat-affected zone, will be evaluated as needed to optimize parameters. If necessary, subsequent postweld annealing and tensile testing would be conducted on optimized welds with the best ductility and microstructure. Due to project cancellation, this activity was terminated after fabrication of the test specimens and holding fixture; no welding trials were performed.

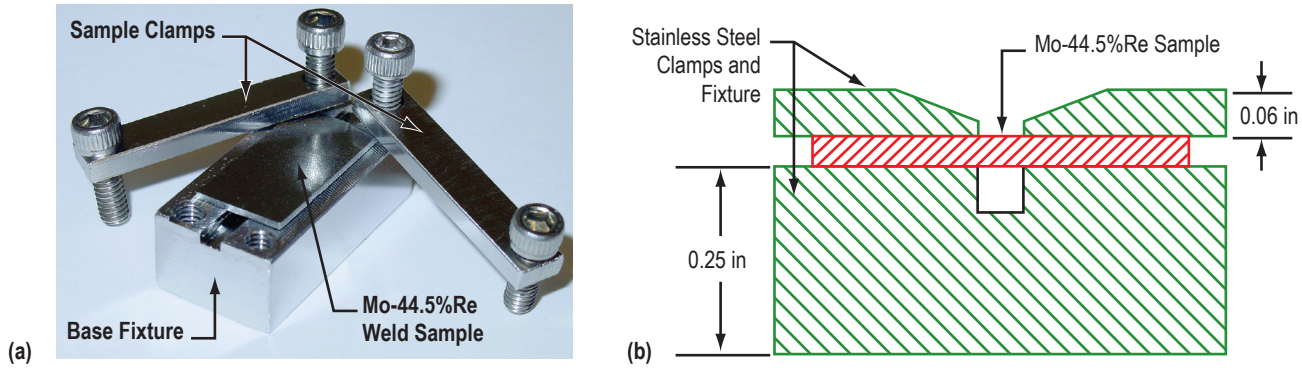

Figure 10. EB welding fixture and sample setup.

Sample weld testing was to be conducted using a general matrix, such as that shown in table 12, in which the parameters are varied about a previous experience base. Typical EB weld parameters found in the literature[9] are as follows:

- Accelerating voltage: 50 kV
- Primary beam current: 50 mA
- Welding speed: 30 mm/s.

Table 12. General EB weld development matrix.

Trial	Voltage (kV)	Current (mA)	Speed (mm/s)	Response Factors		
				Bend Angle @ 77 K	Microstructure	Chemistry
1	1	1	1	–	As Needed	As Needed
2	2	1	1	–	As Needed	As Needed
3	1	2	1	–	As Needed	As Needed
4	2	2	1	–	As Needed	As Needed
5	1	1	2	–	As Needed	As Needed
6	2	1	2	–	As Needed	As Needed
7	1	2	2	–	As Needed	As Needed
8	2	2	2	–	As Needed	As Needed

To eliminate a variable, the EB focus would be set at the smallest possible spot size for each of the trials. After determination of the best welding parameters, a final set of material evaluations would be made at higher temperatures with weld comparison to base metal performance. The use of potential heat treatment could also be examined at this point. Table 13 provides a general test matrix outlining this approach.

Table 13. Final Mo-44.5%Re test matrix.

Sample	DBTT (Bend Test)	Tensile Testing		Chemistry	Hardness	Microstructure
		RT	1,473 K			
Base Metal	As Needed	2	2	1	1	1
Base Metal + Anneal	As Needed	2	2	1	1	1
As-Welded	As Needed	2	2	1	1	1
As-Welded + Anneal	As Needed	2	2	–	1	1

Figure 11 shows the setup of the base metal and as-welded samples that were to be bend tested using procedures developed by the Materials Advisory Board for ductile refractory metal alloys, as reported by Ammon and Buckman.[8] The base metal specimen and weld bead will be perpendicular to the rolling direction of the plate and axis of bending. The topside of the weld bead will be placed in tension. Base metal and optimized weld samples would be tested at multiple temperatures to determine the DBTT.

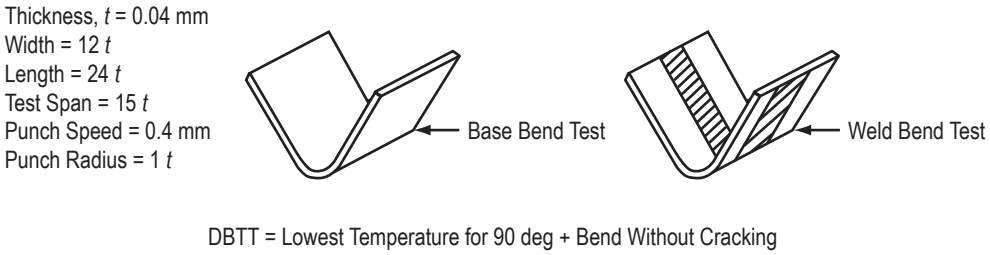

Figure 11. Bend test configuration.

For this project, it was planned to conduct bend test evaluations for both the base metal and welded samples onsite at MSFC and at Pittsburgh Materials and Technology, Inc.

5.2 Heat Pipe Wick and Envelope Development/Manufacture Activity

Manufacture of the refractory metal heat pipes was awarded via competitive procurement to Advanced Methods and Materials, Inc. (AMM), which included development and fabrication activities to produce the wick element, envelope, cleaning, and final assembly with installed wick. As a part of this activity, AMM was to procure all Mo-44.5%Re material and the government was to provide the wick screen material. Due to project cancellation, all contracts were terminated and procured raw material supplied to MSFC.

Prior to cancellation, AMM forcused on developing a method suitable for forming the cylindrical wick element from seven layers of 400 × 400 weave screen material, with a Mo-5%Re composition and a wire diameter of 0.001 in. This mesh material, shown in figure 12, was on hand from a previous government program. After receipt of the material, several chemical composition tests were performed to determine base material impurities in the as-received condition, after chemical cleaning, and lastly after vacuum hot isostatic pressing (HIP).

Analytical results of the Mo-5%Re screen mesh show that, for the ‘as received condition,’ there is an oxygen weight percent (wt%) of 0.37 and nitrogen wt% of 0.136 for the material. After chemically cleaning the screen material, the oxygen wt% was reduced to 0.08 and the nitrogen to 0.031, indicating that a majority of these elements were absorbed on the surface. After the HIP process to form the wick structure, material chemistry shows that the final wt% concentration of oxygen is 0.08 and that of nitrogen is 0.01.

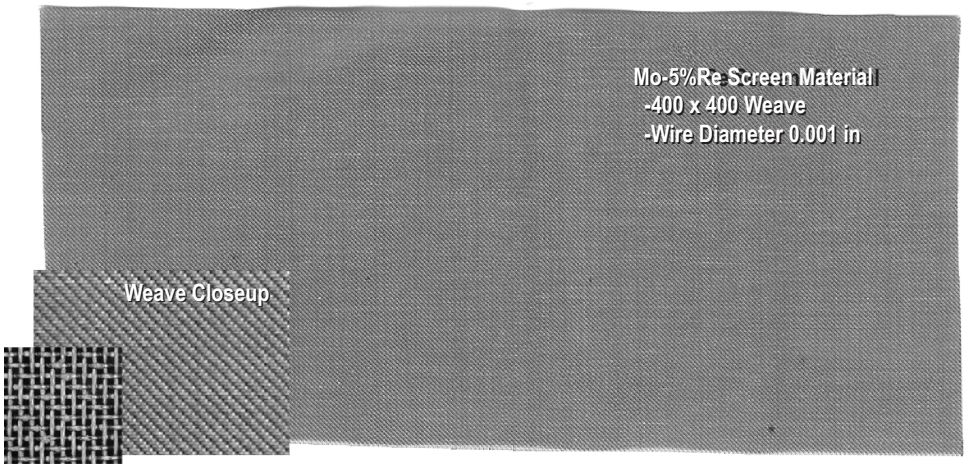

Figure 12. Mo-5%Re screen material.

AMM identified several approaches to fabricate the wick, ranging from a room temperature (RT) swaging/drawing technique to HIP. A HIP procedure was successfully used to bond stainless steel (SS) and niobium (Nb)1%Zr heat pipes, fabricated for MSFC on a prior program. The initial direction was to start with low-temperature techniques to minimize the chance of ductility loss due to recrystallization, which raises the DBTT for this alloy (an issue resulting from the low Re content of the 5% material). A number of trial tests were performed by swaging/drawing short wick sections, using mandrel and sheath materials such as Zr, titanium (Ti), and mild steel. After drawing, acid was used to dissolve the mandrel material from the final wick. The type of acid depended on the mandrel/sheath material—hydrofluoric acid for Ti, and Zr and hydrochloric acid for mild steel. Although Ti would be a preferred mandrel material, especially if using high processing temperatures since it would getter oxygen and other impurities from the screen material, the initial drawing/swaging trials indicated that mild steel provided a better final wick product. All three encapsulant metals—iron (Fe), Zr, and Ti—produced similar quality wicks; however, a very slight reduction in weight was observed for Ti and Zr, suggesting some interdiffusion between the Ti/Zr and the Mo-Re wick material. Because there was no interaction between the mild steel and the Mo-Re, the steel was selected over the two reactive metals. Results of the low-temperature forming techniques indicate that a strong mechanical bonding between the screen layers was formed; however, there was no diffusion bonding of the material to keep it from fraying or pulling apart. Figure 13 shows one of the drawn/swaged samples that was produced.

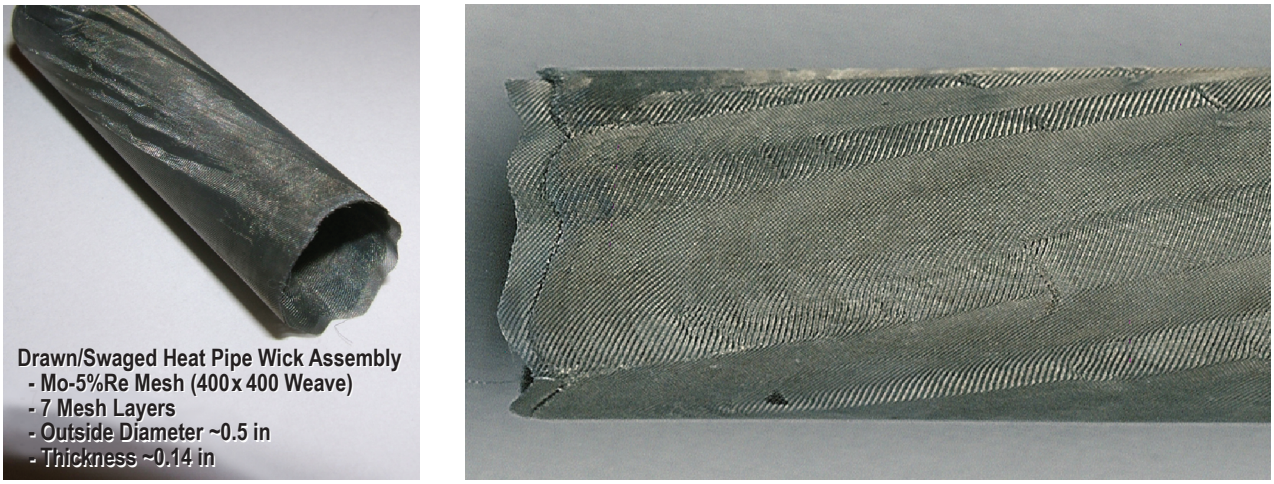

Figure 13. Room-temperature swaged wick element sample.

The layers were tightly packed, retaining considerable ductility and allowing the assembly to be flexed/deformed to a considerable extent. The surface was fairly smooth with the exception of a length-wise ripple pattern, an artifact of the drawing processing which could be resolved. It was noted that the layers could be separated if small tools were used to pry apart and grasp the exposed layer edges. This could be a concern when considering the long-term operation of the heat pipes for this project (thermal cycling and possible chemical attack loosening the bonds between the layers). It was therefore decided that a HIP technique would be evaluated to examine if a diffusion bond could be achieved without a significant loss of ductility.

A 6-in-long wick sample was fabricated to evaluate the HIP technique. The mesh material was wrapped on a mild steel mandrel with sheath and initially drawn to achieve the required wick thickness (≈0.014 in). The mandrel was evacuated, sealed by EB welding, and placed in a HIP chamber. This HIP process included a 1.5-hr ramp to a temperature of 950 °C and a pressure of 30,000 psi, at which it was held for 1 hr. The pressure was released and the furnace turned off to cool over ≈2 hr. The HIP temperature was kept as low as possible to minimize the amount of recrystallization (maximize ductility) yet still provide a satisfactory diffusion bond. The mandrel and sheath assembly were dissolved using hydrochloric acid. The final wick product is shown in figure 14. The outer surface still retains a slight pattern (artifact of the drawing process). This wick assembly is significantly more rigid when compared to the drawn/swaged version and behaves more like a solid piece of tubing, with no visible bond line on the external surface (outer layer). The tube can be flexed very slightly if squeezed, so some ductility has been retained (the wick was not flexed to failure); however, it cannot be deformed to the extent demonstrated by the drawn/swaged sample.

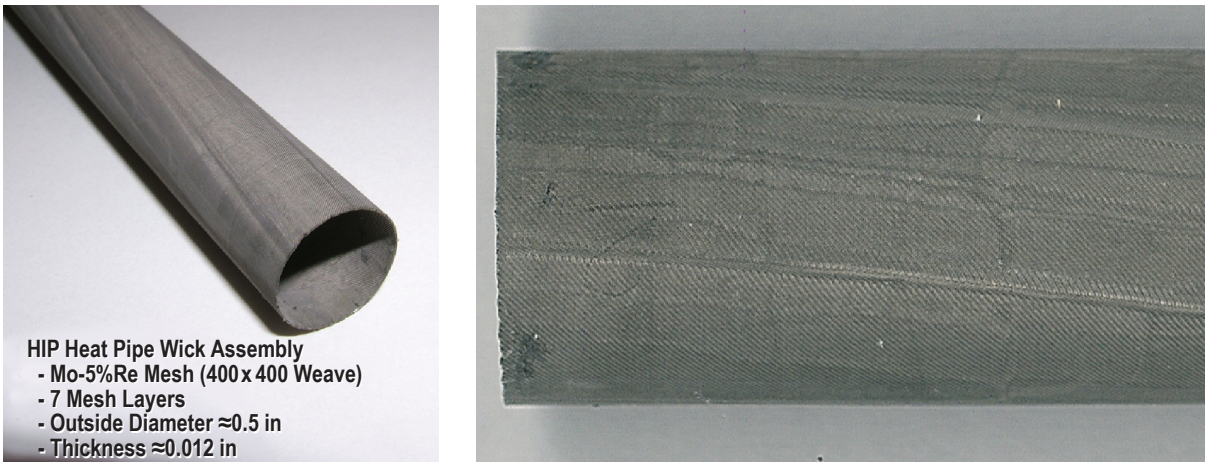

Figure 14. Hot isostatic pressed wick element sample.

A concern with the HIP process was that it could completely close off the screen pores, resulting in a solid cylindrical tube rather then a porous wick structure. To verify the product, it was evaluated by bubble-point testing to determine final pore size. The bubble-point test made use of ethyl alcohol and high-purity He, with results indicating an ≈22-μ wick pore radius, well within the required specification of 16 to 32 μ.

Overall, the final HIP wick element had good geometric consistency and was vastly superior to the RT swaged version, which has the potential to unravel since it is only mechanically bonded. The HIP wick produced in this test was approximately half the length of what would be required for the life test heat pipes. No issues or problems are expected with proceeding to the full-length wick, and the success of the HIP technique was a major project accomplishment. The PM Mo-1 44.5%Re rod stock supplied by Rhenium Alloys, Inc., was provided to MSFC; chemical composition is provided in appendices O and P.

6. SODIUM PURITY EVALUATION USING VANADIUM WIRE EQUILIBRATION

An investigation into the experimental assessment of Na purity in heat pipes has been undertaken. The vanadium (V) wire equilibration method has been identified as the technique of choice to evaluate Na purity within the heat pipe by means of a high-temperature oxygen equilibration process. To support the application of this technique, procedural development governing the processing steps and checkout testing operations for the V wire setup were undertaken with consideration of previous investigations.[12–14] In addition, acquisition of the hardware components and chemicals required to prepare the samples according to the V wire equilibration technique, per ASTM C 997–83,[15] were completed. The Na stock currently in-house at MSFC will be used for all evaluations, as this material was baselined for use with the accelerated life test heat pipes.

6.1 Basic Hardware Setup

In the current approach, the V wire element is sized to fit within the volume constraint of the heat pipe fill stem. The V wire selected has a diameter of 0.25 mm and requires a length of 100 mm to achieve the desired oxygen content sensitivity. The V wire is mounted to an Mo alloy wire bow that is inserted into the fill stem. The bow is held in place by a combination of spring force and a hook (holding tab) that is positioned between the valve body and the end of the fill stem. Figure 15 shows the wire bow layout and a typical installation (a window cut from the sample 0.25-in-diameter fill stem to allow viewing of the V wire).

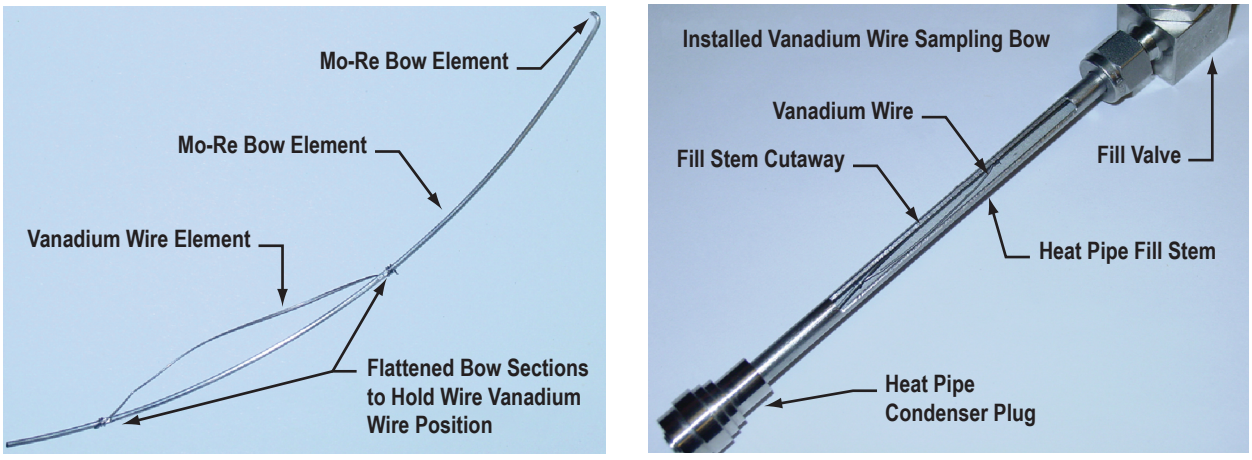

Figure 15. Vanadium wire support and insertion concept using a Mo-alloy bow.

For the Vanadium wire evaluation testing, a nickel (Ni) sample tube was selected to simulate the Mo-44.5%Re fill stem. (Nickel was identified as the containment material in the ASTM specification.) Figure 16 shows the final sample fixture setup, configured for verification testing. The assembly consists

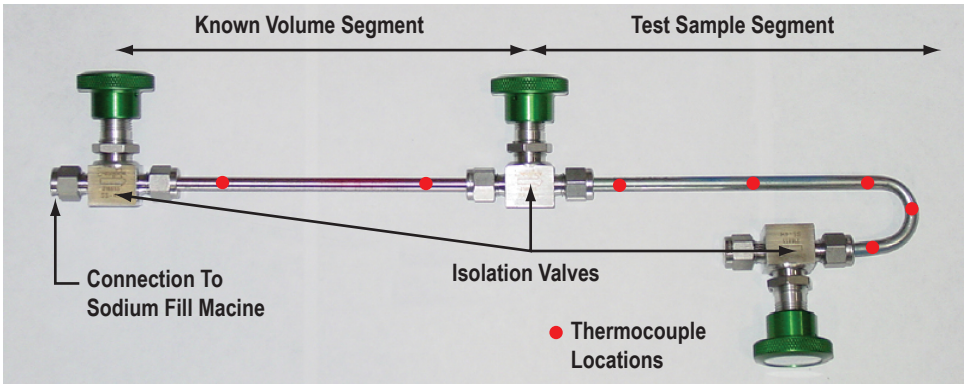

Figure 16. Layout of V wire/Na sampling test setup.

of three isolation valves and seven thermocouples to control and monitor the quantity and position of the Na in the test segment. The Na is initially loaded into the known volume segment, so a precise charge can be determined, and then transferred into the test sample segment. The sample segment has additional void volume to account for Na expansion during heating to the 750 °C equilibration temperature; the Na would be transferred at a temperature of ≈150 °C during filling to minimize oxygen solubility. Prior to filling, all components undergo an extensive cleaning and vacuum bakeout process to minimize the possibility of contamination.

6.2 General Preparation and Operations

To test the operational procedures for this technique, a number of components were processed up to the point of filling the test segments with Na. The initial step was to chemically clean all components (SS valves, Ni tubing, and Mo wire) with pickling procedures to remove surface oxide layers and organics. Appendix Q lists the chemicals, concentrations, and mixtures used for each of the materials. Chemical cleaning was followed by vacuum bakeout of the Ni tubing using a small vacuum furnace system at a pressure in the 10^{-6} torr range and a temperature of 750 °C, the projected equilibration temperature. The SS transfer valves were vacuum baked to 225 °C at a pressure of 10^{-6} torr; this temperature is sufficient due to the low operating temperature during transfer. (The valves will not be attached during equilibration.) The V and Mo wire samples were prepared using an electroetching unit; the V wire was not vacuum baked to avoid gettering oxygen. Vanadium wire samples were etched from an initial diameter of 0.25 to 0.22 mm, producing a clean and oxide-free, lustrous surface appearance. The Mo wire diameter was not monitored, since it functions only as a structural support element. An outline of the operations used for preparation and equilibration testing is provided in appendix R. A total of seven sample V wire segments were processed to test the operations and promote familiarity with the equipment and handling. It was planned that three complete Na equilibration tests would be performed; therefore, an additional three V wire samples and three Mo bow wires were also prepared. All of these items were stored in clean, inert-gas-filled, sealed containers. The results of this activity are documented in appendix S.

To accurately determine the oxygen increase in the V wire resulting from being immersed in a quiescent liquid-Na bath at high temperature, an analysis of the initial and final oxygen concentration in the V wire would be required. The LECO Corporation analysis technique was identified in the ASTM

specification as the appropriate test method. For the heat pipe application, the analysis must be accomplished using a minimal amount (20–30 mg) of V wire. The length of V wire is proportioned to the volume of Na used in the test. This poses an operational concern for the LECO method, which has an industry standard minimum mass requirement of 1 g. Discussions with the LECO Corporation indicate that the preferred 1-g mass provides guaranteed accuracies of 0.05 ppm Na and 0.05 ppm O. Smaller material quantities can be used, however, the measurement uncertainty increases. For materials quantities in the range of interest for the heat pipe Na equilibration, testing accuracy will drop into the 10 to 20 ppm O range. This resolution should be sufficient, because the V-O concentration is expected to increase on the order of 100 to 1,000 ppm during equilibration. For example, (from fig. 17) an initial Na-O concentration ($C_{\underline{O}(Na)I}$) of 20 ppm equilibration produces a final Na-O concentration ($C_{\underline{O}(Na)F}$) of ≈0.04 ppm and a final V wire oxygen concentration ($C_{\underline{O}(V)}$) of ≈900 ppm. This analysis was performed assuming that the V wire segment is immersed and equilibrated in Na using a configuration geometrically consistent with the heat pipe fill stem.

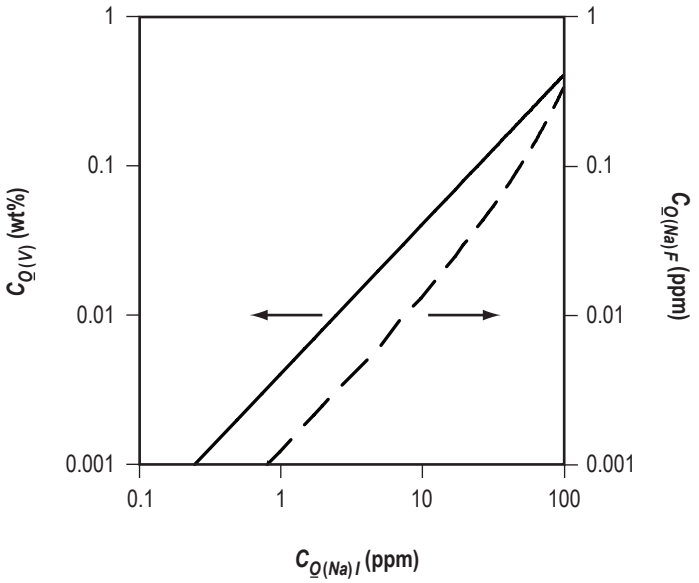

Figure 17. Oxygen concentrations: Na initial, Na final, and V wire.

To evaluate the LECO method, two V wire control samples were prepared and sent to LECO to undergo oxygen determination analysis. These samples, identified as control 6 and control 7 (as listed in app. S), had masses of 23 and 26 mg, respectively. The project was terminated prior to performing material analysis on these samples.

Prior to implementing the approach on actual heat pipes, it was planned that three complete test cycles (Na fill, equilibration, and LECO analysis) would be performed using the samples identified as test 1, test 2, and test 3 (as listed in app. S). Once the operations were found to provide satisfactory results, a complete SS test heat pipe unit would be evaluated. However, due to termination of this project, all activity has been closed out prior to filling the first Ni test units with Na.

7. SUMMARY

The accelerated heat pipe life test project was cancelled due to program selection of a gas-cooled reactor concept. As a result, all activities have been closed out using the most logical approach to terminate procurements and recover costs where possible. A majority of the hardware procurements had been placed for the laboratory equipment required to perform the tests, including fabrication of the Mo-44.5%Re heat pipe units. This Technical Publication (TP) provides details for the specific test systems that included calorimeters, RF inductive heaters, and Na oxide impurity activity. Significant progress was made related to the heat pipe fabrication procurement. The vendor, AMM, had procured material (rod, tube, and plate stock) and successfully manufactured an annular wick structure. This wick was fabricated from Mo-5%Re screen material (existing NASA stock) by a HIP technique (950 °C for 1 hr at 30,000 psi). The final product had a pore radius of 22 μm, and still retained significant ductility. Low-temperature drawing/swaging techniques were also tested, producing wick structures in which the screen layers were only mechanically bonded. This simple technique was found to be unacceptable because there is a risk of layer separation; this was not an issue with the HIP approach. At the time of project termination, no technical showstoppers were encountered, either with heat pipe development or laboratory equipment procurement/layout. The planned focus for this test project was to implement a methodology to establish heat pipe material system life expectancy consistent with a limited schedule, budget, and material availability while conducting comparatively few tests (16 units for this project) to study key variables. Data were expected early in the program (within 6 months of starting the first heat pipe), providing early indications of the aging effect. Additional data obtained over the course of the planned 3-year operation would build confidence in extrapolationing corrision and provide insight into possible random manufacturing and processing defects.

APPENDIX A—LAMINAR FLOW WATER CALORIMETER UNIT SPECIFICATION

Request for Information for Materials and Fabrication of Calorimeter Assemblies Integrated Financial Management Program Procurement

Delivery 6–8 weeks after receipt of order (ARO)

Quantity—16 units

Title—Copper Alloy Laminar Flow Water Calorimeter Units for use in a Vacuum/High-Purity Inert Gas Environment. Request information for both fabrication materials, as well as complete manufacturing of the calorimeter units.

Specification for Water Circulation System

Laminar flow water calorimeter units fabricated from a copper alloy are used to absorb heat energy from a research application. The calorimeters consist of three concentric tubes forming the primary water film flow gap/path and the water return path, shown in figures 18–20. The calorimeter surrounds a process component that operates at high temperature, providing the heat load. Power is transferred to the calorimeter from the process component, a small noncontact gas conduction gap that allows for a large temperature gradient in a short distance. Critical calorimeter dimensional constraints necessary to meet test power and temperature requirements include the following:

- The gas gap distance between the process component surface and the ID of the calorimeter channel tube regulates the power transfer between the process component and the calorimeter. The low-temperature calorimeter cannot come into physical contact with the high-temperature process component, hence the required dimensional tolerances.

- The water film flow gap between the OD of the calorimeter channel tube and the ID of the shell tube controls the water flow regime, maintaining laminar conditions.

- The outermost cover tube should have sufficient ID to provide a water return path approximately an order of magnitude larger than the water film flow gap.

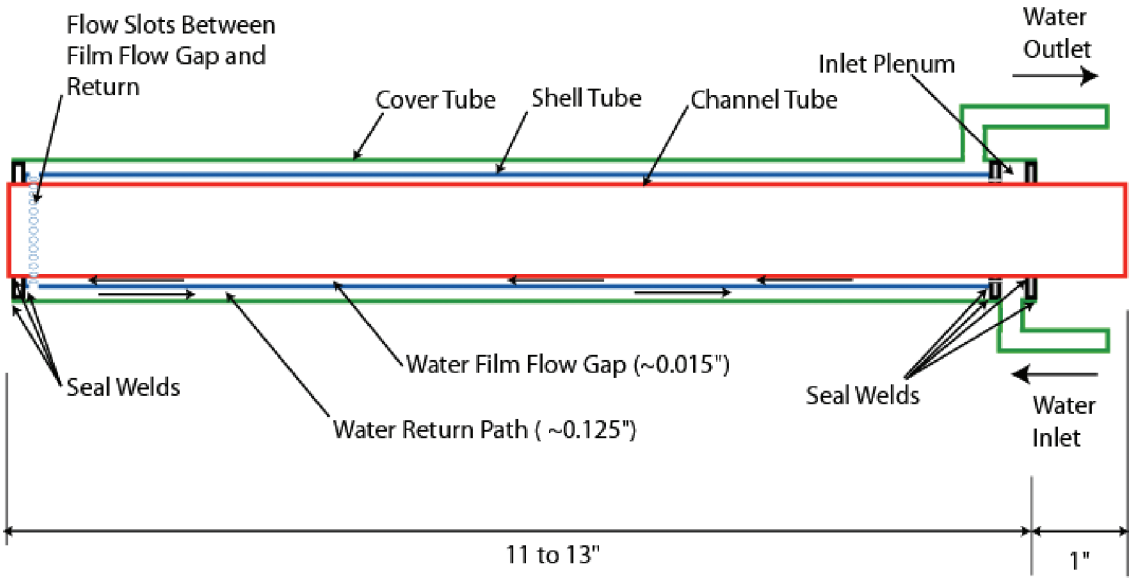

Figure 18. Conceptual calorimeter design.

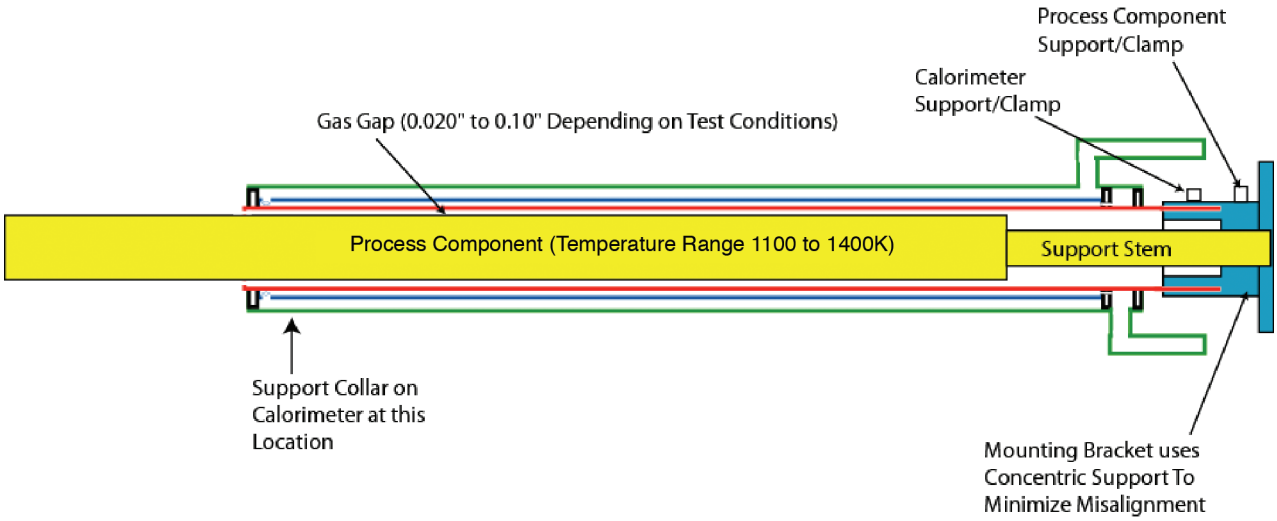

Figure 19. Conceptual process application/calorimeter with mounting setup.

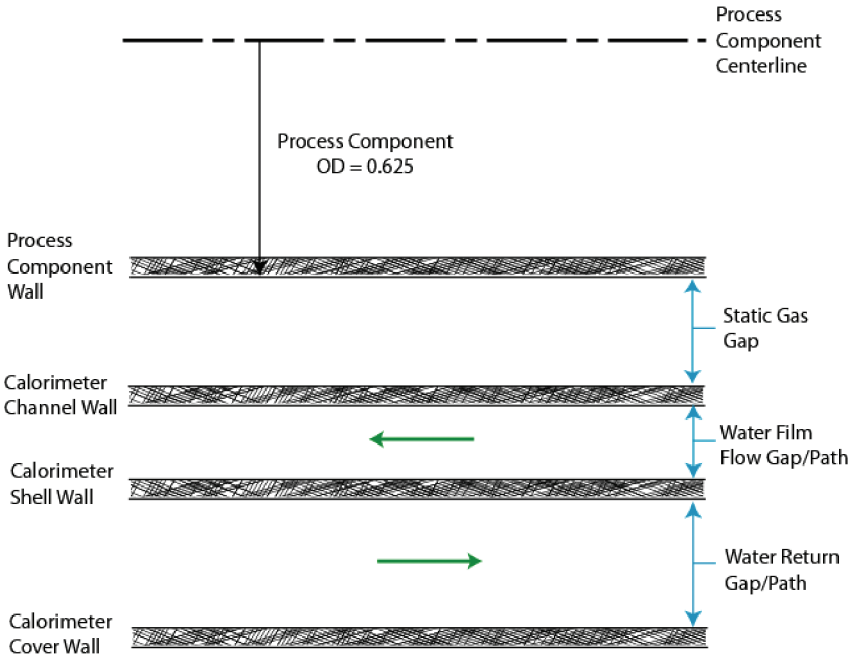

Figure 20. Calorimeter tube layout nomenclature.

The initial engineering drawings of a calorimeter unit are shown in figures 21 and 22. The calorimeter unit is 11–13 in long and currently planned to be fixed at the clamped end with the free-cantilevered section supported by a collar. Specific specifications include the following:

- High-strength (durable) alloy with good thermal conductivity and an excellent ability to hold tolerance. Copper alloy C122 is an option, but other alloys should be suggested for consideration.

- The unit will be operated in a very clean test chamber with either vacuum or low-pressure purified inert gas (He/Ar) environments; therefore, it should have a good, clean external finish (32–64 μin) with no virtual leaks and minimal outgassing properties. Internal coolant will be filtered water with a conductivity between 1 and 40 μ*S*/cm to support operation of a magnetic-type flow meter.

- The calorimeter will be assembled with an all-welded construction to minimize the potential for leakage. This welding should be performed in an inert environment to minimize oxidation and potential for trapping of contaminants in the calorimeter welds. During the assembly process, the primary flow gap width and ID of the channel tube will be monitored to verify compliance with the required sizes. Small tabs that will not interfere with the fluid flow can be used in the primary coolant flow path, between the channel and shell tubes, to assist in maintaining the dimension. The ID of the channel tube will be honed, if necessary, after welding to achieve the required ID.

- Leak checking will be performed to verify leak tightness of all calorimeter assemblies. The assemblies will be checked with an He mass spectrometer leak detector with a sensitivity capable of detecting leak rates of 1×10^{-10} std-cc/s of He or lower. All components (100% of the calorimeter units) will be leak tested and any defective units rejected.

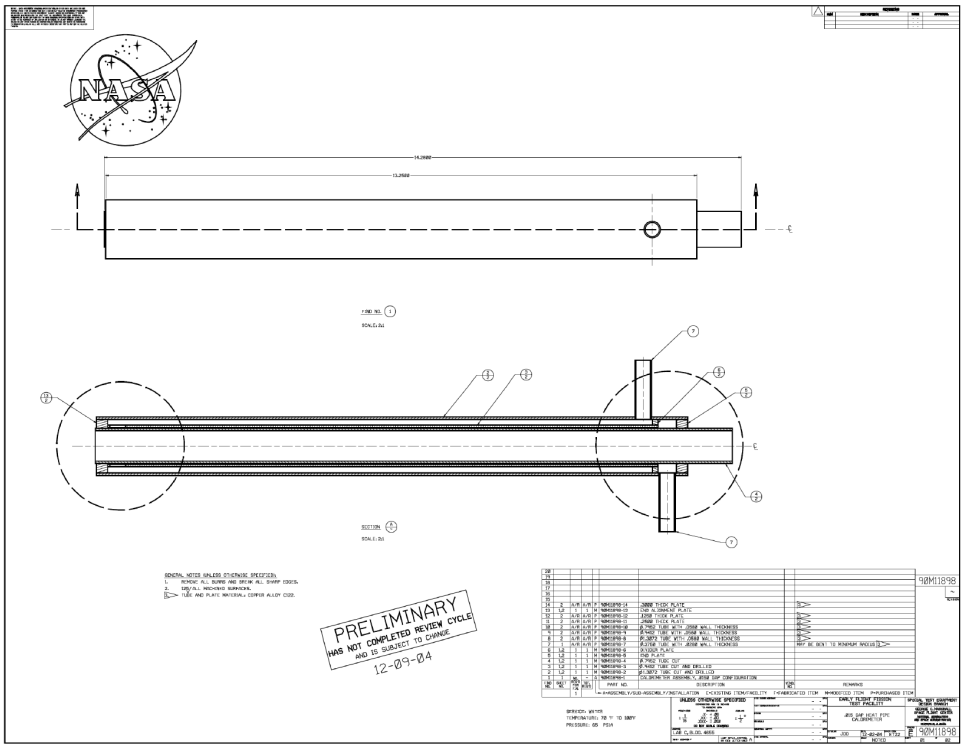

Figure 21. Initial calorimeter concept—engineering design layout.

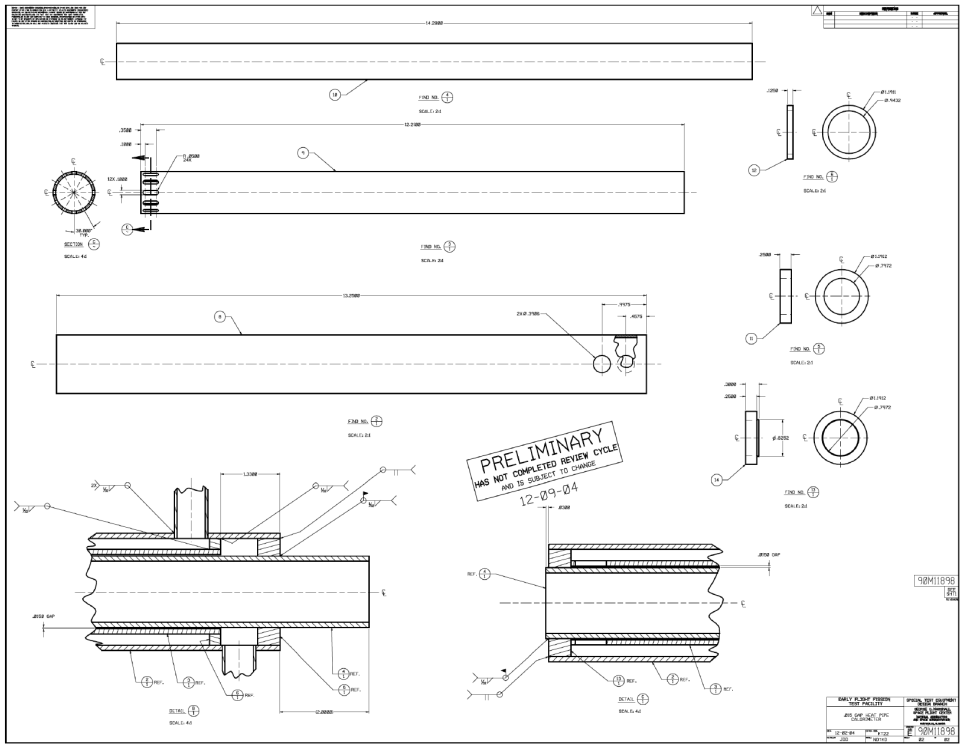

Figure 22. Initial calorimeter concept—engineering design parts detail.

- Water feed lines will be 0.37-in OD by 0.35-in wall nominal copper feed lines with 36-in stub lengths. Feeds are welded to the calorimeter manifolds.

- Material stock and final assembly of the calorimeter should conform to the following target requirements:

  – Tubing wall thickness variation: ±0.001 in.

  – Tubing diameter variation: ±0.002 in.

  – Tubing diameter ovality variation: Cannot exceed ±0.002 in at any cross section.

  – Permissible straightness: 0.002 in over the length of the calorimeter.

The calorimeter length is estimated at 11 to 13 in, based on preliminary design analysis. The calorimeter unit is supported, in cantilever fashion, at one end with a support and at the other end, as indicated in figures 18 and 19, by a 1-in extension of the inner channel tube. Tight tolerances are required to prevent the calorimeter from touching the very hot process component. There are 10 different calorimeter geometry types required to meet the research objectives. Each is composed of a single-channel tube, shell tube, and cover tube with dimensions and quantity as provided in table 14. The following assumptions were made in performing the thermal analysis and generating this table:

- Current design makes use of a constant wall thickness tube for all calorimeter tubes (baseline wall thickness 0.058 in). This approach assumes that the tube manufacturing process is a drawing technique, in which the draw dies can be adjusted to provide the required OD/ID dimensions.

- The primary coolant film flow gap width baseline for all calorimeters is held at 0.015 in.

- The return coolant flow gap width baseline for all calorimeters is held at 0.125 in.

- Inspection/cleaning—Each completed calorimeter unit should be tested for straightness and dimensional consistency along the inner bore (diameter/ovality). Any final machining to bring units into tolerance, remove burrs, finalize the surface, etc., should be performed. Each of the calorimeter units will be cleaned externally and internally by flushing, to remove debris and surface contaminants.

- Operational duty—Calorimeters will be operated in an around-the-clock fashion for 3–5 years.

- Other considerations for tubing selection and dimensions—The use of standard or specialized tube sizes with machining to meet the final geometry is also an acceptable option. If standard/specialized sizes are used, some additional variation can be allowed in the gap widths for the water film flow gap/path and water return path as follows:

  – Water film flow gap (between the OD of the calorimeter channel tube and the ID of the shell tube) can range between 0.010 and 0.015 in.

  – Water return path can range to provide approximately a factor of 10 increase over the film flow gap width.Table 14. Tube sizes required for calorimeter layouts (all dimensions are in inches) for tubing material produced by drawn technique (or other).

Table 14. Tube sizes required for calorimeter layouts (all dimensions are in inches) for tubing material produced by drawn technique (or other).

Calorimeter Geometry	G	F(–4)	F(–3)	F(–2)	F(–1)	F(1)	F(2)	F(3)	F(4)	F(0)
Quantity	**7**	**1**	**1**	**1**	**1**	**1**	**1**	**1**	**1**	**1**
Process Component OD	0.625	0.625	0.625	0.625	0.625	0.625	0.625	0.625	0.625	0.625
Gas Conduction Gap Width	0.027	0.027	0.105	0.033	0.023	0.039	0.018	0.048	0.022	0.027
Calorimeter Channel Tube ID	0.679	0.678	0.835	0.690	0.670	0.702	0.661	0.720	0.669	0.679
Calorimeter Channel Tube OD	0.795	0.794	0.951	0.806	0.786	0.818	0.777	0.836	0.785	0.795
Calorimeter Channel Tube Wall Thickness	0.058	0.058	0.058	0.058	0.058	0.058	0.058	0.058	0.058	0.058
Calorimeter Shell Tube ID	0.825	0.824	0.981	0.836	0.816	0.848	0.807	0.866	0.815	0.825
Calorimeter Shell Tube OD	0.941	0.940	1.097	0.952	0.932	0.964	0.923	0.982	0.931	0.941
Calorimeter Shell Tube Wall Thickness	0.058	0.058	0.058	0.058	0.058	0.058	0.058	0.058	0.058	0.058
Calorimeter Cover Tube ID	1.191	1.190	1.347	1.202	1.182	1.214	1.173	1.232	1.181	1.191
Calorimeter Cover Tube OD	1.307	1.306	1.463	1.318	1.298	1.330	1.289	1.348	1.297	1.307
Calorimeter Cover Tube Wall Thickness	0.058	0.058	0.058	0.058	0.058	0.058	0.058	0.058	0.058	0.058

However, the gas conduction gap between the process component and the calorimeter channel tube ID must remain fixed as specified in table 14; therefore, the selection of the size used for the calorimeter channel tube must be able to meet the required dimensions after machining.

- The following information provides operational specifics regarding the expected flow and temperature conditions for the calorimeter, based on research requirements and a thermal analysis:

  – Water flow rates: Ranging from 0.1 to 1 gpm, depending on thermal load.

  – Power capacity: 1,000 to 5,000 W range.

  – Water temperature inlet: Expected range 15–30 °C.

  – Water temperature rise: Expected up to 40 °C.

  – Process component temperature: From 1,100 to 1,400 K.

  – Inert gas gap environment: He/Ar mixture at 1 to 2 psia.

  – Process component material: Mo-Re refractory metal.

  – Packaging: Calorimeter must be a modular design, since they will be packaged to test component clusters (fig. 23).

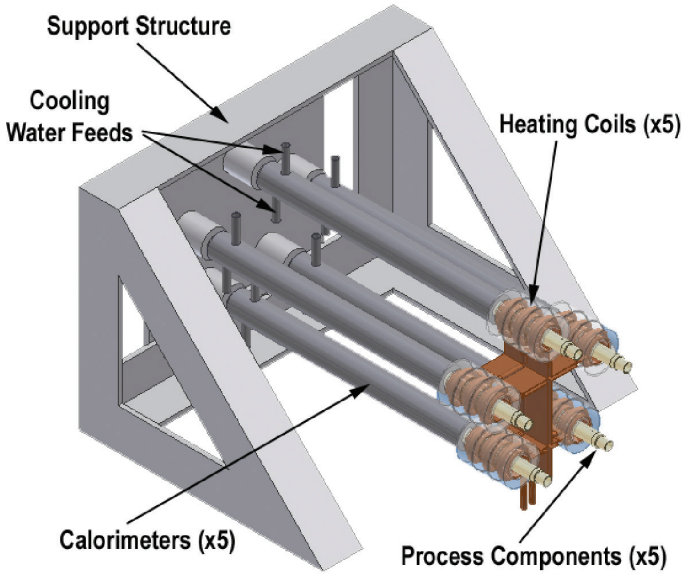

Figure 23. Calorimeter cluster arrangement.

- Additional information sought:
  - Copper alloy materials that provide a robust and durable calorimeter unit to better meet the goal.
  - Alternate calorimeter-type cooling designs that will provide the same function in a similar package (commercial).
  - Enhancement to the water film flow gap cooling channel design (improved heat transfer) with predicted thermal performance with known correlations.
  - Low-cost welded transition elements from copper alloy to SS to simplify routing the calorimeter water feeds out of the test chamber and avoid the use of mechanical fittings.

APPENDIX B—TWO-BAND OPTICAL PYROMETER SPECIFICATION

Specification for Procurement for Optical Pyrometer Temperature Sensors
Integrated Financial Management Program Procurement

Estimated delivery 4–6 weeks ARO

Title—Turnkey Two-Band Optical Pyrometer Temperature Sensors

Vendors:

- Ircon, Inc.
  7300 N. Natchez Ave.
  Niles, IL 60714
  Telephone: 847–967–5151
  POC: Randy Cutrara
  Telephone: 704–604–4165

- PEI Group
  2815 Winterberry Way
  Hampton Cove, AL 35763
  POC: William Burnette
  Telephone: 256–534–5949

- Mikron Infrared, Inc.
  16 Thornton Road
  Oakland, NJ 07436
  POC: Korhan Gazi
  Telephone: 201–405–0900

- Uni-Tech Engineering
  983 Yeager Parkway
  P.O. Box 510
  Pelham, AL 35124
  Telephone: 205–999–7983

- Omega Engineering
  One Omega Drive
  P.O. Box 4047
  Stamford, CT 06907
  Telephone: 203–359–1660

Quantity—17 complete units

Specification for Two-Band Pyrometer Units

Turnkey two-band optical pyrometer units, such as the Ircon® series/model 5R–1410 complete system or equivalent with the following specifications:

- Temperature range: 600–1,400 °C.
- Mode: Operates in one- or two-color (ratio) mode.
- Wavelength: Ratio mode (0.75–1.05 and 1–1.1 mm range). Single-color 1–1.15 mm.
- Focusing range: 13 in to infinity.
- Measurement spot size: 0.13-in diameter at 13 in and 0.24-in diameter at 24 in.
- Sighting method: Through lens, no filter.
- Response time: 10 μs to 60 s.
- Analog output: 4–20 mA.
- Analog input: 4–20 mA.
- Digital input/output: RS–485.
- Accuracy: 0.5% of reading plus 2 °C.
- Resolution: 1 K.
- Emissivity slope: 0.8 to 1.2.
- Repeatability: 0.1% of full-scale plus 1 digit (25 °C).
- Sensor rear panel control: Temperature, setup display, and keypad for independent configuration and operation.
- Operating voltage: 24 VDC.
- Operating temperature: Ambient 0–55 °C.
- Cable assembly: 25 ft.
- Weight: Under 4 lb.
- Mount: Universal two-axis support.
- Operators manual: Included.
- Normal operation: No cooling required.

APPENDIX C—WATER-COOLING PALLET SPECIFICATION

Procurement Specification for Water-Cooling Recirculation System
Integrated Financial Management Program Procurement

Estimated delivery 6 weeks ARO

Title—Turnkey Water-to-Water Heat Exchanger System (Recirculation Flow Separated from Plant Service Cooling Water) to Remove up to 100 kW from Test Hardware

Vendors:

- Thermo Electron Corporation
  Control Technologies Division
  25 Nimble Hill Road
  Hewington, NH 03801
  POC: Kathy Payne
  Telephone: 972–867–9769

- Fluid Flow of Georgia
  1135 Powers Place
  Alpharetta, GA 30004
  POC: Jeff Norford
  Telephone: 800–849–5947

- Advantage Engineering
  525 East Stop 18 Road
  Greenwood, In 46142
  POC: Kip Kelly
  Telephone: 317–887–0729

Quantity—1 complete unit

Specification for Water Circulation System

Complete turnkey recirculation water-cooling system, such as the Sentry closed-water isolation skid or the NESLAB recirculating system, with water-to-water heat exchanger to dump waste heat to a plant cooling water system. Nonrefrigerated system with the following specifications:

- Temperature range: 5–40 °C.
- Temperature stability: ±2 °C.
- Cooling capacity: 90 kW or more.
- Operating voltage: 440–480 VAC 3–P (preferred) or 208–240 VAC 3–P.
- Power consumption: 2–5 kVA.
- Pumping capacity: 40 gpm or more.
- Maximum operating press: 100 psi or better.
- Pump pressure rise: 40 psig or better.
- Reservoir/expansion tank: Included.
- Inlet/outlet fitting type: Pipe connections.
- Unit controller: Easy to use, programmable control capability for automatic, closed-loop control, regulation of recirculation water temperature with modulating valves. User-selectable temperature set points, limits, and alarms. High temperature, low level, and loss of flow indicators, alarms, and interlocks. Display with keypad entry for user to input settings. Automatic restart capability should power fail.
- Isolation valves: As necessary on recirculation and plant cooling connections.
- Heat exchanger: Heavy-duty SS construction with provisions for cleaning with minimal system impact.
- Make-up water: Allocation for introducing clean treated water into system.
- Instrumentation: Pressure, temperature, and flow-on recirculation.
- Material: Recirculation system piping, etc. should be made of SS parts and other materials that will not rust or slough off debris into the clean water flow (steel should not be used).
- Plant water: Untreated nonpotable water.
- Recirculation water: Capable of long-duration operation with clean filtered water and a nominal resistive in the 0.05 to 1 MΩ/cm range. Maximum return water temperature of 40° (from process).
- Operational duty: 24/7 operation for 3–5 years. Unit is located on the floor of an environmentally controlled high bay.

Include the following options in the quote, if possible, and break out as separate costs:

(1) Dual heat exchanger and/or oversized heat exchanger to deal with potential fouling on plant water side.

(2) Dual pump unit to serve as backup should the primary fail (with switchover capability).

(3) Inline filter unit on the recirculation side, downstream of the pumps to stop any potential debris from reaching the process.

(4) Bacteria/algae control options, using treatment or inline ultraviolet (UV) filter.

(5) Allocation to deaerate the recirculation system water to remove dissolved gases.

APPENDIX D—WATER FLOW METER SPECIFICATION

Specification for Procurement of Magnetic-Type Flow Meters
Integrated Financial Management Program Procurement

Estimated delivery 4–6 weeks ARO

Title—Turnkey Magnetic-Type Flow Meters for Both Small- and Large-Line Sizes With No Moving Parts and No Flow Restrictions, Ready for Inline Water Service

Vendors:

- Total Temperature Instrumentation, Inc.
  8 Leroy Road
  P.O. Box 1073
  Williston, VT 05495
  POC: Lou Phelps
  Telephone: 802–863–0085

- Trinova, Inc.
  P.O. Box 2806
  Mobile, AL 36601
  POC: Chad Green
  Telephone: 251–378–7837

- Rosemount Inc.
  8200 Market Blvd
  Chanhassen, MN 55317
  POC: Sales
  Telephone 800–999–9307

Quantity—17 low-flow range units

Specification for Small Magnet Flow Meter Units

Complete ready-to-use magnetic flow meters, providing no flow restriction, with no moving parts to include the flow element, converter, or other assemblies as required with the following specifications:

- Flow range: 0.03 to 2 gpm water.

- Overrange capability: Up to 4 gpm water.

- Water temperature range: Room temperature to 100 °C.
- Flow accuracy: ±0.5% or better.
- Operating pressure: 150 psi or more.
- Operating voltage: 120 VAC.
- Line size: Suitable for 0.25 to 0.5-in-diameter line.
- Inlet/outlet fitting type: Compression, pipe-type fittings, flanges.
- Signal output: 4–20 mA.
- Flow meter setup: Unit has a display window, attached or remote position, that can be used to set up the meter and also provides display of current flow in user-selected units.
- Material: All wetted surface should be made of SS or other materials that will not rust or contribute debris to the clean water flow (steel should not be used).
- Water type: Capable of long-duration operation with clean filtered water and a nominal conductivity in the 1–20 μS/s range.
- Operational duty: Around-the-clock operation for 3–5 years.
- Calibration data: Provided for water flow measurement (covering high- and low-flow conditions).
- Options for consideration with the units—break out as separate costs:
  - Embedded temperature and pressure measurement that provides water flow media conditions.
  - Internal provisions for self-cleaning the meter electrodes.
  - Suggested water specifications for long-term operation. Also, water treatment or conditioning if the nominal conductivity of the water is out of range, and meter to indicate conductivity problems impacting accuracy of the measurement.
  - 485 digital communication interface.
  - Calibration interval and how it is accomplished.

Quantity—Two high-flow rate units.

Specification for Large-Magnet Flow Meter Units

Complete ready-to-use magnetic flow meters, providing no flow restriction, with no moving parts to include the flow element, converter, or other assemblies as required with the following specifications:

- Flow range: 10 to 100 gpm water.
- Over range capability: Up to 150 gpm water.
- Water temperature range: Room temperature to 100 °C.
- Flow accuracy: ±0.5% or better.
- Operating pressure: 150 psi or more.
- Operating voltage: 120 VAC.
- Line size: Suitable for 2-in-diameter line.
- Inlet/outlet fitting type: Compression, pipe type fittings, flanges.
- Signal output: 4–20 Ma.
- Flow meter setup: Unit has a display window, attached or remote position, that can be used to set up the meter and also provides a display of current flow in user-selected units.
- Material: All wetted surface should be made of SS or other materials that will not rust or contribute debris to the clean water flow (steel should not be used).
- Water type: Capable of long-duration operation with clean filtered water and a nominal conductivity in the 1–20 µS/s range.
- Operational duty: Around-the-clock operation for 3–5 years.
- Calibration data: Provided for water flow measurement, covering high- and low-flow conditions.
- Options for consideration with the units—break out as separate costs:
  - Embedded temperature and pressure measurement that provides water flow media conditions.
  - Internal provisions for self-cleaning the meter electrodes.

– Suggested water specifications for long-term operation. Also, water treatment or conditioning if the nominal conductivity of the water is out of range, and meter to indicate conductivity problems impacting accuracy of measurement.

– 485 digital communication interface.

– Calibration interval and how it is accomplished.

APPENDIX E—INERT GAS PURIFIER SPECIFICATION

Specification for Procurement of an Inline Inert Gas Purifier Unit
Integrated Financial Management Program Procurement

Estimated delivery 6 weeks ARO

Title—Inert Gas Purifier Unit for Use with He and Ar in a Closed-Loop Gas Circulation System

Vendors:

- SAES Pure Gas Inc.
  4175 Santa Fe Road
  San Luis Obispo, CA 93401
  POC: Greg Perry
  Telephone: 805–786–2130

- Johnson Matthey USA
  Gas Purification Technology Group
  1397 King Road
  West Chester, PA 19380
  Telephone: 610–232–1900

- NuPure III
  67 Iber Road, Unit 107
  Ottawa ON K2S 1E7 Canada
  Telephone: 1–613–836–0336

Quantity—Two complete units

Specification for Turbopump Unit

Complete turnkey heated getter purifiers (getter material irreversibly binds with impurities) for rare gas (He and Ar). SAES® MonoTorr PS4–MT3–R1 complete turnkey system or equivalent with the following specifications:

- Setup: Device contained in an enclosure.

- Surface mountable: Enclosure can be mounted.

- Cooling: Fan unit in enclosure.

- Voltage: 120 VAC.
- Power consumption: Less than 400 W.
- Operating temperature: 400 °C.
- Operating pressure: Vacuum to 150 psig.
- Maximum flow rate: 50 slpm.
- Nominal flow rate: 20 slpm.
- Fittings: VCR type.
- Tubing internal roughness: 10-µin finish for low outgassing.
- Filter: 0.003-mm metal filter.
- Valves: SS diaphram type.
- Valve actuation: Air (80–100 psig).
- Pressure drop: Low-pressure drop unit at nominal flow rate.
- Life and status sensor: Included.
- Bypass assembly: Included.
- Control: Thermocouple interface with multifunction controller.

Table 15. Guaranteed delivered gas purity at flow rate.

	Flow Rate	
Impurity	0–20 slpm	20–50 slpm
O_2	<1 ppb	<1 ppb
H_2O	<1 ppb	<1 ppb
CO	<1 ppb	<1 ppb
CO_2	<1 ppb	<1 ppb
N_2	<1 ppb	<10 ppb
H_2	<1 ppb	<10 ppb
CH_4	<1 ppb	<10 ppb

APPENDIX F—WATER AND GAS SYSTEM HAND VALVE SPECIFICATION

Specification for Procurement of Stainless Steel Hand-Valve Hardware for Water and Purified Gas Systems Integrated Financial Management Program Procurement

Estimated delivery 4–6 weeks ARO

Title—SS Hand Valves for Water and High-Purity Gas Systems

Vendors:

- Alabama Fluid Systems (primary)
  237 Cahaba Valley Parkway
  Pelham, AL 35124
  Telephone: 205–988–4812

- Hile Controls
  311 Applegate Parkway
  Pelham, AL 35124
  Telephone: 205–620–4000

- Parker Hannifin Corporation
  6035 Parkland Boulevard
  Cleveland, OH 44124-4141 USA
  Telephone: 1–800–272–7537

Deliverables and Specifications

- Six 2-in SS hand-operated ball valves, Swagelok® SS–68TSW32T or equivalent with the following specifications:

  – Reinforced polytetrafluoroethylene (PFTE) seats.

  – Manual operation.

  – Operating temperature rating up to 200 °C.

  – Working pressure of 880 psi at 120 °C.

  – 2-in diameter with SS construction.

  – Tube socket weld connections.

- Five 1-in SS hand-operated ball valves, Swagelok SS–65TS16 or equivalent with the following specifications:
  - Reinforced PFTE seats.
  - Manual operation.
  - Operating temperature rating up to 200 °C.
  - Working pressure of 1,150 psi at 120 °C.
  - 1-in diameter with SS construction.
  - Swagelock compression connections.
- Twenty-two ½-in SS hand-operated ball valves, Swagelok SS–63TS8 or equivalent with the following specifications:
  - Reinforced PFTE seats.
  - Manual operation.
  - Operating temperature rating up to 200 °C.
  - Working pressure of 1,150 psi at 120 °C, ½-in diameter with SS construction.
  - Swagelock compression connections.
- Twenty ½-in all SS straight bellows valves with compression fittings, Swagelok SS–8BW or equivalent with the following specifications:
  - Completely welded bellows valve design.
  - Manual operation.
  - Temperature rated to at least 900 °F continuous operation.
  - Pressure rated to at least 200 psig (at full temperature).
  - All SS wetted surfaces.
  - ½-in Swagelok connection.

- Fifteen ½-in all SS straight bellows valves with VCR fittings, Swagelok SS–8BW–V47 or equivalent with the following specifications:
  - Completely welded bellows valve design.
  - Manual operation.
  - Temperature rated to at least 900 °F continuous operation.
  - Pressure rated to at least 200 psig (at full temperature).
  - ½-in VCR female connection.
  - All SS wetted surfaces.
  - Handles may be rated to less than 900 °F if they are removable.
- Eight 3/8-in all SS straight bellows valves with compression fittings, Swagelok SS–6BW or equivalent with the following specifications:
  - Completely welded bellows valve design.
  - Manual operation.
  - Temperature rated to at least 900 °F continuous operation.
  - Pressure rated to at least 200 psig (at full temperature).
  - All SS wetted surfaces.
  - Handles may be rated to less than 900 °F if they are removable.
  - ½-in Swagelok connection.

APPENDIX G—VACUUM PUMP UNITS SPECIFICATION

Specification for Procurement of Stainless Steel Hand-Valve Hardware for Water and Purified Gas Systems Integrated Financial Management Program Procurement

Estimated delivery 6 weeks ARO

Title—Turbopump System (Turbopump With Controller) Varian V–301 Navigator Complete System or Equivalent Unit. Dry rough pump unit Alcatel model ACP40 or equivalent unit

Vendors:

- Varian Vacuum Technologies
  121 Hartwell Ave.
  Lexington, MA 02173
  POC: Thomas J. Drisgill
  Telephone: 407–366–8602

- Alcatel Vacuum Products
  67–T Sharp St
  Hingham, MA 02043
  Sales: 781–331–4200

- Osaka Vacuum Ltd.
  911 Bern Court, Suite 140
  San Jose, CA 95112
  Telephone: 408–441–7658

- Leybold Vacuum Inc.
  5700 Mellon Road
  Export, PA 15632
  Sales: 724–327–5700

- BOC Edwards
  301 Ballardvale St.
  Wilmington, MA 01887
  Sales: 978-658-5410

- Pfeiffer Vacuum Inc.
  24 Trafalgar Sq.
  Nashua, NH 03063
  Sales: 603–578–6500

Quantity—two units.

General Specification for Turbopump Unit

Turbopump system (turbopump with controller) Varian V–301 navigator complete system or equivalent with the following specifications:

- Cooling: Natural air convection.
- Protective screen: Inlet screen factory installed.
- Pumping speed: 250 L/s N, 200 L/s H, 220 L/s He.
- Compression ratio: 7×10^{8} for N.
- Ultimate pressure: 8×10^{-10} mbar or less.
- Operating voltage: 120 VAC.
- Bake-out temperature: Up to 120 °C on the inlet flange.
- Startup time: 2 to 5 min.
- Installation position: Any.
- Ambient temperature: Up to 40 °C (for operation).
- Inlet flange: 6-in conflat.
- Outlet flange: KF25.

Quantity—1 unit

General Specification for Rough Pump

Alcatel model ACP40 equivalent with the following specifications:

- Oil-free pumping.
- 500 L/min pumping speed or better.
- Operating pressure range from atmospheric to less than 10^{-2} torr.
- NW40 inlet flange.
- 120 VAC single phase.

- Air-cooled.
- Operating temperature 5–40 °C.
- Gas ballast fitting provided.
- Noise level 68 dB or lower.
- Time between overhauls >20,000 hr.

APPENDIX H—FORTRAN 90 SOURCE CODE LISTING—LOSS OF COOLANT TRANSIENT ANALYSIS

A Fortran code was developed to assess the transient calorimeter heating trends during a loss of recirculation coolant condition.

```
************************************************************************************************************************
**  trans_anular.f90 (4-7-2005)
************************************************************************************************************************
**      Eric Stewart
**      (256) 544-7099
**      Eric.T.Stewart@nasa.gov
************************************************************************************************************************
PROGRAM trans_anular
  IMPLICIT NONE
  INTEGER :: lumps=6,id,pc,jd
  REAL, DIMENSION(1:6) :: vol=0.,cp=0.,k=0.,rho=0.,t1,to,heff=0.,rvc=0.,dtrvc=0.
  REAL, DIMENSION(1:8) :: diam=0.
  REAL :: em1=.2,em2=.2,em6=.2,length=0.33,pi,to=0,dt=.0001,kgas=.205,sig=5.67E-08,qin=5000.
  REAL :: dr23,dr32,pi,qrad,qcon,time,ts=290.
  REAL :: c1,d1,e1,c2,d2,e2,c3,d3,e3,c4,d4,e4,c5,d5,e5,c6,d6,e6,energy,energyo
  pi = 4.0*ATAN(1.0)
  diam(1) = .014097
  diam(2) = .015977
! diam(1) = diam(2)-3.*(diam(2)-diam(1))
  diam(3) = .017252
  diam(4) = .020198
  diam(5) = .020960
  diam(6) = .023906
  diam(7) = .030256
  diam(8) = .033203
  to(1)   = 1273.
  to(2)   = 400.
  to(3)   = 325.
  to(4)   = 325.
  to(5)   = 325.
  to(6)   = 325.
  t1      = to
  vol(1)  = 0.25*pi*(diam(2)*diam(2)-diam(1)*diam(1))*length
  vol(2)  = 0.25*pi*(diam(4)*diam(4)-diam(3)*diam(3))*length
  vol(3)  = 0.25*pi*(diam(5)*diam(5)-diam(4)*diam(4))*length
  vol(4)  = 0.25*pi*(diam(6)*diam(6)-diam(5)*diam(5))*length
  vol(5)  = 0.25*pi*(diam(7)*diam(7)-diam(6)*diam(6))*length
  vol(6)  = 0.25*pi*(diam(8)*diam(8)-diam(7)*diam(7))*length
  cp(1)   = 250.
  cp(2)   = 380.
  cp(3)   = 4200.
  cp(4)   = 380.
  cp(5)   = 4200.
  cp(6)   = 380.
  rho(1)  = 13800.
  rho(2)  = 8900.
  rho(3)  = 985.
  rho(4)  = 8900.
```

```
 rho(5)  = 985.
 rho(6)  = 8900.
 k(1)    = 90.
 k(2)    = 400.
 k(3)    = 0.65
 k(4)    = 400.
 k(5)    = 0.65
 k(6)    = 400.
 rvc(1)  = rho(1)*vol(1)*cp(1)
 rvc(2)  = rho(2)*vol(2)*cp(2)
 rvc(3)  = rho(3)*vol(3)*cp(3)
 rvc(4)  = rho(4)*vol(4)*cp(4)
 rvc(5)  = rho(5)*vol(5)*cp(5)
 rvc(6)  = rho(6)*vol(6)*cp(6)
 dtrvc   = dt/rvc
!*************************************************************************************************************************************
 dr23 = diam(2)/diam(3)
 dr32 = diam(3)/diam(2)
 qrad = (t1(1)-t1(2))*sig*pi*diam(2)*length*(to(1)+to(2))*(to(1)*to(1)+to(2)*to(2))/(1./em1+(1-em2)*dr23/em2)
 qcon = (t1(1)-t1(2))*(2.*pi*length*kgas)/LOG(dr32)
 WRITE(6,'(/,»  t of mo-re is  «,3E15.8)') to(1),qcon,qrad
 WRITE(6,'(/,»  mass is  «,6E15.8)') rho(1)*vol(1),rho(2)*vol(2),rho(3)*vol(3),rho(4)*vol(4),rho(5)*vol(5),rho(6)*vol(6)
 WRITE(6,'(/,»  rvc is  «,6E15.8)') rvc(1),rvc(2),rvc(3),rvc(4),rvc(5),rvc(6)
!*************************************************************************************************************************************
 OPEN(UNIT=81,FILE='temperature.txt',STATUS='REPLACE',FORM='FORMATTED')
 WRITE(81,'(4X,»time»,7X,»temp1»,6X,»temp2»,6X,»temp3»,6X,»temp4»,6X,»temp5»,6X,»temp6»,5X,»energy»)')
 time = 0
 energyo = 0.
 DO jd=1,6
   energyo = energyo + to(jd)*rvc(jd)
 ENDDO
 WRITE(81,'(8E11.3)') time,to(1),to(2),to(3),to(4),to(5),to(6),energyo
 c1 = dtrvc(1)*(sig*pi*diam(2)*length/(1./em1+(1-em2)*(diam(2)/diam(3))/em2))
 d1 = dtrvc(1)*(2.*pi*length*kgas/LOG(diam(3)/diam(2)))
 c2 = dtrvc(2)*(sig*pi*diam(2)*length/(1./em1+(1-em2)*(diam(2)/diam(3))/em2))
 d2 = dtrvc(2)*(2.*pi*length*kgas/LOG(diam(3)/diam(2)))
 e2 = dtrvc(2)*(2.*pi*length*k(3)/LOG((diam(5)+diam(4))/(2.*diam(4))))
 c3 = dtrvc(3)*(2.*pi*length*k(3)/LOG((diam(5)+diam(4))/(2.*diam(4))))
 d3 = dtrvc(3)*(2.*pi*length*k(3)/LOG((2.*diam(5))/(diam(5)+diam(4))))
 c4 = dtrvc(4)*(2.*pi*length*k(3)/LOG((2.*diam(5))/(diam(5)+diam(4))))
 d4 = dtrvc(4)*(2.*pi*length*k(5)/LOG((diam(7)+diam(6))/(2.*diam(6))))
 c5 = dtrvc(5)*(2.*pi*length*k(5)/LOG((diam(7)+diam(6))/(2.*diam(6))))
 d5 = dtrvc(5)*(2.*pi*length*k(5)/LOG((2.*diam(7))/(diam(7)+diam(6))))
 c6 = dtrvc(6)*(2.*pi*length*k(5)/LOG((2.*diam(7))/(diam(7)+diam(6))))
 d6 = dtrvc(6)*(sig*pi*diam(8)*length*em6)
 pc = 0
 DO id=1,1000000
   pc = pc + 1
   time = time + dt
   t1(1) = to(1) - c1*(to(1)**4-to(2)**4) - d1*(to(1)-to(2))
   t1(2) = to(2) + c2*(to(1)**4-to(2)**4) + d2*(to(1)-to(2)) - e2*(to(2)-to(3))
   t1(3) = to(3) + c3*(to(2)-to(3)) - d3*(to(3)-to(4))
   t1(4) = to(4) + c4*(to(3)-to(4)) - d4*(to(4)-to(5))
   t1(5) = to(5) + c5*(to(4)-to(5)) - d5*(to(5)-to(6))
   t1(6) = to(6) + c6*(to(5)-to(6)) - d6*(to(6)**4-ts**4)
   IF(pc == 1000)THEN
     energy = 0.
     DO jd=1,6
       energy = energy + t1(jd)*rvc(jd)
     ENDDO
```

```
      WRITE(81,'(8E11.3)') time,t1(1),t1(2),t1(3),t1(4),t1(5),t1(6),energy
      pc = 0
    ENDIF
    to = t1
  ENDDO
  CLOSE(UNIT=81)
*****************************************************************************************************************************
END PROGRAM trans_anular
```

APPENDIX I—HEAT PIPE CALORIMETER GEOMETRY—STANDARD TUBE SIZES

Due to difficulty obtaining quotes for drawn tubing, an assessment, shown in table 16, was made using standard copper tube sizes. Machining of the inner diameter would be required.

Table 16. Heat pipe calorimeter geometry based on standard tubing dimensions.

Fabrication of Copper Alloy Heat Pipe Calorimeters Using Standard Tubing Sizes										
Standard Sizes Taken From Parker Instrument Tubing Selection Guide Bulletin 4200-TS (June 2004)										
Actual Sizes may vary based on Vendors and Alloys - Will Require Slight Adjustments										
Possible Copper Alloys include C122 and Beryllium Copper C172										
Calorimeter Geometry	G	F(-4)	F(-3)	F(-2)	F(-1)	F(1)	F(2)	F(3)	F(4)	F(0)
Quantity	7	1	1	1	1	1	1	1	1	1
Process Component (OD)	0.625	0.625	0.625	0.625	0.625	0.625	0.625	0.625	0.625	0.625
Gas Conduction Gap Width	0.027	0.027	0.105	0.033	0.023	0.039	0.018	0.048	0.022	0.027
Calorimeter Channel Tube										
Std Tube OD	0.875	0.875	1.000	0.875	0.875	0.875	0.875	0.875	0.875	0.875
Std Tube Wall	0.109	0.109	0.083	0.095	0.109	0.095	0.109	0.083	0.109	0.109
Caloirmeter Channel Tube OD	0.875	0.875	1.000	0.875	0.875	0.875	0.875	0.875	0.875	0.875
Calorimeter Channel Tube ID	0.679	0.679	0.835	0.691	0.671	0.703	0.661	0.721	0.669	0.679
Calorimeter Channel Tube Wall -Target	0.098	0.098	0.0825	0.092	0.102	0.086	0.107	0.077	0.103	0.098
Std Tube Wall Material to Remove	0.0110	0.0110	0.0005	0.0030	0.0070	0.0090	0.0020	0.0060	0.0060	0.0110
Calorimeter Shell Tube										
Water Film Flow Gap - Target	0.0135	0.0135	0.0135	0.0135	0.0135	0.0135	0.0135	0.0135	0.0135	0.0135
Std Tube OD	1.000	1.000	1.125	1.000	1.000	1.000	1.000	1.000	1.000	1.000
Std Tube Wall	0.049	0.049	0.049	0.049	0.049	0.049	0.049	0.049	0.049	0.049
Caloirmeter Shell Tube OD	1.000	1.000	1.125	1.000	1.000	1.000	1.000	1.000	1.000	1.000
Calorimeter Shell Tube ID	0.902	0.902	1.027	0.902	0.902	0.902	0.902	0.902	0.902	0.902
Calorimeter Shell Tube Wall -Target	0.049	0.049	0.049	0.049	0.049	0.049	0.049	0.049	0.049	0.049
Std Tube Wall Material to Remove	0.0000	0.0000	0.0000	0.0000	0.0000	0.0000	0.0000	0.0000	0.0000	0.0000
Calorimeter Cover Tube										
Water Return Path Width - Target	0.135	0.135	0.135	0.135	0.135	0.135	0.135	0.135	0.135	0.135
Std Tube OD	1.500	1.500	1.500	1.500	1.500	1.500	1.500	1.500	1.500	1.500
Std Tube Wall	0.083	0.083	0.065	0.083	0.083	0.083	0.083	0.083	0.083	0.083
Caloirmeter Cover Tube OD	1.500	1.500	1.500	1.500	1.500	1.500	1.500	1.500	1.500	1.500
Calorimeter Cover Tube ID - Target	1.27	1.27	1.395	1.27	1.27	1.27	1.27	1.27	1.27	1.27
Calorimeter Cover Tube Wall -Target	0.115	0.115	0.0525	0.115	0.115	0.115	0.115	0.115	0.115	0.115
Std Tube Wall Material to Remove	-0.0320	-0.0320	0.0125	-0.0320	-0.0320	-0.0320	-0.0320	-0.0320	-0.0320	-0.0320
Water Return Path Width - No Machining	0.167	0.167	0.1225	0.167	0.167	0.167	0.167	0.167	0.167	0.167
Calorimeter Cover Tube ID - No Machining	1.334	1.334	1.37	1.334	1.334	1.334	1.334	1.334	1.334	1.334

For Calorimeters G, F(-4), F(-1), F(2), F(4) and F(0)
Channel Tube
Std Tubing OD = 0.875
Std Tubing Wall Thickness = 0.109
Shell Tube
Std Tubing OD = 1.000
Std Tubing Wall Thickness = 0.049
Cover Tube
Std Tubing OD = 1.500
Std Tubing Wall Thickness = 0.083

For Calorimeters F(-3)
Channel Tube
Std Tubing OD = 1.000
Std Tubing Wall Thickness = 0.083
Shell Tube
Std Tubing OD = 1.125
Std Tubing Wall Thickness = 0.049
Cover Tube
Std Tubing OD = 1.500
Std Tubing Wall Thickness = 0.065

For Calorimeters F(-2) and F(1)
Channel Tube
Std Tubing OD = 0.875
Std Tubing Wall Thickness = 0.095
Shell Tube
Std Tubing OD = 1.000
Std Tubing Wall Thickness = 0.049
Cover Tube
Std Tubing OD = 1.500
Std Tubing Wall Thickness = 0.083

For Calorimeters F(3)
Channel Tube
Std Tubing OD = 0.875
Std Tubing Wall Thickness = 0.083
Shell Tube
Std Tubing OD = 1.000
Std Tubing Wall Thickness = 0.049
Cover Tube
Std Tubing OD = 1.500
Std Tubing Wall Thickness = 0.083

Notes:
1) Wall thickness for the Channel Tube is approx. 2X that of the baseline drawn case. For Copper this should be no issue due to the high themal conductivity.
2) The size and wall thickness of the Shell Tube are adjusted to achieve a film flow gap width which is between 0.010 and 0.015 inch so that no machining is required.
3) The size and wall thickness of the Cover Tube is adjusted so that it is approx. 10 times the film flow gap width. It is suggested that no machining be performed on this tube and the ID/OD are used as is (machined amount is very small).
4) Total of 8 different types of tubing material are required to build all calorimeters.
5) The calorimeter cover tube could potentially be reduced to save weight possible to a 1-3/8" diameter tube with a 0.065 wall if available. This would provide a water flow return path of approx. 0.122" and an cover tube mass reduction of approx 0.5 lbs.

Approximate Weight per Calorimeter

Copper Density	0.323	lb/in^3	
Calorimeter length	14	in	
Channel Tube	1.08	lb	
Shell Tube	0.67	lb	
Cover Tube	1.67	lb	(1.5" OD x 0.083 wall)
Cover Tube	1.21	lb	(1.3755" OD x 0.065 wall)
Manifold End Caps	0.24	lb	
Total	3.66	lb	(with 1.5" OD cover)

APPENDIX J—CALORIMETER POWER EXTRACTION PERFORMANCE WORKSHEET FOR STANDARD TUBING

The full spreadsheet, shown in table 17, was used in assessing the calorimeter configuration based on standard size tubing holding this water film flow gap at 0.0135 in.

Table 17. Calorimeter geometry and performance for a cooling film annulus of 0.0135 in.

For NRPCT Work Item #2	Updated on 5-15-2005 for Std Tubing inputs										
Water Calorimeter Quick Assessment for Heat pipe life time testing											
Assumes: helium/argon gas flooded test chamber at low pressure to improve coupling to calorimeter											
						- Direct Input Value					
						- Value Carried From Other Input Location					
Heat pipe Inputs						parameters of interest					
Heat pipe length	0.3048		12	inch	ratio Cond/Evap						
Evaporator length	0.06985	m	2.75	inch							
Adiabatic length	0	m	0	inch							
Condenser length	0.23495	m	9.25	inch							
Diameter	0.015875	m	0.625	in OD							
Calorimeter Inputs											
length of calorimeter	0.3302	m	13	inch							
Calorimeter Area	0.01171167	m^2	18.153125	inch^2	covering heat pipe						
Calorimeter Area	0.004747974	m^3	7.359375	inch^3	covering support						
Nominal Inlet Temperature	299.8166667	K	80	deg F							
Nominal Flow rate	0.027491492	kg/sec	0.435	gallons/min							
inlet water pressure	446599	Pa	65	psi							
Target Surface Temp (ID)	351	K	172.13	F	on the ID surface exposed to hot heat pipe (boiling = 420 K at 65psia)						
Channel Wall thickness	0.0014732	m	0.058	inch	inner tube exposed to hot heat pipe						
Shell Wall thickness	0.0014732	m	0.058	inch	middle tube creating the film flow path						
Cover Wall thickness	0.0014732	m	0.058	inch	outer tube sealing the return path						
film flow Gap	0.0003429	m	0.0135	inch	water flow gap on inner annulus (outlet flow) next to heat pipe - this absorbs the heat						
Return Flow Gap	0.0042418	m	0.167	inch	water flow gap on outer annulus (inlet flow)						
	Test Condition --->	**G series**	**F(-4)**	**F(-3)**	**F(-2)**	**F(-1)**	**F(1)**	**F(2)**	**F(3)**	**F(4)**	**F(0)**
Variables	**Units**										
Power (W)	W	3000	5000	1000	3000	3000	2000	4000	2000	4000	3000
Heat Pipe Surface Temperature	K	1273	1273	1273	1373	1173	1223	1223	1323	1323	1273
Average Gas Gap Temperature	K	814	831.5	802.5	864	764	780	798	830.5	848	814
Calorimeter Channel ID Temperature	K	355	390	332	355	355	337	373	338	373	355
Calorimeter Channel Wall OD Temperature	K	353.48	387.46	331.64	353.58	353.41	336.12	370.76	337.23	370.85	353.48
Calorimeter Channel Wall Delta Temp	K	1.52	2.54	0.36	1.42	1.59	0.88	2.24	0.77	2.15	1.52
Dimensions (meters)											
Heat Pipe OD at Room Temperature	m	0.01588	0.01588	0.01588	0.01588	0.01588	0.01588	0.01588	0.01588	0.01588	0.01588
Heat Pipe OD at Temperature	m	0.01597	0.01597	0.01597	0.01598	0.01595	0.01596	0.01596	0.01597	0.01597	0.01597
Condenser Length	m	0.23495	0.23495	0.23495	0.23495	0.23495	0.23495	0.23495	0.23495	0.23495	0.23495
Gas Gap Width - HP OD to Calorimeter ID	m	0.000646	0.000631	0.002638	0.000782	0.000531	0.000942	0.000423	0.001166	0.000508	0.000646
Calorimeter Channel Wall ID	m	0.01725	0.01725	0.02121	0.01755	0.01704	0.01786	0.01679	0.01831	0.01699	0.01725
Calorimeter Channel Wall OD	m	0.02223	0.02223	0.02540	0.02223	0.02223	0.02223	0.02223	0.02223	0.02223	0.02223
Calorimeter Channel Wall Thickness	m	0.00249	0.00249	0.00210	0.00234	0.00259	0.00218	0.00272	0.00196	0.00262	0.00249
Calorimeter Shell Wall ID	m	0.02291	0.02291	0.02609	0.02291	0.02291	0.02291	0.02291	0.02291	0.02291	0.02291
Calorimeter Shell Wall OD	m	0.02540	0.02540	0.02858	0.02540	0.02540	0.02540	0.02540	0.02540	0.02540	0.02540
Calorimeter Shell Wall Thickness	m	0.00124	0.00124	0.00124	0.00124	0.00124	0.00124	0.00124	0.00124	0.00124	0.00124
Calorimeter Cover Wall ID	m	0.03388	0.03388	0.03480	0.03388	0.03388	0.03388	0.03388	0.03388	0.03388	0.03388
Calorimeter Cover Wall OD	m	0.03810	0.03810	0.03810	0.03810	0.03810	0.03810	0.03810	0.03810	0.03810	0.03810
Calorimeter Cover Wall Thickness	m	0.00211	0.00211	0.00165	0.00211	0.00211	0.00211	0.00211	0.00211	0.00211	0.00211
Film Flow Gap Thickness	m	0.00034	0.00034	0.00034	0.00034	0.00034	0.00034	0.00034	0.00034	0.00034	0.00034
Return Flow Gap Thickness	m	0.00424	0.00424	0.00312	0.00424	0.00424	0.00424	0.00424	0.00424	0.00424	0.00424
Film Hydraulic Diameter (Douter-Dinner)	m	0.000686	0.000686	0.000686	0.000686	0.000686	0.000686	0.000686	0.000686	0.000686	0.000686
Dimensions (inches)											
Heat Pipe OD at Room Temperature	in	0.6250	0.6250	0.6250	0.6250	0.6250	0.6250	0.6250	0.6250	0.6250	0.6250
Heat Pipe OD at Temperature	in	0.6286	0.6286	0.6286	0.6290	0.6281	0.6283	0.6283	0.6288	0.6288	0.6286
Condenser Length	in	9.2500	9.2500	9.2500	9.2500	9.2500	9.2500	9.2500	9.2500	9.2500	9.2500
Gas Gap Width - HP OD to Calorimeter ID	in	0.0254	0.0248	0.1038	0.0308	0.0209	0.0371	0.0166	0.0459	0.0200	0.0254
Calorimeter Channel Wall ID	in	0.6790	0.6790	0.8350	0.6910	0.6710	0.7030	0.6610	0.7210	0.6690	0.6790
Calorimeter Channel Wall OD	in	0.8750	0.8750	1.0000	0.8750	0.8750	0.8750	0.8750	0.8750	0.8750	0.8750
Calorimeter Channel Wall Thickness	in	0.0980	0.0980	0.0825	0.0920	0.1020	0.0860	0.1070	0.0770	0.1030	0.0980
Calorimeter Shell Wall ID	in	0.9020	0.9020	1.0270	0.9020	0.9020	0.9020	0.9020	0.9020	0.9020	0.9020
Calorimeter Shell Wall OD	in	1.0000	1.0000	1.1250	1.0000	1.0000	1.0000	1.0000	1.0000	1.0000	1.0000
Calorimeter Shell Wall Thickness	in	0.0490	0.0490	0.0490	0.0490	0.0490	0.0490	0.0490	0.0490	0.0490	0.0490
Calorimeter Cover Wall ID	in	1.3340	1.3340	1.3700	1.3340	1.3340	1.3340	1.3340	1.3340	1.3340	1.3340
Calorimeter Cover Wall OD	in	1.5000	1.5000	1.5000	1.5000	1.5000	1.5000	1.5000	1.5000	1.5000	1.5000
Calorimeter Cover Wall Thickness	in	0.0830	0.0830	0.0650	0.0830	0.0830	0.0830	0.0830	0.0830	0.0830	0.0830
Film Flow Gap Thickness	in	0.0135	0.0135	0.0135	0.0135	0.0135	0.0135	0.0135	0.0135	0.0135	0.0135
Return Flow Gap Thickness	in	0.1670	0.1670	0.1230	0.1670	0.1670	0.1670	0.1670	0.1670	0.1670	0.1670
Film Hydraulic Diameter (Douter-Dinner)	in	0.0270	0.0270	0.0270	0.0270	0.0270	0.0270	0.0270	0.0270	0.0270	0.0270
Material Emissivity											
Emissivity Mo-44.5Re @ Temp		0.16	0.16	0.16	0.17	0.15	0.16	0.16	0.16	0.16	0.16
Emissivity Copper C122		0.44	0.44	0.44	0.44	0.44	0.44	0.44	0.44	0.44	0.44
Effective Emissivity		0.13	0.14	0.13	0.14	0.13	0.13	0.13	0.14	0.14	0.13
Heat Transfer Gas Gap											
Radiation Heat Transfer Gap	W	235.23	234.72	235.60	333.91	160.73	195.53	194.99	281.53	280.99	235.23
Conduction Heat Transfer Gap	W	2764.77	4765.28	764.40	2666.09	2839.27	1804.47	3805.01	1718.47	3719.01	2764.77
Gas Gap Composition	Helium -Argon	32% Ar	6% Ar	32% Ar	32% Ar	32% Ar	32% Ar	32% Ar	32% Ar	32% Ar	32% Ar
Helium Thermal conductivity @ Avg Temp	W/m-K	0.31	0.32	0.31	0.33	0.30	0.30	0.31	0.32	0.32	0.31
Gas Gap Compensation factor		0.51	0.88	0.51	0.51	0.51	0.51	0.51	0.51	0.51	0.51
Effective Gas Gap Thermal Conductivity	W/m-K	0.1588	0.2783	0.1572	0.1658	0.1517	0.1540	0.1565	0.1611	0.1636	0.1588
Calorimeter Material		copper C122	copper C122	copper C122	copper C122	copper C122	copper C122	copper C122	copper C122	copper C122	copper C122
Calorimeter Channel Wall Thermal Conductivity	W/m-K	339.0	339.0	339.0	339.0	339.0	339.0	339.0	339.0	339.0	339.0
Calorimeter Cooling Fluid		Water	Water	Water	Water	Water	Water	Water	Water	Water	Water
Avg Temp Used for Fluid Properties	K	312.8	320.9	314.6	312.8	312.8	308.6	317.2	309.5	317.2	312.8
Water Flow Rate	kg/sec	0.028	0.028	0.008	0.028	0.028	0.027	0.027	0.025	0.027	0.028
Water Flow Rate	gal/min	0.436	0.449	0.128	0.436	0.436	0.430	0.435	0.392	0.435	0.436
Inlet Water Pressure	Pa	446599	446599	446599	446599	446599	446599	446599	446599	446599	446599
Inlet Water Pressure	psi	65.00	65.00	65.00	65.00	65.00	65.00	65.00	65.00	65.00	65.00
Water Inlet Temperature	K	299.82	299.82	299.82	299.82	299.82	299.82	299.82	299.82	299.82	299.82
Log mean Water Film Flow temp Wall to Fluid	K	40.80	66.90	11.87	40.80	40.80	27.46	53.91	27.40	53.91	40.80
Average Water Film Flow Temperature	K	312.82	320.90	314.57	312.82	312.82	308.61	317.23	309.47	317.23	312.82
Water film flow temp delta (inlet to outlet)	K	26.02	42.17	29.51	26.02	26.02	17.59	34.83	19.31	34.83	26.02
Water Outlet Temperature	K	325.83	341.99	329.32	325.83	325.83	317.41	334.65	319.13	334.65	325.83
Water specific heat Cp	J/kg-K	4180.28	4180.26	4180.15	4180.28	4180.28	4180.86	4180.09	4180.71	4180.09	4180.28
Water thermal conductivity k	W/m-K	0.63	0.64	0.63	0.63	0.63	0.62	0.63	0.62	0.63	0.63
water density rho	kg/m3	993.64	990.52	992.99	993.64	993.64	995.12	991.98	994.82	991.98	993.64
Water Absolute Viscosity mu	kg/m-s	0.000665	0.000570	0.000642	0.000665	0.000665	0.000725	0.000610	0.000712	0.000610	0.000665
Log Mean Temperature Difference Wall to Fluid	K	40.80	66.90	11.87	40.80	40.80	27.46	53.91	27.40	53.91	40.80
Heat Transfer To Cooling Fluid											
Channel Flow Tube surface		smooth	smooth	smooth	smooth	smooth	smooth	smooth	smooth	smooth	smooth
Shell Flow Tube surface		smooth	smooth	smooth	smooth	smooth	smooth	smooth	smooth	smooth	smooth
Type of flow (Re<2300 = Laminar)		Laminar	Laminar	Laminar	Laminar	Laminar	Laminar	Laminar	Laminar	Laminar	Laminar
Film Flow Area	m^2	2.43E-05	2.43E-05	2.77E-05	2.43E-05	2.43E-05	2.43E-05	2.43E-05	2.43E-05	2.43E-05	2.43E-05
Film Flow Velocity	m/sec	1.14	1.18	0.29	1.14	1.14	1.12	1.14	1.02	1.14	1.14
Reynolds Number		1171.24	1403.80	312.43	1171.24	1171.24	1058.46	1271.16	981.78	1271.16	1171.24
Nusselt Number		4.89	4.89	4.89	4.89	4.89	4.89	4.89	4.89	4.89	4.89
Convective heat Transfer Coeff h	W/m^2-K	4484.26	4558.33	4497.51	4484.26	4484.26	4442.60	4525.62	4451.28	4525.62	4484.26
Check on power balance -convection side	*W*	*3000.00*	*5000.00*	*1000.00*	*3000.00*	*3000.00*	*2000.00*	*4000.00*	*2000.00*	*4000.00*	*3000.00*
Check power balance - water flow side	*W*	*3000.00*	*5000.00*	*1000.00*	*3000.00*	*3000.00*	*2000.00*	*4000.00*	*2000.00*	*4000.00*	*3000.00*
Pressure Drop in Film Channel											
viscosity ratio (mu-bulk to mu-wall)		1.87	2.50	1.35	1.87	1.87	1.64	2.13	1.63	2.13	1.87
annular passage dia ratio dinner/douter		0.970	0.970	0.974	0.970	0.970	0.970	0.970	0.970	0.970	0.970
annular passage adjustment factor		1.49998	1.49998	1.49998	1.49998	1.49998	1.49998	1.49998	1.49998	1.49998	1.49998
factor for #/Re expression		82.0	76.3	89.1	82.0	82.0	84.9	79.5	85.0	79.5	82.0
friction factor f smooth channel		0.070	0.054	0.285	0.070	0.070	0.080	0.063	0.087	0.063	0.070
Calorimeter Length	m	0.330	0.330	0.330	0.330	0.330	0.330	0.330	0.330	0.330	0.330
Delta pressure in Film Channel	Pa	21873.3	18009.0	5914.0	21873.3	21873.3	24303.4	19398.4	21768.7	19398.4	21873.3
Delta pressure in Film Channel	psi	3.2	2.6	0.9	3.2	3.2	3.5	2.8	3.2	2.8	3.2
Delta Pressure/Inlet Pressure		0.049	0.040	0.013	0.049	0.049	0.054	0.043	0.049	0.043	0.049

APPENDIX K—SIMPLIFIED CALORIMETER UNCERTAINTY ANALYSIS

Water Calorimeter Power Assessment—Simple Uncertainty Analysis

Water flow calorimeter was selected as the method to assess the heat pipe condenser power output for accelerated heat pipe life tests. This power is assessed using measurement of the water temperature increase (ΔT), specific heat (C_p), and flow rate ( ) per the following formulation:

$$Q = \dot{m} C_p \Delta T \quad . \tag{14}$$

The temperature difference (ΔT) is based on thermocouple readings taken both upstream and downstream of the calorimeter as,

$$\Delta T = T_o - T_i \quad . \tag{15}$$

The mass flow rate is based on the measured water flow velocity (V), density (ρ), and area (A) of the flow meter duct as,

$$\dot{m} = \rho V A \quad . \tag{16}$$

The flow rate is measured with a flow meter that has an accuracy ranging from 0.3% to 3% depending on the type (magnetic meter or paddle wheel-style). The temperature difference is based on the reading of two thermocouples, with accuracy on the order of 2%. Fluid properties are assessed based on standard water tables at the flow meter temperature, with accuracy typically of 0.5%.

General Uncertainty Equations

The expression in equation (14) is used for the current uncertainty analysis. The power can be expressed as a function of the following terms:

$$Q = f(\dot{m}, C_p, \Delta T) \quad . \tag{17}$$

The propagation of errors results in,

$$dQ = \frac{\partial Q}{\partial \dot{m}} d\dot{m} + \frac{\partial Q}{\partial C_p} dC_p + \frac{\partial Q}{\partial \Delta T} d\Delta T \quad . \tag{18}$$

Squaring, expanding, and setting all correlated terms to zero results in the following final expression:

$$dQ^2 = \left(\frac{\partial Q}{\partial \dot{m}}\right)^2 d\dot{m}^2 + \left(\frac{\partial Q}{\partial C_p}\right)^2 dC_p^2 + \left(\frac{\partial Q}{\partial \Delta T}\right)^2 d\Delta T^2 \quad . \tag{19}$$

Defining all partial derivatives listed in equation (19) by using equation (14):

$$\frac{\partial Q}{\partial \dot{m}} = C_p \Delta T \quad , \tag{20}$$

$$\frac{\partial Q}{\partial C_p} = \dot{m} \Delta T \quad , \tag{21}$$

and

$$\frac{\partial Q}{\partial \Delta T} = \dot{m} C_p \quad . \tag{22}$$

Substituting equations (20), (21), and (22) into equation (19) results in,

$$dQ^2 = \left(C_p \Delta T\right)^2 d\dot{m}^2 + \left(\dot{m} \Delta T\right)^2 dC_p^2 + \left(\dot{m} C_p\right)^2 d\Delta T^2 \quad . \tag{23}$$

Rearranging each derivative term in equation (23) by dividing it by its square results in the following:

$$dQ^2 = \left(C_p \Delta T \dot{m}\right)^2 \left(\frac{d\dot{m}}{\dot{m}}\right)^2 + \left(\dot{m} \Delta T C_p\right)^2 \left(\frac{dC_p}{C_p}\right)^2 + \left(\dot{m} C_p \Delta T\right)^2 \left(\frac{d\Delta T}{\Delta T}\right)^2 \quad . \tag{24}$$

Further rearrangement results in the following:

$$dQ^2 = \left(C_p \Delta T \dot{m}\right)^2 \left[\left(\frac{d\dot{m}}{\dot{m}}\right)^2 + \left(\frac{dC_p}{C_p}\right)^2 + \left(\frac{d\Delta T}{\Delta T}\right)^2\right] . \tag{25}$$

Each of the derivative terms $\frac{d\dot{m}}{\dot{m}}$, $\frac{dC_p}{C_p}$, and $\frac{d\Delta T}{\Delta T}$ must now be determined.

Mass Flow Rate Uncertainty Determination

For the mass flow rate expression, given in equation (16), a propagation of errors must be evaluated. For this formulation, the flow meter produces a flow velocity, while the flow area is measured and the density is taken from the water property tables as follows:

$$d\dot{m}^2 = \left(\frac{\partial \dot{m}}{\partial \rho}\right)^2 d\rho^2 + \left(\frac{\partial \dot{m}}{\partial V}\right)^2 dV^2 + \left(\frac{\partial \dot{m}}{\partial A}\right)^2 dA^2 \quad . \tag{26}$$

Find all partial derivatives listed in equation (26) by using equation (16) as follows:

$$\frac{\partial \dot{m}}{\partial \rho} = VA \quad , \tag{27}$$

$$\frac{\partial \dot{m}}{\partial V} = \rho A \quad , \tag{28}$$

$$\frac{\partial \dot{m}}{\partial A} = \rho V \quad . \tag{29}$$

Substitute the partials from equations (27), (28), and (29) into equation (26) resulting in the following:

$$d\dot{m}^2 = (VA)^2 d\rho^2 + (\rho A)^2 dV^2 + (\rho V)^2 dA^2 \quad . \tag{30}$$

Rearrange each derivative term in equation (30) by dividing it by its square, resulting in the following:

$$d\dot{m}^2 = (VA\rho)^2 \left(\frac{d\rho}{\rho}\right)^2 + (\rho AV)^2 \left(\frac{dV}{V}\right)^2 + (\rho VA)^2 \left(\frac{dA}{A}\right)^2 \quad . \tag{31}$$

Factor out the term $\rho VA = \dot{m}$, and divide both sides of the expression by it, resulting in this final form,

$$\left(\frac{d\dot{m}}{\dot{m}}\right)^2 = \left(\frac{d\rho}{\rho}\right)^2 + \left(\frac{dV}{V}\right)^2 + \left(\frac{dA}{A}\right)^2 \quad . \tag{32}$$

Each of these terms can now be determined as follows:

- $\left(\frac{dV}{V}\right)$ = uncertainty in determining velocity (0.3%=0.003 to 3%=0.03 depending on the magnitude of the flow rate).

- $\left(\frac{dA}{A}\right)$ = uncertainty in determining the duct area, which is assumed to be a negligible error (0%).

- $\left(\frac{d\rho}{\rho}\right)$ = uncertainty in determining the density, which is composed of two components:

  – Uncertainty over a temperature range of 300 to 350 K (2% = 0.02), assuming a single average density value is used to cover this temperature range.

  – Uncertainty in the reference density data (0.5% = 0.005).

The uncertainty of the density term can be reduced considerably by curve fitting the referenced density data as a function of temperature, and replacing the single average value. A more suitable density value can be determined by using the measured temperature at the flow meter. This density value will have an associated uncertainty that is approximately that of the reference data, as temperature measurement uncertainty is relatively small over the range.

For the flow rate, the uncertainty term can be approximated assuming maximums as,

$$\left(\frac{d\dot{m}}{\dot{m}}\right)^2 = (0.03)^2 + (0.02)^2 + (0.0)^2 \quad , \tag{33}$$

$$\left(\frac{d\dot{m}}{\dot{m}}\right) = 0.036 \quad \text{or} \quad 3.6\% \quad . \tag{34}$$

If the density is assumed to be found as a function of the temperature, with uncertainty approximating the reference data, the overall uncertainty tracks that of the flow meter.

Specific Heat Uncertainty Determination

The specific heat (C_p) assessment is calculated from the tabulated water data. The value of C_p varies by approximately 0.3% over the expected flow temperature range of 300 to 350 K. For conservatism and simplicity in this exercise, uncertainty is based on a combination of temperature affect and reference accuracy:

- $\frac{dC_p}{C_p}$ = Uncertainty based on a temperature range of 300 to 350 K (0.3% = 0.003), assuming that a single-average (C_p) value is used to cover this temperature range.

- $\frac{dC_p}{C_p}$ = Uncertainty from the reference C_p data (0.5% = 0.005).

As with the density calculation, uncertainty in the specific heat term can be reduced by curve fitting the referenced specific heat data, and using the measured temperature at the flow meter to determine a more suitable density value. This approach reduces the overall uncertainty by eliminating the use of a single average value. However, it is seen that there is only a small uncertainty in the C_p value as a function of temperature, on the order of that for the reference data; therefore, the use of a single value is not a bad approach.

The specific heat uncertainty term can be approximated with maximum values by,

$$\left(\frac{dC_p}{C_p}\right)^2 = (0.003)^2 + (0.005)^2 \quad , \tag{35}$$

$$\left(\frac{dC_p}{C_p}\right) = 0.0058 \quad \text{or} \quad 0.58\% \quad . \tag{36}$$

Temperature Difference Uncertainty Determination

The temperature difference across the calorimeter (ΔT) is assessed using the expression from equation (15) and propagating errors. This measurement is strictly based on two thermocouple measurements as follows:

$$d\Delta T^2 = \left(\frac{\partial \Delta T}{\partial T_o}\right)^2 dT_o^2 + \left(\frac{\partial \Delta T}{\partial T_i}\right)^2 dT_i^2 \quad . \tag{37}$$

Find all partial derivatives listed in equation (37) by using equation (15):

$$\frac{\partial \Delta T}{\partial T_o} = 1 \tag{38}$$

and

$$\frac{\partial \Delta T}{\partial T_i} = -1 \quad . \tag{39}$$

Substitute the partials from equations (38) and (39) into equation (37), resulting in the following:

$$d\Delta T^2 = (1)^2 dT_o^2 + (-1)^2 dT_i^2 \quad . \tag{40}$$

Divide both sides by the temperature difference, resulting in the following:

$$\left(\frac{d\Delta T}{\Delta T}\right)^2 = \left(\frac{dT_o}{(T_o - T_i)}\right)^2 + \left(\frac{dT_i}{(T_o - T_i)}\right)^2 \quad . \tag{41}$$

Each of these terms can now be determined as,

- $\left(\frac{dT_o}{(T_o - T_i)}\right)^2$ = uncertainty in thermocouple measurement at outlet (2%=0.02)

- $\left(\frac{dT_i}{(T_o - T_i)}\right)^2$ = uncertainty in thermocouple measurement at inlet (2%=0.02).

The flow rate uncertainty term is

$$\left(\frac{d\Delta T}{\Delta T}\right)^2 = (0.02)^2 + (0.02)^2 \quad , \tag{42}$$

$$\left(\frac{d\Delta T}{\Delta T}\right) = 0.028 \quad \text{or} \quad 2.8\% \quad . \tag{43}$$

The uncertainty value for each of these independent thermocouples is based on the combined accuracy of both the thermocouple probe/wire and the reading device. This uncertainty can be improved if the thermocouples are used in a differencing mode with a common reading device, because the accuracy of the device is related to its ΔT (a small number) rather than to the accuracy of each absolute and independent measurement (large numbers). A typical ΔT measurement can have an accuracy approaching 1%, half that of a single thermocouple.

Overall Uncertainty Assessment

Collecting all the $\frac{d\dot{m}}{\dot{m}}$, $\frac{dC_p}{C_p}$, and $\frac{d\Delta T}{\Delta T}$ terms and substituting them into equation (25) results in the following expression:

$$\left(\frac{dQ}{Q}\right)^2 = \left[\left(\frac{d\rho}{\rho}\right)^2 + \left(\frac{dV}{V}\right)^2 + \left(\frac{dA}{A}\right)^2 + \left(\frac{dC_p}{C_p}\right)^2 + \left(\frac{dT_o}{(T_o - T_i)}\right)^2 + \left(\frac{dT_i}{(T_o - T_i)}\right)^2\right] . \tag{44}$$

In the case of a paddle-wheel-style flow meter setup (3%) with thermocouples for temperature measurement (2%), taking reference uncertainties for both C_p and ρ, and assuming curve fits, the overall uncertainty in power is as follows:

$$\left(\frac{dQ}{Q}\right)^2 = \left[(0.005)^2 + (0.03)^2 + (0.0)^2 + (0.0058)^2 + (0.02)^2 + (0.02)^2\right] \tag{45}$$

$$\left(\frac{dQ}{Q}\right) = 0.042 \quad \text{or} \quad 4.2\% \ . \tag{46}$$

In the case of a magnetic-style flow meter setup (0.3%) with thermocouples for temperature measurement (2%), the overall uncertainty in power is

$$\left(\frac{dQ}{Q}\right)^2 = \left[(0.005)^2 + (0.003)^2 + (0.0)^2 + (0.0058)^2 + (0.02)^2 + (0.02)^2\right] , \tag{47}$$

$$\left(\frac{dQ}{Q}\right) = 0.029 \quad \text{or} \quad 2.9\% \ . \tag{48}$$

The uncertainty bars for the setup using a paddle-wheel flow meter are approximately 45% wider than those for the magnetic meter configuration. If the thermocouples used to measure the temperature are configured in a delta temperature arrangement (1%), the uncertainty for the paddle-wheel configuration is reduced as given by the following:

$$\left(\frac{dQ}{Q}\right)^2 = \left[(0.005)^2 + (0.03)^2 + (0.0)^2 + (0.0058)^2 + (0.01)^2\right] , \tag{49}$$

$$\left(\frac{dQ}{Q}\right) = 0.033 \quad \text{or} \quad 3.3\% \ . \tag{50}$$

The uncertainty is reduced by approximately 20%, a small value since the overall uncertainty is dominated by the flow meter velocity calculation. A similar assessment for the magnetic flow meter can be performed as follows:

$$\left(\frac{dQ}{Q}\right)^2 = \left[(0.005)^2 + (0.003)^2 + (0.0)^2 + (0.0058)^2 + (0.01)^2\right] , \tag{51}$$

$$\left(\frac{dQ}{Q}\right) = 0.013 \quad \text{or} \quad 1.3\% \ . \tag{52}$$

Since the temperature term carries the largest weight of any of the factors, there is nearly a 60% reduction in the overall uncertainty.

Summary

For all the cases examined, flow meter and temperature types, the maximum overall uncertainty in the calorimeter power is expected to be on the order of 5%, which translates to 50 W out of 1,000 W for the low-powered test case, and 250 W out of 5,000 W for the high-powered case. An error of this magnitude is certainly acceptable for the level of operation expected for the heat pipe evaluations; therefore, the final selection of measurement devices should be performed based on a combination of cost and durability (lasting up to 3 years). Paddle-wheel-type flow meters cost approximately $1.4k each and have the benefit of including both a temperature and pressure measurement, while magnetic meters cost up to $2.4k each for the planned heat pipe system.

APPENDIX L—RADIO FREQUENCY INDUCTIVE COIL ASSEMBLY CONTRACTOR REPORT

Fluxtrol® Inc.
1388 Atlantic Blvd.
Auburn Hills, MI 48326
Telephone: 248–393–2200/Fax: 248–393–0277

Date: June 3, 2005
Project name: Radio Frequency Induction Coil Assembly
Customer: NASA MSFC
Project type: Induction coil development
Process type: Heating for device validation
Author: Robert Goldstein

Background

This report contains the results of the computer simulation design phase. The report is for "Final Modeling of the Configuration of the RF Inductive Coils." This modeling should be used as a basis for engineering and manufacturing induction coils that fit the project specifications.

Fluxtrol, Inc. is an induction company specializing in advanced induction coil design including computer simulation, induction coil manufacturing, and magnetic flux control. Fluxtrol manufactures Fluxtrol and Ferrotron products, which are the primary materials used for RF induction heating magnetic flux control.

The induction coil assemblies for the heat pipe testing should be reliable to meet the stringent demands of the testing procedure. The test coils should run maintenance-free for a period of 3 years in a low-pressure environment, with or without a load. This means that careful calculation of the power that needs to be removed from the induction coil is required to ensure reliable performance.

Design Considerations

Computer Modeling and the Role of Magnetic Flux Controllers

The heat pipe test configuration, shown in figures 24 and 25, maximizes space utilization within the test chamber and minimizes the number of test chambers required. To accomplish this, the following issues must be considered:

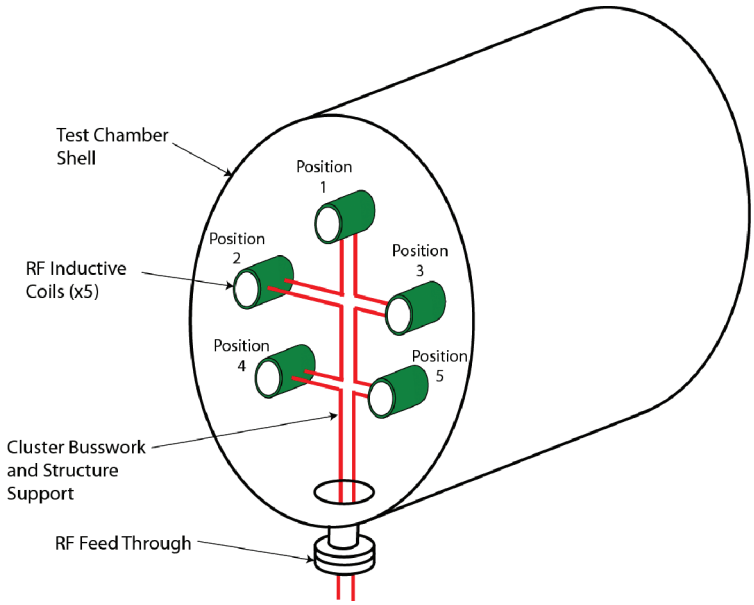

Figure 24. General layout RF inductive coil assemblies (cluster with five positions).

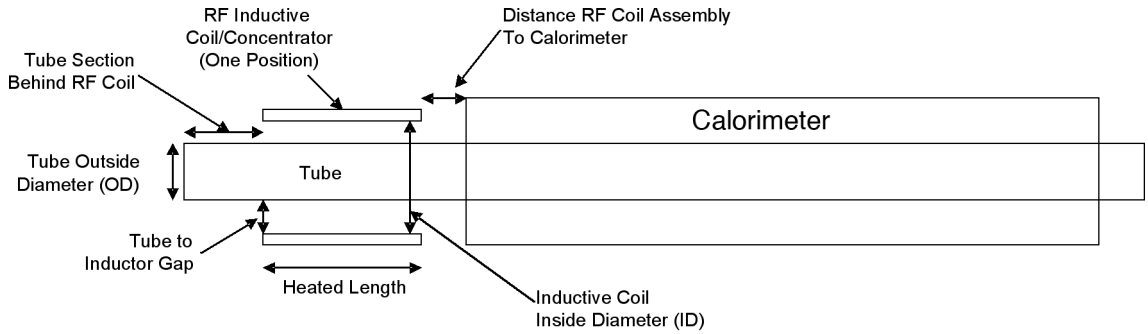

Tube Material is a Mo-Re alloy
Tube wall thickness = 0.050 inch
Heated Length = 2.75 to 3 inches
Tube length behind RF Coil = 1 to 1.5 inch
RF coil to Calorimeter Spacing = 0.2 to 0.25 inch (Required Visble Path Cannot Be Blocked)
Tube Temperatures 1150 to 1400 K
RF Coil ID to Tube OD adjusted to maximize efficiency and minimize thermal loss/voltage breakdown

Figure 25. General dimensional layout of a single RF inductive coil position.

- Variation in azimuthal power-density distribution, due to mutual inductance of adjacent inductors.
- Variation in azimuthal power-density distribution, due to proximity to the chamber wall.
- Power induced in the water-cooling calorimeters.

Flux® 2D software was used for two-dimensional electromagnetic computer simulation to evaluate the level of these influences on a 5/8-in OD Mo-Re (50% Mo) heat pipe tube with a 0.05-in wall thickness and liquid Na inside at a temperature of 1,000 °C. Flux 2D is a two-dimensional, finite element code for simulation of induction heating systems. Flux 2D is written and developed by the Cedrat Group (www.cedrat.com) based in Grenoble, France. Magsoft Corporation (www.magsoft-flux.com) based out of Ballston Spa, NY, is the U.S. distributor of the software.

The RF frequency used for the simulation was 50 kHz. Magnetic field lines from the simulation demonstrate the mutual inductance between a neighboring coil 3.5-in center-to-center (fig. 26(a)), and without a neighbor (fig. 26(b)) using Fluxtrol 50 magnetic flux controller. Figure 27 shows the same conditions without a magnetic flux controller. The results, contained in table 18, indicate that without a magnetic flux controller the variation in power around the circumference of the heat pipe will be greater than 5%. With Fluxtrol 50 applied, the variation will be a very small percentage of the overall power.

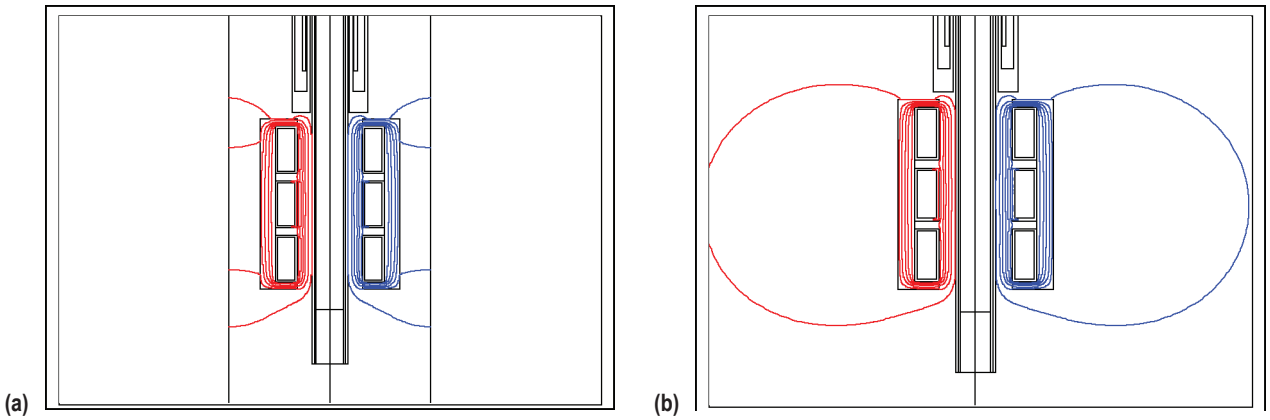

Figure 26. Magnetic field lines (a) with and (b) without a neighboring inductor for a three-turn coil with Fluxtrol 50 magnetic flux controller.

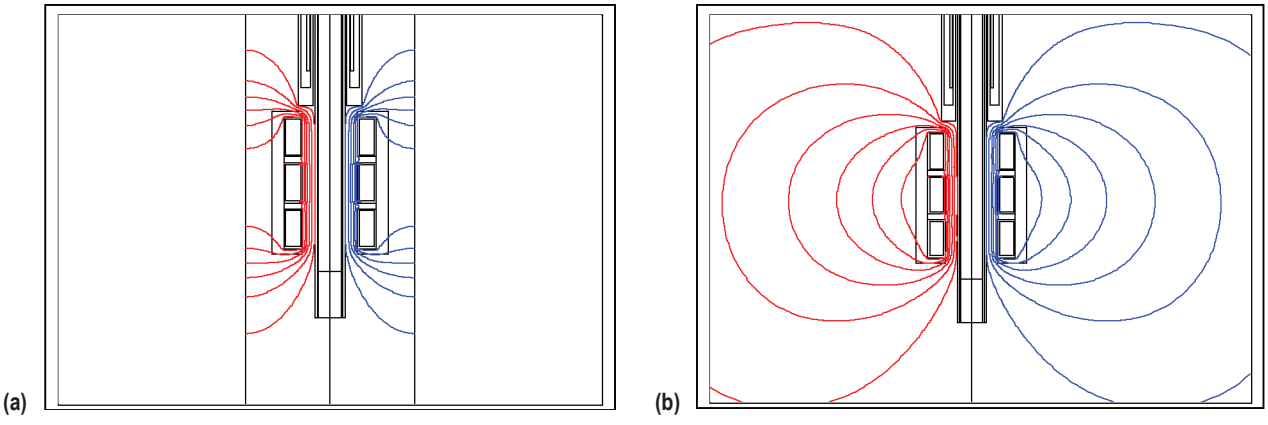

Figure 27. Magnetic field lines (a) with and (b) without a neighboring inductor for a three-turn coil without a magnetic flux controller.

Table 18. Results of two-dimensional simulation for 5/8-in OD Mo-Re heat pipe tube with 0.05-in wall thickness.

Frequency (Hz)	Boundary Type	Concentrator Type	Electrical Efficiency	Cal. Losses (W)	Pipe Power (W)	Total Power (W)	Coil Current (A)	Coil Voltage (V)
50,000	Infinity	Fluxtrol 50	66.9%	5.5	3,000	4,484	1,385	31.2
50,000	Infinity	None	65.5%	61.5	3,000	4,582	1,575	30.5
50,000	Close	Fluxtrol 50	66.9%	5.7	3,011	4,499	1,385	31.2
50,000	Close	None	65.7%	66.3	3,179	4,841	1,575	29.7

The results also show that when Fluxtrol 50 is applied, power induced in the heat pipe reduces the heat induced in the calorimeter by approximately a factor of 10. It is necessary to limit and quantify the power induced in the calorimeter, since it will result in an error when measuring the heat pipe power throughput by water flow rate and temperature difference.

Besides the value of power induced in the calorimeter, the calorimeter also shunts the power induced in the heat pipe on the side closest to it. For a coil without a concentrator, this effect exaggerates the naturally occurring reduction in power density for the outer turns. When Fluxtrol 50 is applied, this effect is reduced and power density is more uniform along the evaporator length, nearly the same on the calorimeter and terminal side. Figure 28 shows the relative power density distribution in the heat pipe for these two cases.

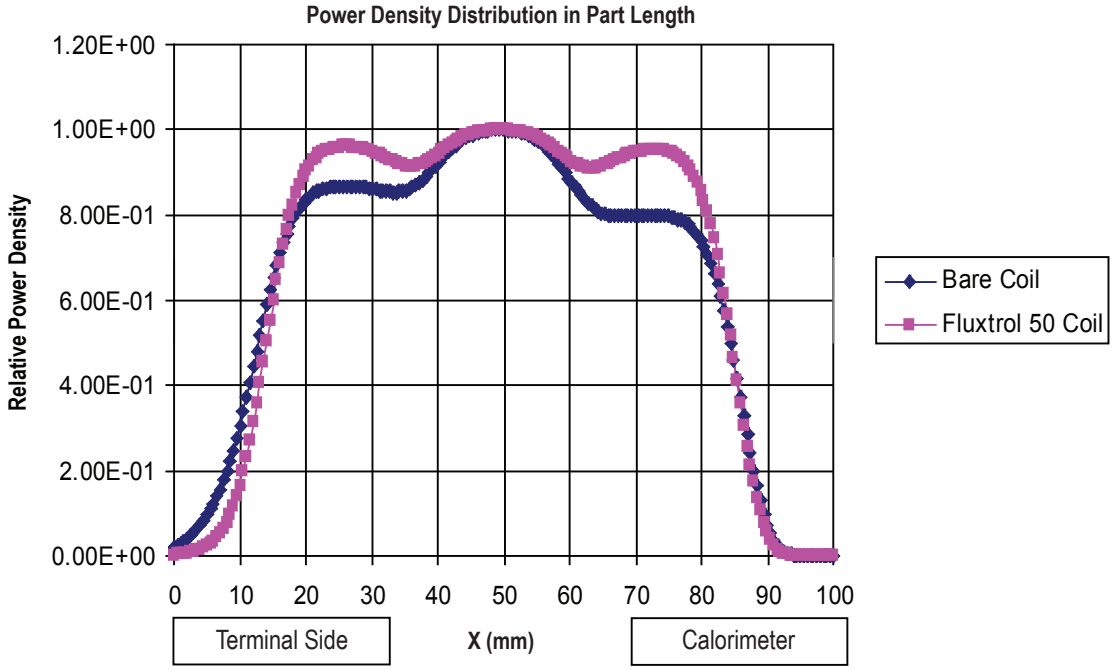

Figure 28. Axial power-density distribution in the heat pipe.

Voltage Breakdown

The DC voltage breakdown potential is shown in figure 29 in the form of Paschen curves. These curves are shown for various atmospheres at different pressure distance products. As atmospheric pressure increases, the breakdown voltage increases dramatically. Also, as the pressure distance product rises, breakdown voltage also increases. Voltage breakdown can be prevented either by limiting applied voltage, increasing the distance between components, or providing proper physical insulation of live components. Voltage breakdown levels are frequency dependent; however, operation at 50 kHz can be approximated as a DC potential. The factors that determine the voltage are as follows:

- Frequency.
- Busswork.
- Induction coil design.
- Power in the heat pipe.

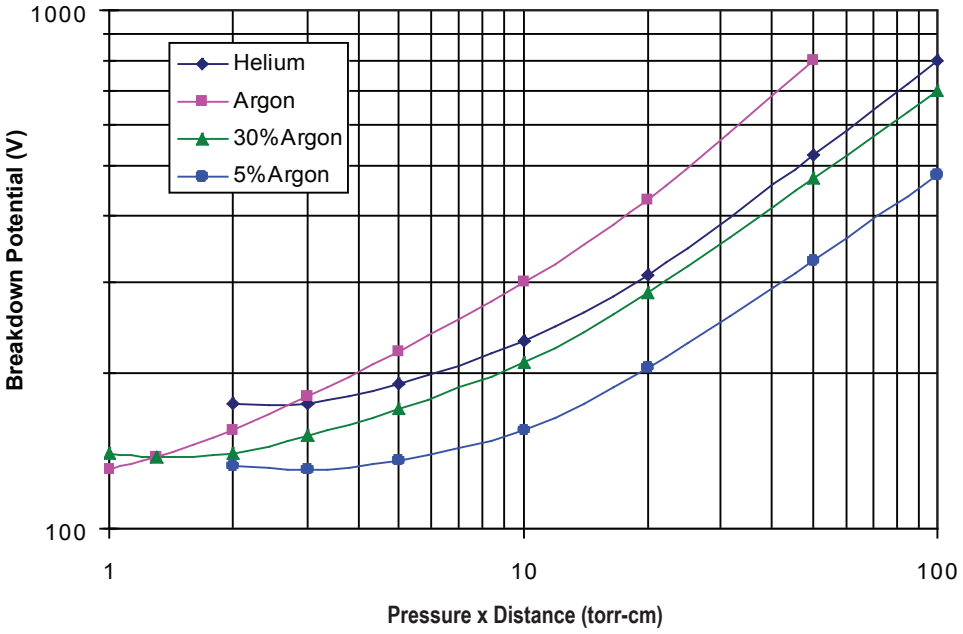

Figure 29. DC breakdown voltages in various atmospheres.

There will be different voltages in different areas of the heat pipe RF assembly, since all components are connected in series. The highest voltage will be at the output of the power supply, but this will be at one atmosphere, and the levels of acceptable voltage are much higher. Inside the chamber, the highest voltage will be at the feedthrough outputs/busswork input. Physical insulation should be provided for the busswork components to prevent breakdown; however, sufficient spacing is necessary in the connection areas to allow for electrical hookup.

The biggest determinant of the total voltage for a well-designed assembly is the induction coil geometry and frequency. Figure 30 illustrates the relationship between coil head voltage and frequency for five single-turn induction coils connected in series with selected coupling gaps as predicted by ELTA, a one-dimensional computer simulation program. The induction coil voltage not only depends on the coupling gap, but also upon the number of turns. If we assume that the system is linear, then for the same power the voltage will be directly proportional to the number of turns, with corresponding inverse dependence of coil current.

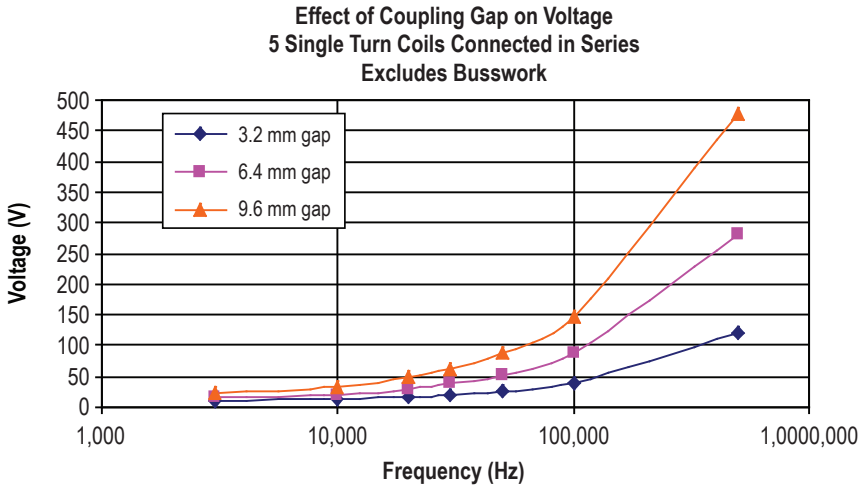

Figure 30. Relationship between voltage and frequency for various coupling gaps.

The final induction coil geometry should be tested with respect to the selected induction power supply. For example, a minimum voltage is required to properly match the coils to the induction power supply. At a given power level, increasing the number of coils requires higher coil head voltages and a corresponding lower coil current, reducing losses in the power supplying the circuitry (busswork, transformer, etc.). At the same time, the breakdown voltage is strongly dependent upon chamber pressure and gap distance. The best compromise between coil geometry and system efficiency should be determined for each test chamber.

Heat Transfer in the System

When designing the induction coils, it is important to keep in mind that the required RF power induced in the pipes does not include thermal losses. This is only the value that is transferred to the calorimeter in the tests. The real power necessary in a given heat pipe is the required RF power plus the heat transfer (loss) from the evaporator to the induction coil. Radiation and conduction are the two components for heat transfer to the induction coil. The heat loss values are independent of the required RF power.

There are three dominant factors that influence the thermal losses from the heat pipe to the RF inductor: (1) Emissivity of the coil surface, (2) coil to work piece coupling gap, and (3) temperature of the heat pipe. Radiant heat transfer is mainly dependent upon the coil surface emissivity, and is proportional

to the 4th power of the absolute temperature. Conductive heat transfer is dependent upon the coil to work piece coupling gap and the evaporator to induction coil temperature difference. Figure 31 shows heat loss to the RF coil, as a function of gap, for a heat pipe with a temperature of 1,373 K, based upon calculations made by Jim Martin of NASA.

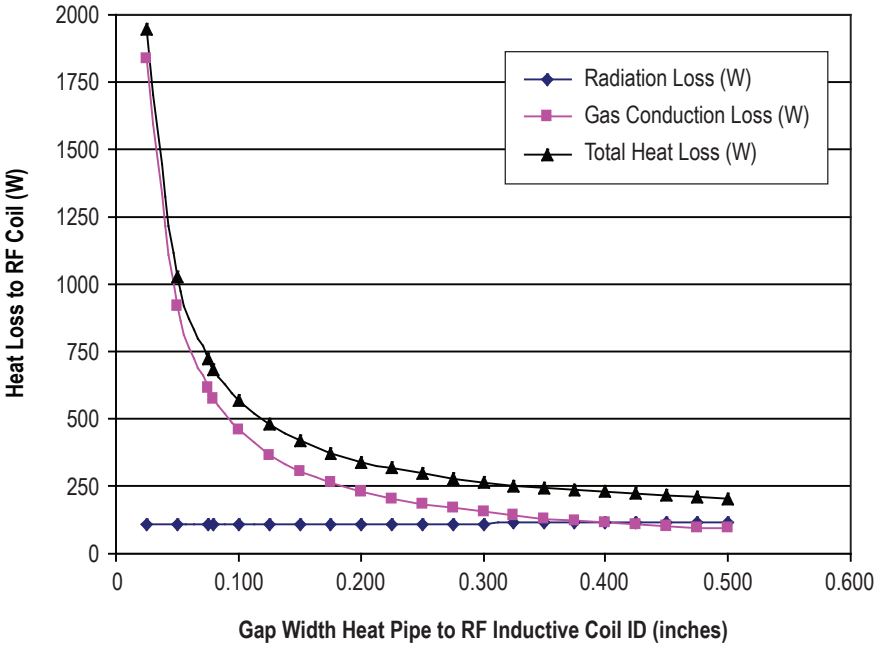

Figure 31. Heat transferred from heat pipe to induction coil (curves based upon calculations and information provided by Jim Martin from NASA for 1,373 K heat pipe temperature).

Design of Assemblies

RF Assembly 1

RF assembly 1 consists of all G-series heat pipes. The atmosphere in the chamber is He-32%Ar at 75 torr. All of these heat pipes should be at 1,273 K and the power transferred to the calorimeter should be 3,000 W. At these conditions, the thermal losses for a 0.25-in coupling gap will be ≈250 W. This means the required RF power will be 3,250 W for each heat pipe.

Since the power requirement to all heat pipes is the same, all of the induction coils should be of an identical design. The parameters of the three-turn coil with a Fluxtrol 50 concentrator, described earlier in this TP, fit well to the requirements for the G-series. The system is nearly linear and required voltage and current are proportional to the root square of the power. To deliver the required 3,250 W of RF power of to the heat pipe, each individual coil will require a voltage around 33 V and carry a current of around 1,450 A. The power in each inductor head will be ≈4,910 W.

To design the assembly, it is also necessary to take into account the busswork. The primary parameters for determining busswork performance are the busswork height and the gap between adjacent conductors. The conductor thickness, provided it is electrically thick, influences the mechanical strength and weight of the assembly.

Taller busswork and smaller gaps are beneficial for reducing voltage drop. Optimal busswork, in terms of voltage drop, would be infinitely tall with zero gap. This is not practical and dimensions are required that fit well to the system size and available space. For the busswork height, it is natural to initially set it equal to the coil length (3 inches). The gap between the conductors should depend upon the breakdown voltage in this area.

Based upon the supplied Paschen curves, breakdown voltage in the He-30%Ar chamber at various gaps should be approximately as follows:

- 2-mm gap—250 V
- 3-mm gap—310 V
- 6-mm gap—450 V

Table 19 shows the electrical parameters for 3-in tall busswork carrying a current of 1,450 A at 50 kHz.

Table 19. Electrical parameters per meter for 3-in-tall busswork carrying 1,450 A at 50 kHz.

Gap (mm)	Current (A)	Voltage Drop (V/m)	Losses (W/m)	Reactive *P* (kVA/m)
2	1,450	17	3,110	24.4
3	1,450	23	3,040	33.9
6	1,450	42	2,900	60.8

A conceptual layout of the test chamber RF coil assembly is shown in figure 32. There are different voltages at various points within the RF assembly. Because the coils are connected in series to ensure uniform loading and insensitivity to the presence of a heat pipe, the voltage in area 1 is the highest and represents the full-voltage drop on all coils and busswork inside the chamber. The voltage in area 2 is significantly less than in area 1, because it does not include the voltage drop for the G1 and G5 heat pipe inductors, plus their respective connection zones. The voltage in area 3 is lower still, representing the connection zone voltage and the individual coil head voltage. If a uniform length connection buss were used, the RF assembly 1 area 3 voltage would be the same at all coils.

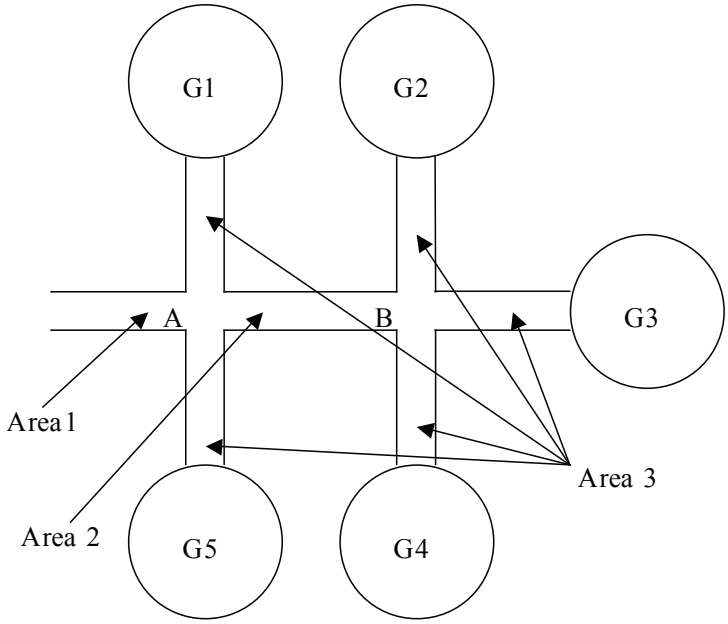

Figure 32. Conceptual layout of the heat pipe inductive coil assembly.

The voltage drop, losses, and reactive power in a given section of busswork are all directly proportional to the length of that section. For this reason, it is beneficial to make all the sections of busswork as short as possible. From a practical sense, the following need to be considered for the respective areas:

- Area 1—Distance from chamber ceiling/floor to assembly.
- Area 2—Space between coil heads.
- Area 3—Space for making electrical and water connections.

To calculate losses for the whole assembly, each of the areas must be assessed. The first step for area 3 is to determine the length and acceptable portion of the connecting busswork. Based upon estimates from coil manufacturing specialists, a 7.5-cm distance is a reasonable estimate for minimum length. The individual coil head voltages are 33 V. For this level of voltage, a 2- or 3-mm gap with break down voltages of 250 V and 310 V, respectively, can be safely used. The voltage drop would be less than 2 V for the 7.5-cm busswork, for a total section voltage of around 35 V. Losses in this section of busswork are ≈230 W.

At point B in figure 32, the coil voltage should be around 105 V (3×35 V). This voltage is still relatively low, and a 2- or 3-mm gap may be used in area 2. The length of area 2 should be equal to the OD of an induction coil plus sufficient space for limiting mutual inductance. Figure 32 and table 20 show that if the length of area 2 is 3.5 in (8.9 cm), there will be minimal variation in circumferential heating of the heat pipe. This means the voltage drop in area 2 will be around 2 V and losses will be ≈270 W.

Table 20. Electrical parameters of RF inductor assembly 1.

Component	Gap (mm)	Length (cm)	Turns	Voltage Drop (V)	Power (W)	Reactive Power (kVA)
G1 Inductor	6.4	NA	3	33	4,860	47.9
G1 Buss	3.0	7.5	NA	2	230	2.9
G2 Inductor	6.4	NA	3	33	4,860	47.9
G2 Buss	3.0	7.5	NA	2	230	2.9
G3 Inductor	6.4	NA	3	33	4,860	47.9
G3 Buss	3.0	7.5	NA	2	230	2.9
G4 Inductor	6.4	NA	3	33	4,860	47.9
G4 Buss	3.0	7.5	NA	2	230	2.9
G5 Inductor	6.4	NA	3	33	4,860	47.9
G5 Buss	3.0	7.5	NA	2	230	2.9
Area 2	3.0	8.9	NA	3	270	4.4
Area 1	6.0	7.5	NA	3	230	4.4
Total Value	**NA**	**NA**	**NA**	**180**	**25,950**	**263**

At point A in figure 32, the coil voltage should be around 177 V (5×35 V+2 V). This voltage is probably too high to safely use a gap of only 2 mm, but 3 mm should be sufficient. If the distance from point A to the chamber feedthrough is assumed to be 7.5 cm, the voltage drop in this section should be around 2 V and the losses ≈230 W. If a 6-mm gap was used, the voltage drop would be around 3 V and losses ≈230 W.

Due to the small difference, it may be better to use the larger 6-mm gap in area 1 for a breakdown voltage close to 450 V and a higher safety factor. Total coil voltage would be 180 V and total inductor power would be ≈26 kW. The values for all components are summarized in table 20.

RF Assembly 2

RF assembly 2 consists of two G-series and three F-series (0, –1, –2) heat pipes. The atmosphere in the chamber is He-32%Ar at 75 torr. For all of these heat pipes, the power transferred to the calorimeter should be 3,000 W. Three heat pipes should be at 1,273 K and the other two heat pipes at 1,173 and 1,373 K, respectively.

The temperature in the heat pipe has an influence upon the required RF power, because it changes the thermal losses from the heat pipe to the induction coil. As stated earlier, radiation heating is proportional to the 4th power of temperature and convective heating should be directly proportional to the temperature difference. For the two G-series heat pipes and the F(0) heat pipe, thermal losses with a ¼-in gap would be 250 W, leading to a required RF power of 3,250 W—the same as RF assembly 1. For F(–1), with a temperature of 1,173 K, thermal losses would be reduced to 207 W, leading to a required RF power of 3,207 W with the same ¼-in coupling gap. For F(–2) with a temperature of 1,373 K, thermal losses would be 295 W with a required RF power of 3,295 W. The difference between the required RF power for this assembly is ±45 W or around 1.5%. Based upon the magnitude of this effect, it is better to maintain

consistency by using the same inductor for each case, and balance the temperature with the calorimeter static gas gap by a slight adjustment of the coolant flow. Therefore, the RF assembly 2 design is identical to RF assembly 1.

RF Assembly 3

RF assembly 3 consists of five F-series (–3, 1, 2, 3, 4) heat pipes. The atmosphere in the chamber is He-32%Ar at 75 torr. All five of these pipes have at least one factor (temperature or power) different from the others in the test chamber. The required power and temperature for these heat pipes are detailed in table 21.

Table 21. Description of RF assembly 3 heat pipes.

Heat Pipe	Calorimeter Power (W)	Heat Pipe Temperature (K)
F(–3)	1,000	1,273
F(1)	2,000	1,223
F(2)	4,000	1,223
F(3)	2,000	1,323
F(4)	4,000	1,323

In RF assembly 2, there was only a relatively small change in the required RF power for a ±100 K change in temperature. Heat pipes F(1) and F(3) represent a similar situation with a ±50 K temperature difference, and the same can be said of F(2) and F(4). For this reason, these heat pipes can be paired up and only three unique coils designs are required to satisfy the 1,000-, 2,000-, and 4,000-W power levels. A mean heat pipe temperature of 1,273 K will be used for the 2,000- and 4,000-W heat pipes.

A conceptual layout of the RF assembly in the test chamber is shown in figure 33. The coils are all connected in series to ensure insensitivity to the presence of a heat pipe, and the coil length maintained constant to keep power densities proportional to heat pipe power. Therefore, the three available methods to control the power delivered to the respective heat pipes include: (1) Number of coil turns, (2) coupling gap between coil and heat pipe, and (3) distance between the coil liner and heat pipe.

When the coil length, space factor (ratio of copper length to total coil length), and coupling gap are held constant, the power induced in the heat pipe will be proportional to the ratio of the number of turns squared. This should be the primary method of power balance between the different heat pipes.

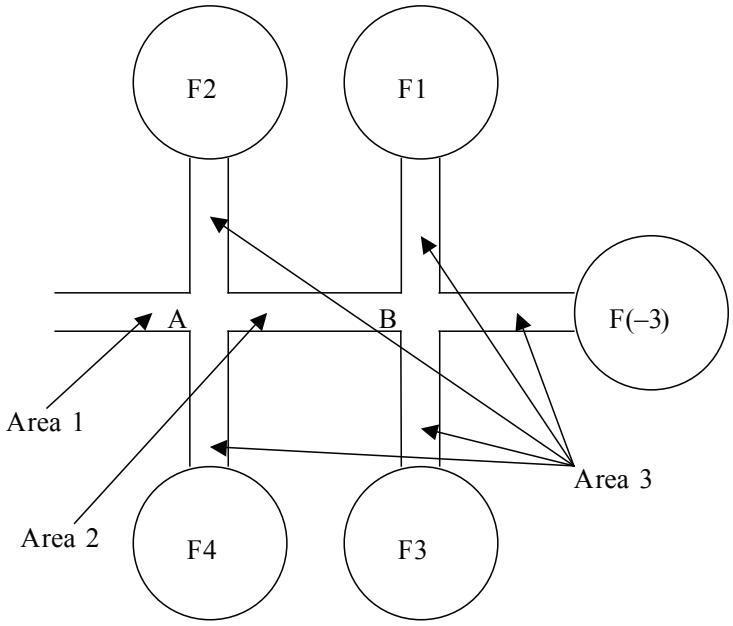

Figure 33. Conceptual layout of the RF inductor assembly 3.

The coupling gap also influences the power induced in a given heat pipe, but not as strongly as the number of turns, since there are the same number of ampere turns. As the coupling gap is increased, the power will slowly decrease. The opposite will occur if the coupling gap is decreased. At the same time though, as the coupling gap increases, the coil voltage will dramatically increase, leading to higher reactive powers and larger gaps required for the busswork. Finally, if the coupling gap gets much larger than ¼ in, heating of the calorimeter will increase, and power-density uniformity in the coil length will decrease.

The last factor, distance between the coil liner and heat pipe, is new, and is used to match the required RF power to the induced power from the inductor, in effect, adjusting the thermal losses. For this, a new factor is introduced called the potting gap, to separate this value from the classic electromagnetic coupling gap. The two parameters are shown in figure 34.

An iterative process to adjust the three factors was used until a solution was achieved that balanced these three factors. The assumption was made that the surface temperature of the liner would be 350 K in all cases. This will not be the case in reality, because as the temperature difference between the coil liner and the coil copper ID grows, the liner temperature will increase. This will have some effect upon the conductive losses but the difference should be relatively small in terms of required RF power, provided the liner has reasonably good thermal conductivity.

The final design utilizes a three-turn inductor for the 1,000-W heat pipe (F–3), four-turn inductors for the 2,000-W heat pipes (F1 and F3), and five-turn inductors for the 4,000-W heat pipes (F2 and F4). The necessary design factors are shown in table 22. The desired RFP in the table is the required RF power based upon adding the heat pipe/calorimeter power to the thermal losses. The actual RFP is the value of power from the computer simulation for that geometry. The goal is for these

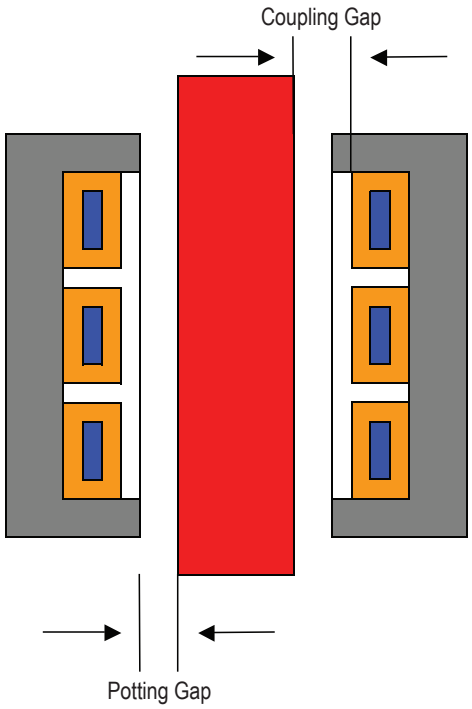

Figure 34. Conceptual induction coil head cross section.

two values to converge. The coil parameters in table 22 achieve the desired conformance within a convergence of approximately 1%. The values for the actual heat pipe RF assembly 3 will be slightly larger due to different heat pipe temperatures, but this can be compensated for by adjusting calorimeter properties.

Table 22. Parameters of RF assembly 3.

Cal. Power (W)	Coup. Gap (mm)	Potting Gap (mm)	Therm. Loss (W)	Desired RFP (W)	Turns	Actual RF Power (W)	Ind. Power (W)	Coil I (A)	Coil U (V)
1,000	6.4	3.2	490	1490	3	1490	2190	990	22
2,000	6.4	2.0	680	2680	4	2660	3920	990	39
4,000	5.4	5.4	330	4330	5	4360	6260	990	52

The mean coil voltages for RF assembly 3 are higher due to the larger turns number. On the other side, the coil current is significantly lower than in RF assemblies 1 and 2 (990 A compared to 1,450 A). This means that the voltage drop in the busswork will be lower proportionally, and the losses in the busswork will drop as the square of current, allowing for the use of larger gaps without significant penalty.

The same section lengths used for RF assemblies 1 and 2 can be used to calculate the whole assembly. The difference in RF assembly 3 is that there are new voltages for each of the different coil heads. Fortunately, even the highest voltage (52.1 V) is well below the breakdown voltage for the 2-mm gap (250 V), allowing the use of uniform area 3's for all cases. The voltage drop in area 3 of the busswork will be around 1.4 V for each inductor head, due to the lower coil current. Losses in these sections of busswork are ≈110 W each.

To determine the voltage at point B in figure 33, the final arrangement of the inductors must be decided. Point A will see the same voltage regardless of the inductor/heat pipe arrangement. The most favorable arrangement for point B is to have the lowest voltage coils in the last three positions. This means F(–3), F(1), and F(3) heat pipes should be placed here to reduce area 2 busswork requirements. The voltage at point B should be around 104 V (22 V+2×39 V+3×1.4 V), which is still relatively low, and a 2- or 3-mm gap may be used in area 2. The voltage drop in area 2 would be around 1.7 V with losses of ≈130 W.

The point A coil voltage (fig. 33) should be around 212 V (104 V+2×1.4 V+1.7 V+2×52 V). This voltage is probably too high to safely use a gap of only 2 mm, but 3 mm should be sufficient. Assuming the distance from point A to the chamber feedthrough is 7.5 cm, the voltage drop in this section would be around 1.4 V and the losses ≈110 W. The voltage drop using a 6-mm gap would be around 2 V and losses ≈110 W.

Due to the small difference, it may be better to use the larger 6-mm gap in area 1 for a higher safety factor, with a breakdown voltage close to 450 V. The total coil voltage would be 214 V and the total inductor power would be ≈23 kW. Values for all of the components are summarized in table 23.

RF Assembly 4

RF assembly 4 is much simpler than the previous assemblies, because it consists of a single inductor and heat pipe (F–4) as shown in the conceptual layout in figure 35. The heat pipe power is 5,000 W with a He-6%Ar chamber atmosphere, instead of the He-32%Ar gas mixture used in the other test chamber setups. Breakdown voltages for this atmosphere are lower than for the other chambers, but it should not present a problem since only one coil and buss system are required.

In addition, this unit is connected to a smaller power supply, where lower voltages are favorable for coupling. The optimal voltage for matching to this unit is in the 50–100 V range. For this reason, the same induction coil used for the F4 and F5 heat pipes fits well. It is only necessary to recalculate the values for the new power level, as shown in table 24.

To assess the losses on the complete assembly, only a single section of busswork needs to be evaluated. The busswork should be ≈6 in (15 cm) long to center the coil in the test chamber. Due to the relatively low voltage, 2- or 3-mm busswork can be used. Voltage drop in the busswork will be around 3.1 V, and losses in these busswork sections are ≈270 W. Details of this assembly are contained in table 25.

Table 23. Electrical parameters of RF inductor assembly 3.

Component	Gap (mm)	Length (cm)	Turns	Voltage Drop (V)	Power (W)	Reactive Power (kVA)
F–3 Inductor	6.4	NA	3	22	2,190	21.8
F–3 Buss	3.0	7.5	NA	1.4	110	1.4
F1 Inductor	6.4	NA	4	39	3,920	38.6
F1 Buss	3.0	7.5	NA	1.4	110	1.4
F3 Inductor	6.4	NA	4	39	3,920	38.6
F3 Buss	3.0	7.5	NA	1.4	110	1.4
F2 Inductor	5.4	NA	5	52	6,260	51.5
F2 Buss	3.0	7.5	NA	1.4	110	1.4
F4 Inductor	5.4	NA	5	52	6,260	51.5
F4 Buss	3.0	7.5	NA	1.4	110	1.4
Area 2	3.0	8.9	NA	1.7	130	1.7
Area 1	6.0	7.5	NA	1.4	110	2
Total Value	NA	NA	NA	212	23,340	213

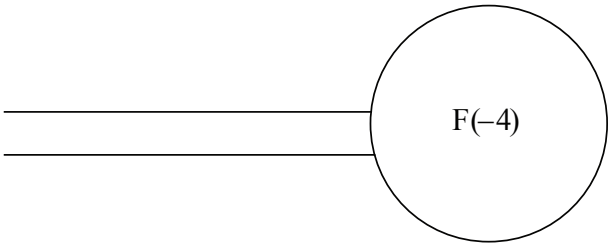

Figure 35. Conceptual layout of the RF inductor assembly 4.

Table 24. Recalculating five-turn inductor for use in RF assembly 4 configuration.

Cal. P (W)	Coup. Gap (mm)	Pot. Gap (mm)	Therm. Loss (W)	Turns	Required RF Power (W)	Electrical Efficiency	Ind. Power (W)	Coil I (A)	Coil U (V)
4,000	5.4	5.4	330	5	4,360	69.6%	6,260	990	52
5,000	5.4	5.4	330	5	5,360	69.6%	7,650	1,090	57.5

Table 25. Electrical parameters of RF inductor assembly 4.

Component	Gap (mm)	Length (cm)	Turns	Voltage Drop (V)	Power (W)	Reactive Power (kVA)
F–3 Inductor	5.4	NA	5	57.5	7,650	62.7
F–3 Buss	3.0	15	NA	3.1	270	3.4
Total Value	NA	NA	NA	60.6	7,920	66.1

Summary

Four RF assemblies for heat pipe testing have been designed. The operational parameters of each set of RF assemblies matches well to the power supply that they are connected. The required voltages for all test chamber configurations are at reasonable levels and are well below, typically by a factor of 2, the breakdown levels predicted by the Paschen voltage breakdown curves.

Engineering of the final assemblies is still required before fabrication can begin. Also, the design for connecting the power supplies to the chambers must still be finalized. This requires input from NASA on the complete system layout and exact RF power supply output parameters. External to the test chambers, few space restrictions should allow the power supplies to be closely coupled, lowering transmission losses. In addition, the projected power requirements are well within the range of the 50 kW units identified for this task.

Table 25 can be used to effectively determine the effect the busswork will have on the electrical parameters of RF assemblies 1 and 2. The values only need to be recalculated based upon the length. The RF assembly 3 voltage drop per meter and power loss per meter should be multiplied by 0.68, due to the lower current, while RF assembly 4 values should be multiplied by 0.75.

APPENDIX M—MO-44.5%RE PLATE MATERIAL ANALYSIS

Rhenium Alloys, Inc. provided the following material information for the Mo-44.5%Re plate material procured to support welding tests. The material consisted of two plates with dimensions of 12 in length by 3 in width by 0.04 in thickness.

RHENIUM ALLOYS, INC.

1329 Taylor St.
P.O. Box 245
Elyria, Oh 44036-0245
Voice (440) 365-7388
Fax (440) 366-9831

MATERIAL CERTIFICATION

DATE: February 16, 2005

SOLD TO: Marshall Space Flight Center
Central Receiving Building 4471
Huntsville, AL 35812

PURCHASE ORDER: Master Card

MATERIAL: Moly/44.5%Re

This is a shipment against your order # Master Card which completes the requirement for the Moly/44.5%Re sheet .004" thick. The Moly/44.5%Re sheet meets the requirements of our typical .004" specifications.

Lot number MR-1254

Todd Leonhardt
Director of Technology

Rhenium Alloys, Inc
Yesterday's Pioneer, Today's Leader
Email: rhenium@rhenium.com
Web Page: http://www.rhenium.com

RHENIUM ALLOYS, INC.

1329 Taylor St.
P.O. Box 245
Elyria, Oh 44036-0245
Voice (440) 365-7388
Fax (440) 366-9831

Report No. B-843

Customer Name

Marshall Space Flight Center
Central Receiving Building 4471
Huntsville, AL 35812

Subject

Molybdenum 44.5% Rhenium sheet 0.040" thick. Lot # MR-1254

Submitted to Our Laboratory on Purchase Order Number- Master Card

Rhenium Alloy, Inc
Email: rhenium@rhenium.com
Web page at http://www.rhenium.com

REPORT NO. B-843

BACKGROUND

Samples identified as Molybdenum 44.5% Rhenium sheet 0.040" thick. lot number MR-1254 was submitted to our laboratory.

TEST REQUESTED

Grain Size and Microhardness

TEST RESULTS

MICROHARDNESS TEST

Microhardness was performed in accordance with ASTM E384 using a Vickers diamond indentor with a **500**-gram load for **15**sec.

Avg. Vickers microhardness was **282.3 ±3.8 VHN**

GRAIN SIZE EXAMINATION

The submitted specimen was prepared in accordance with ASTM E3-95 for grain size. The sample was examined at **100X** for grain size determination. The average grain size was rated in accordance with the ASTM E112-96 comparison method for determining grain size.

The average grain size was **6**

Rhenium Alloys, Inc
Email: rhenium@rhenium.com
Web site: http://www.rhenium.com

REPORT NO. B-843

PHOTOGRAPH

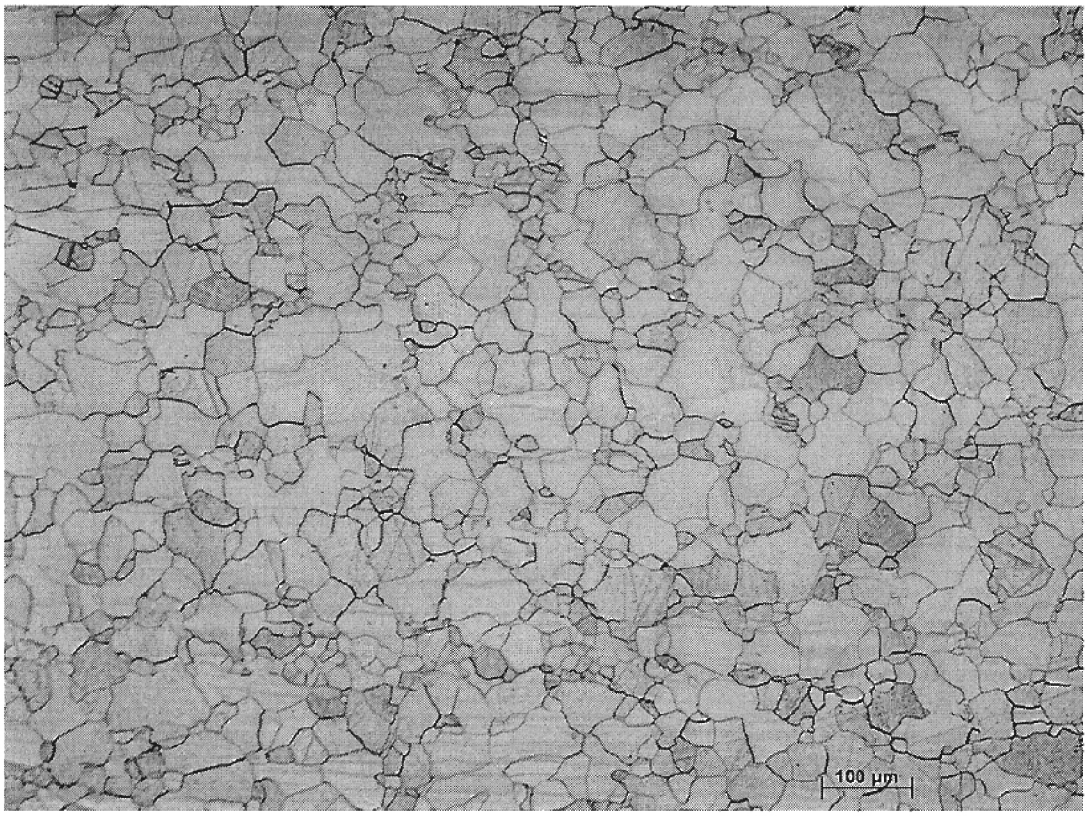

Magnification of photo: 100X

Etchant: Modified Murakami's Reagent

This is a representative view of the microstructure from the submitted sample.

Rhenium Alloys, Inc
Email: rhenium@rhenium.com
Web site: http://www.rhenium.com

REPORT NO. B-843

PHOTOGRAPH

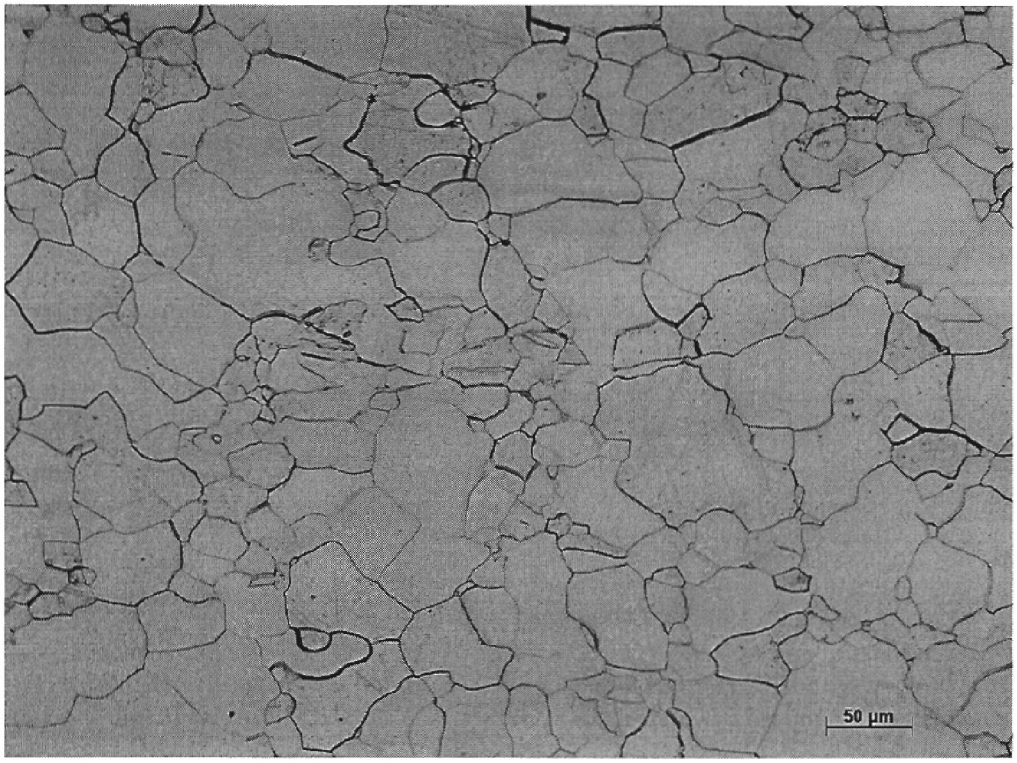

Magnification of photo: 200X

Etchant: Modified Murakami's Reagent

This is a representative view of the microstructure from the submitted sample.

Respectfully,

for

Todd A. Leonhardt
Director of Research and Development

Rhenium Alloys, Inc
Email: rhenium@rhenium.com
Web site: http://www.rhenium.com

IMR TEST LABS
A Division of Ithaca Materials Research & Testing Incorporated

131 Woodsedge Drive
Lansing Business & Technology Park
Lansing, NY 14882

Phone 607.533.7000 • Fax 607.533.9210
www.imrtest.com • E-mail imr@imrtest.com
Toll Free 888.464.8422

CERTIFIED MATERIAL ANALYSIS

IMR Report Number 200500525A

February 15, 2005

Cliff Guthman
Rhenium Alloys Inc.
1329 Taylor Street
PO Box 245
Elyria, OH 44036-0245
USA

PO Number
11643

Date Received
January 20, 2005

Lot#
MR-1254

SUMMARY

One sample was received for chemical analysis. The GDMS portion of the analysis was outsourced by IMR to a qualified outside facility (non-A2LA accredited). Per customer request the sample was analyzed by combustion for hydrogen, nitrogen, oxygen, and carbon. Note that the combustion methods used for hydrogen, nitrogen, oxygen, and carbon are the referee methods of analysis.

A2LA ACCREDITED 1140.01 • 1140.02

Accredited Nadcap Materials Testing Laboratory

Reviewed by

Hank Balduzzi
Chemist

Reviewed by

Peter Damian
Chemistry Dept. Manager

CHEMISTRY

Element	MR-1254
H[1]	2.53
Li	< 0.005
Be	< 0.005
B	< 0.005
C[2]	17.0
N[1]	4.0
O[2]	12.5
F	< 0.05
Na	1.1
Mg	< 0.01
Al	2.1
Si	0.43
P	0.11
S	0.13
Cl	0.05
K	15
Ca	0.63
Sc	< 0.005
Ti	< 10
V	0.09
Cr	10
Mn	0.89
Fe	9.5
Co	0.25
Ni	6.7
Cu	0.65
Zn	< 0.1
Ga	< 0.05
Ge	< 0.05
As	< 0.05
Se	< 0.05
Br	< 0.05
Rb	0.05
Sr	< 0.1
Y	< 0.1
Zr	< 0.1
Nb	< 0.1
Mo	55.85 wt%
Ru	< 0.01
Rh	< 0.01
Pd	< 0.01
Ag	< 1
Cd	< 1

In	< 0.1
Sn	0.17
Sb	0.05
Te	< 0.01
I	< 0.01
Cs	< 0.01
Ba	< 0.5
La	< 0.01
Ce	< 0.01
Pr	< 0.01
Nd	< 0.01
Sm	< 0.01
Eu	< 0.01
Gd	< 0.01
Tb	< 0.01
Dy	< 0.01
Ho	< 0.01
Er	< 0.01
Tm	< 0.01
Yb	< 0.01
Lu	< 0.01
Hf	< 0.01
Ta	< 50
W	80
Re	Balance
Os	< 0.01
Ir	< 0.01
Pt	< 0.05
Au	< 0.5
Hg	< 0.05
Tl	< 0.01
Pb	< 0.01
Bi	< 0.01
Th	0.007
U	0.13

[1]Determined by inert gas fusion-thermal conductivity.

[2]Determined by combustion-infrared absorbance.

Unless otherwise indicated, elements were analyzed by GDMS.

Results in ppm (ppm = parts per million = mg/Kg); 0.1000% by wt = 1000 ppm unless otherwise indicated.

Methods: ASTM E 1937-04, ASTM E 1409-97, ASTM E 1447-01, ASTM E 1941-98 and GDMS.

APPENDIX N—MO-44.5%RE CLEANING PROCEDURE FOR WELDING

The typical procedures used to clean or process Mo-44.5%Re samples prior to welding are as follows:

Pickling for Mo-Re alloys

(1) Handle with clean gloves and appropriate tools, such as tweezers, forceps, etc.

(2) Wipe with acetone/alcohol to remove grease, permanent marker, etc.

(3) Submerge in acetic, nitric, and HF using a 10:4:1 ratio to remove oxide scale (typically <1 min, based on the level of oxidation).

(4) Submerge as needed in pure HCL to remove any visible staining (typically <1 min, based on visual observation).

(5) Water rinse.

(6) Acetone/alcohol rinse.

(7) Dry using heat gun or forced air.

(8) Visually inspect the part for remaining contaminants/oxide layers and if necessary, repeat pickling steps (2) through (7).

Degas Anneal

(1) 800–1,000 °C for 1 hr.

(2) H2 or vacuum furnace at 1×10^{-6} torr.

(3) Avoid having samples sit for more than a few days. Store samples in a dry, controlled atmosphere.

(4) Wipe samples with alcohol or acetone prior to welding.

APPENDIX O—MO-44.5%RE 0.5-INCH-DIAMETER ROD STOCK MATERIAL ANALYSIS

Rhemium Alloys, Inc. provided the following information for the Mo-44.5%Re 0.5-in diameter rod stock material procured for the heat pipe envelopes:

Re RHENIUM ALLOYS, INC.

1329 Taylor St.
P.O. Box 245
Elyria, Oh 44036-0245
Voice (440) 365-7388
Fax (440) 366-9831

MATERIAL CERTIFICATION

DATE: April 27, 2005

SOLD TO: Advanced Method's & Materials
1190 Mountain View Alviso Rd. Suite P
Sunnyvale, CA 94089

PURCHASE ORDER: 884

MATERIAL: Mo/44.5%Re Rod

This is a partial shipment against your order #884 which completes the requirement for the Mo/44.5%Re rod .500" dia.

Lot number MR-1516

Todd Leonhardt
Director of Technology

Rhenium Alloys, Inc
Yesterday's Pioneer, Today's Leader
Email: rhenium@rhenium.com
Web Page: http://www.rhenium.com

RHENIUM
ALLOYS, INC.

1329 Taylor St.
P.O. Box 245
Elyria, Oh 44036-0245
Voice (440) 365-7388
Fax (440) 366-9831

Report No. B-853

Advanced Method's & Materilas
1190 Mountain View Rd. Suite P
Sunnyvale, CA 94089

Subject

Mo/44.5%Re .500 dia. rod lot # MR-1516

Submitted to Our Laboratory on Purchase Order Number 884

Rhenium Alloy, Inc
Email: rhenium@rhenium.com
Web page at http://www.rhenium.com

REPORT NO. B-853

BACKGROUND

Samples identified as Mo/44.5%Re rod .500 dia. lot number MR1516 was submitted to our laboratory. The following tests were conducted.

TEST REQUESTED

Grain Size, Microscopic exam, Density

TEST RESULTS

GRAIN SIZE EXAMINATION

The submitted specimen was prepared in accordance with ASTM E112 for grain size. The sample was examined at **100X** for grain size determination. The average grain size was rated in accordance with the ASTM E112 comparison method for determining grain size.

The average grain size was **6.5**

.MICROSCOPIC EXAMINATION

Shows that porosity is uniformly dispersed throughout the sample.

DENSITY

Density was preformed in accordance with the ASTM B328.

The density is **13.24g/cm3 or 99.9%**

Rhenium Alloys, Inc
Email: rhenium@rhenium.com
Web site: http://www.rhenium.com

REPORT NO. B-853
PHOTOGRAPH

Magnification of photo: 100X

Etchant: Modified Murakami's Reagent

This is a representative view of the microstructure from the submitted sample.

Rhenium Alloys, Inc
Email: rhenium@rhenium.com
Web site: http://www.rhenium.com

REPORT NO. B-853
PHOTOGRAPH

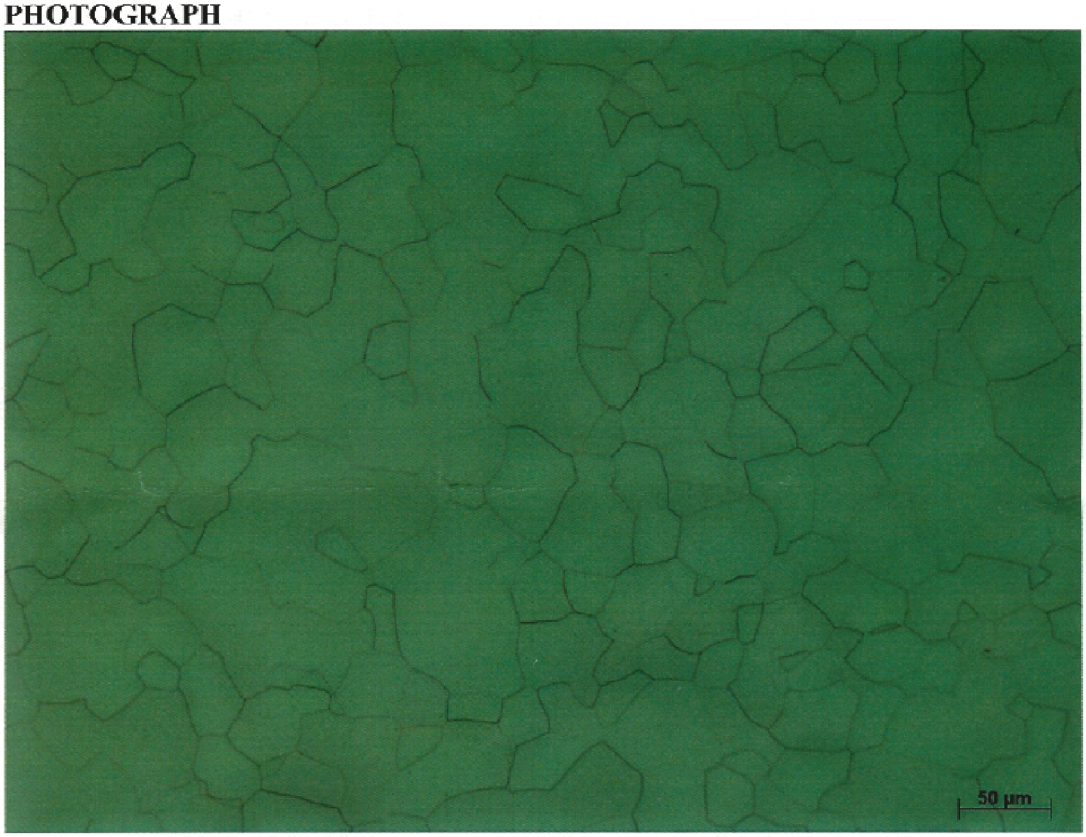

Magnification of photo: 200X

Etchant: Modified Murakami's Reagent

This is a representative view of the microstructure from the submitted sample.

Respectfully,

Todd A. Leonhardt
Director of Research and Development

Rhenium Alloys, Inc
Email: rhenium@rhenium.com
Web site: http://www.rhenium.com

IMR TEST LABS
A Division of Ithaca Materials Research & Testing Incorporated

131 Woodsedge Drive
Lansing Business & Technology Park
Lansing, NY 14882

Phone 607.533.7000 • Fax 607.533.9210
www.imrtest.com • E-mail imr@imrtest.com
Toll Free 888.464.8422

April 13, 2005

Cliff Guthman
Rhenium Alloys Inc.
1329 Taylor Street
PO Box 245
Elyria, OH 44036-0245
USA

PO Number
12066

Date Received
April 11, 2005

Sample #
MR-1516

Material
Mo 44.5% Re

Description
Rod .500 diameter

Specification
As supplied by Customer

CERTIFIED MATERIAL ANALYSIS

IMR Report Number 200503258

SUMMARY

The sample meets the chemical requirements of Attachment 001 to NNM05105903Q for Molybdenum-44.5% Rhenium (Mo-Re) materials as supplied by the customer. The GDMS portion of the analysis was outsourced by IMR to a qualified outside facility (non-A2LA accredited). Per customer request the sample was analyzed by combustion for hydrogen, oxygen, nitrogen and carbon. Note that the combustion methods used for hydrogen, oxygen, nitrogen and carbon are the referee methods of analysis.

The results are given on the following page.

A2LA ACCREDITED 1140.01 • 1140.02

Accredited Nadcap Materials Testing Laboratory

Reviewed by

Hank Balduzzi
Chemist

Reviewed by

Peter Damian
Chemistry Dept. Manager

CHEMISTRY

Element	MR-1516	Specification
H[1]	7.1	25 Maximum
Li	< 0.005	---
Be	< 0.005	---
B	< 0.005	20 Maximum
C[2]	20	20 Maximum
N[1]	5	30 Maximum
O[2]	13	20 Maximum
F	< 0.05	---
Na	0.52	---
Mg	< 0.01	10 Maximum
Al	1.5	---
Si	0.93	30 Maximum
P	0.23	---
S	0.41	---
Cl	0.11	---
K	14	---
Ca	0.32	7 Maximum
Sc	< 0.005	---
Ti	< 10	---
V	0.11	---
Cr	7.8	---
Mn	0.31	4 Maximum
Fe	10	75 Maximum
Co	0.52	30 Maximum
Ni	6.6	50 Maximum
Cu	0.74	---
Zn	< 0.1	---
Ga	< 0.05	---
Ge	< 0.05	---
As	< 0.05	---
Se	< 0.05	---
Br	< 0.05	---
Rb	0.03	---
Sr	< 0.1	---
Y	< 0.1	---
Zr	< 0.1	---
Nb	< 0.1	---
Mo	55.24 wgt %	---
Ru	< 0.01	---
Rh	< 0.01	---
Pd	< 0.01	---
Ag	< 1	---
Cd	< 1	---

In	< 0.1	---
Sn	0.08	20 Maximum
Sb	0.21	---
Te	< 0.01	---
I	< 0.01	---
Cs	< 0.01	---
Ba	< 0.5	---
La	0.16	---
Ce	0.03	---
Pr	< 0.01	---
Nd	< 0.01	---
Sm	< 0.01	---
Eu	< 0.01	---
Gd	< 0.01	---
Tb	< 0.01	---
Dy	< 0.01	---
Ho	< 0.01	---
Er	< 0.01	---
Tm	< 0.01	---
Yb	< 0.01	---
Lu	< 0.01	---
Hf	< 0.01	---
Ta	< 50	---
W	86	300 Maximum
Re	Matrix	---
Os	< 0.01	---
Ir	< 0.01	---
Pt	< 0.05	---
Au	< 0.5	---
Hg	< 0.05	---
Tl	< 0.01	---
Pb	< 0.01	---
Bi	< 0.01	---
Th	0.01	---
U	0.08	---

[1]Determined by inert gas fusion-thermal conductivity.

[2]Determined by combustion-infrared absorbance.

Unless otherwise indicated, elements were analyzed by GDMS.

Results in ppm (ppm = parts per million = mg/Kg); 0.1000% by wt = 1000 ppm unless otherwise indicated.

Methods: ASTM E 1019-03, ASTM E 1447-01, CAP-046A (ICP-AES) and GDMS.

APPENDIX P—MO-44.5%RE 0.625-INCH-DIAMETER ROD STOCK MATERIAL ANALYSIS

Rhenium Alloys, Inc. provided the following information for the Mo-44.5%Re 0.625-in diameter rod stock material procured for the heat pipe envelopes:

RHENIUM ALLOYS, INC.

1329 Taylor St.
P.O. Box 245
Elyria, Oh 44036-0245
Voice (440) 365-7388
Fax (440) 366-9831

MATERIAL CERTIFICATION

DATE: May 19, 2005

SOLD TO: Advanced Methods & Materials
1190 Mountain View Alviso Rd.
Suite P
Sunnyvale, CA 94089

PURCHASE ORDER: 884

MATERIAL: Mo/44.5%Re Rod

This is a partial shipment against your order #884 which completes the requirement for the Mo/44.5%Re rod .625" dia.

Lot number MR-1512

Todd Leonhardt
Director of Technology

Rhenium Alloys, Inc
Yesterday's Pioneer, Today's Leader
Email: rhenium@rhenium.com
Web Page: http://www.rhenium.com

RHENIUM
ALLOYS, INC.

1329 Taylor St.
P.O. Box 245
Elyria, Oh 44036-0245
Voice (440) 365-7388
Fax (440) 366-9831

Report No. B-855

Advanced Methods & Materials
1190 Mountain View Alviso Rd.
Suite P
Sunnyvale, CA 94089

Subject

Mo/44.5%Re .625dia. rod lot # MR1512

Submitted to Our Laboratory on Purchase Order Number 884

Rhenium Alloy, Inc
Email: rhenium@rhenium.com
Web page at http://www.rhenium.com

REPORT NO. B-855

BACKGROUND

Samples identified as Mo/44.5%Re rod .625 dia. lot number MR1516 was submitted to our laboratory. The following tests were conducted.

TEST REQUESTED

Grain Size, Microscopic exam, Density

TEST RESULTS

GRAIN SIZE EXAMINATION

The submitted specimen was prepared in accordance with ASTM E112 for grain size. The sample was examined at **100X** for grain size determination. The average grain size was rated in accordance with the ASTM E112 comparison method for determining grain size.

The average grain size was **6**

.MICROSCOPIC EXAMINATION

Shows that porosity is uniformly dispersed throughout the sample.

DENSITY

Density was preformed in accordance with the ASTM B328.

The density is **13.25 g/cm3 or 99.99%**

Rhenium Alloys, Inc
Email: rhenium@rhenium.com
Web site: http://www.rhenium.com

REPORT NO. B-855
PHOTOGRAPH

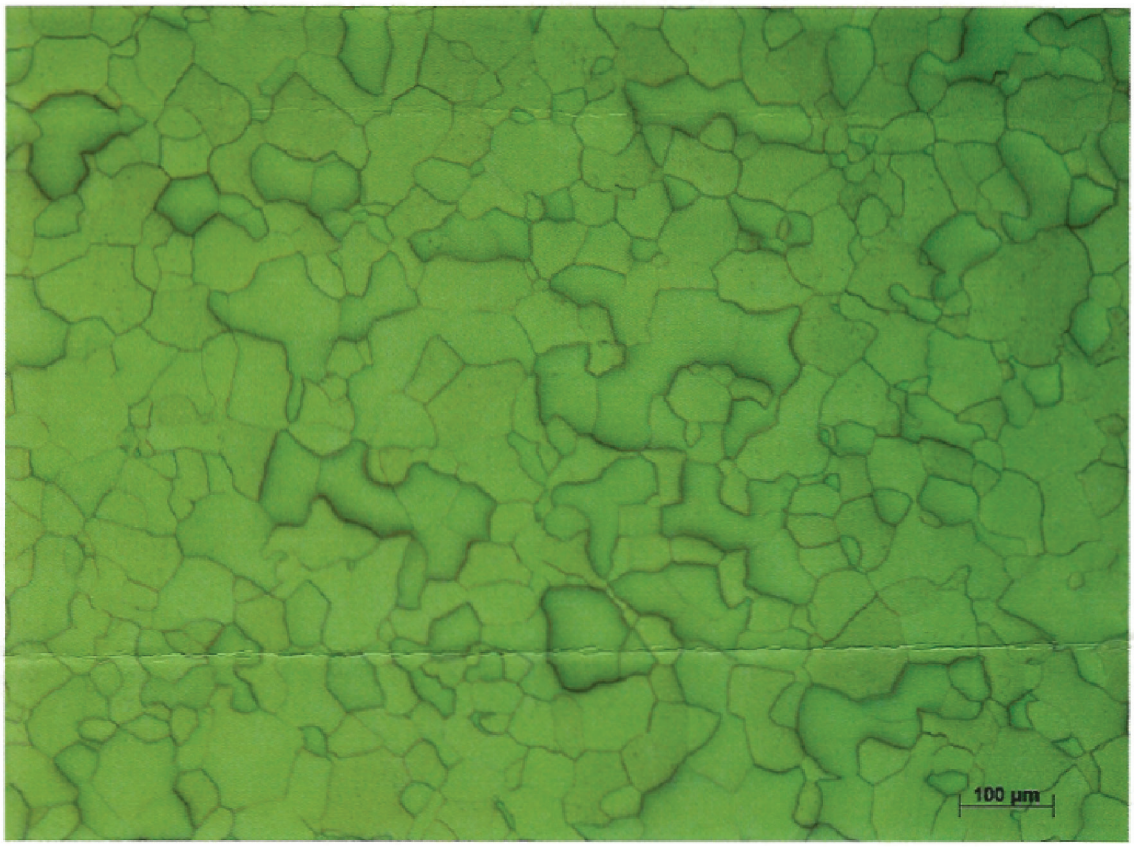

Magnification of photo: 130X

Etchant: Modified Murakami's Reagent

This is a representative view of the microstructure from the submitted sample.

Rhenium Alloys, Inc
Email: rhenium@rhenium.com
Web site: http://www.rhenium.com

REPORT NO. B-855
PHOTOGRAPH

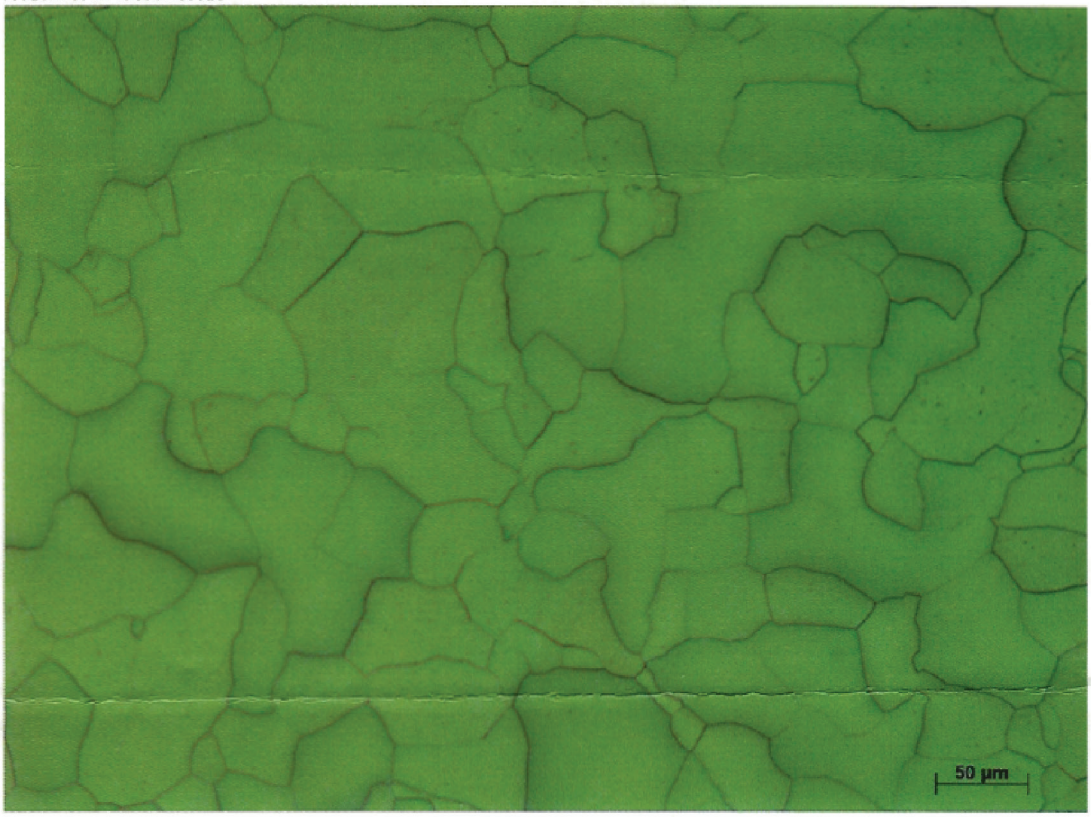

Magnification of photo: 260X

Etchant: Modified Murakami's Reagent

This is a representative view of the microstructure from the submitted sample.

Respectfully,

Todd A. Leonhardt
Director of Research and Development

Rhenium Alloys, Inc
Email: rhenium@rhenium.com
Web site: http://www.rhenium.com

IMR TEST LABS
A Division of Ithaca Materials Research & Testing Incorporated

131 Woodsedge Drive
Lansing Business & Technology Park
Lansing, NY 14882

Phone 607.533.7000 • Fax 607.533.9210
www.imrtest.com • E-mail imr@imrtest.com
Toll Free 888.464.8422

April 13, 2005

Cliff Guthman
Rhenium Alloys Inc.
1329 Taylor Street
PO Box 245
Elyria, OH 44036-0245
USA

PO Number
12066

Date Received
April 11, 2005

Sample #
MR-1516

Material
Mo 44.5% Re

Description
Rod .500 diameter

Specification
As supplied by Customer

CERTIFIED MATERIAL ANALYSIS

IMR Report Number 200503258

SUMMARY

The sample **meets** the chemical requirements of Attachment 001 to NNM05105903Q for Molybdenum-44.5% Rhenium (Mo-Re) materials as supplied by the customer. The GDMS portion of the analysis was outsourced by IMR to a qualified outside facility (non-A2LA accredited). Per customer request the sample was analyzed by combustion for hydrogen, oxygen, nitrogen and carbon. Note that the combustion methods used for hydrogen, oxygen, nitrogen and carbon are the referee methods of analysis.

The results are given on the following page.

A2LA ACCREDITED 1140.01 • 1140.02

Accredited Nadcap Materials Testing Laboratory

Reviewed by

Hank Balduzzi
Chemist

Reviewed by

Peter Damian
Chemistry Dept. Manager

CHEMISTRY

Element	MR-1516	Specification
H[1]	7.1	25 Maximum
Li	< 0.005	---
Be	< 0.005	---
B	< 0.005	20 Maximum
C[2]	20	20 Maximum
N[1]	5	30 Maximum
O[2]	13	20 Maximum
F	< 0.05	---
Na	0.52	---
Mg	< 0.01	10 Maximum
Al	1.5	---
Si	0.93	30 Maximum
P	0.23	---
S	0.41	---
Cl	0.11	---
K	14	---
Ca	0.32	7 Maximum
Sc	< 0.005	---
Ti	< 10	---
V	0.11	---
Cr	7.8	---
Mn	0.31	4 Maximum
Fe	10	75 Maximum
Co	0.52	30 Maximum
Ni	6.6	50 Maximum
Cu	0.74	---
Zn	< 0.1	---
Ga	< 0.05	---
Ge	< 0.05	---
As	< 0.05	---
Se	< 0.05	---
Br	< 0.05	---
Rb	0.03	---
Sr	< 0.1	---
Y	< 0.1	---
Zr	< 0.1	---
Nb	< 0.1	---
Mo	55.24 wgt %	---
Ru	< 0.01	---
Rh	< 0.01	---
Pd	< 0.01	---
Ag	< 1	---
Cd	< 1	---

In	< 0.1	---
Sn	0.08	20 Maximum
Sb	0.21	---
Te	< 0.01	---
I	< 0.01	---
Cs	< 0.01	---
Ba	< 0.5	---
La	0.16	---
Ce	0.03	---
Pr	< 0.01	---
Nd	< 0.01	---
Sm	< 0.01	---
Eu	< 0.01	---
Gd	< 0.01	---
Tb	< 0.01	---
Dy	< 0.01	---
Ho	< 0.01	---
Er	< 0.01	---
Tm	< 0.01	---
Yb	< 0.01	---
Lu	< 0.01	---
Hf	< 0.01	---
Ta	< 50	---
W	86	300 Maximum
Re	Matrix	---
Os	< 0.01	---
Ir	< 0.01	---
Pt	< 0.05	---
Au	< 0.5	---
Hg	< 0.05	---
Tl	< 0.01	---
Pb	< 0.01	---
Bi	< 0.01	---
Th	0.01	---
U	0.08	---

[1]Determined by inert gas fusion-thermal conductivity.

[2]Determined by combustion-infrared absorbance.

Unless otherwise indicated, elements were analyzed by GDMS.

Results in ppm (ppm = parts per million = mg/Kg); 0.1000% by wt = 1000 ppm unless otherwise indicated.

Methods: ASTM E 1019-03, ASTM E 1447-01, CAP-046A (ICP-AES) and GDMS.

APPENDIX Q—CHEMICALS USED FOR VANADIUM WIRE EQUILIBRATION MATERIAL CLEANING

Cleaning chemicals, concentration ratios, and mixtures used for each of the specific materials used in performing the V-wire equilibration technique.

Chemicals Required for Vanadium Wire Equilibration Method Material Prep

Item	Chemical		Vol (L)	Grade	Container Material
1	Freon TF		1	Technical	HDPE
2	De-ionized Water	H_2O	5	Technical	HDPE, Glass
3	Sodium Hydroxide	NaOH	1	Technical	HDPE
4	Hydrogen Peroxide	H_2O_2	1	Technical	HDPE
5	Ethanol	CH_3CH_2OH	1	Technical	HDPE
6	Sulfuric Acid	H_2SO_4	0.5	Technical	HDPE
7	Nitric Acid	HNO_3	0.5	Technical	PTFE
8	Sodium Chloride	NaCl	10g	Technical	N/A
9	Ammonia	NH_3	1	Technical	HDPE, PTFE
10	Hydrochloric Acid	HCl	0.5	Technical	HDPE
11	Acetone	$(CH_3)_2CO$	1	Technical	PTFE
12	PF solvent		1	Technical	HDPE
14	Methanol	CH_3OH	1	Technical	HDPE

Container Selection for VEM Chemicals

Procedure	Bath Fluid	No. Cont.	Poss. Cont Matl	Rec Matl
Stainless Steel	Freon TF	1	HDPE	HDPE
(Valves)	Caustic Soln (11p-2, 1p-3, 1p-4)	1	HDPE	HDPE
	Hot Deionized Water	1	Glass, HDPE	HDPE
	Ethanol	1	HDPE	HDPE
Nickel	Hot Deionized Water	1	HDPE	HDPE
(Tubes)	Sol (6,7, 8, 2)	1	PTFE or glass	PTFE
	De-ionized Water	1	HDPE	HDPE
	Diluted Ammonia	1	HDPE	HDPE
Molybdenum	PF Solvent (Freon?)	1	HDPE	HDPE
(Wire)	Solution (1p-10, 1p-2)	1	HDPE	HDPE
	Caustic Soln (11p-2, 1p-3, 1p-4)	1	HDPE	HDPE
	De-ionized Water	1	HDPE	HDPE
	Ethanol	1	HDPE	HDPE
Vanadium	Elec-Pol Soln (1p-6, 4p-14)	1	Glass (see proc)	Glass
(Wire)	Acetone	1	PTFE	PTFE
	De-ionized Water	1	HDPE	HDPE
	Methanol	1	HDPE	HDPE
	Total HDPE	14	Need 11	
	Total Glass	1	1 to heat then trans to multi HDPE	
	Total PTFE	1	cut to shape, clean/reuse in V pickling	

APPENDIX R—VANADIUM WIRE EQUILIBRATION OPERATIONAL PROCEDURE

Raw Material Preparation

Materials required to perform the V wire equilibration analysis method:

(1) 201 series Ni tubes: Diameter =1/4 in (0.035-in wall)×L=10 in; bent as shown in figure 36.

(2) 201 Ni tubes: Diameter = 1/4 in (0.035-in wall)×L = 6.35 in.

(3) Mo wires: Diameter = 0.762 mm×L=118 mm.

(4) V wires: Diameter = 0.25 mm×L=130 mm.

(5) SS–4H Swagelok SS valves; three per setup.

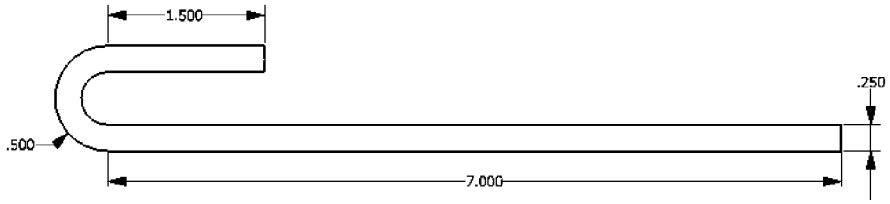

Figure 36. Typical Ni tube.

Pickling Procedures

The following process is applied to the experiment components to minimize the risk of contamination. Pickling methods, conducted in a fume hood as shown in figure 37, are necessary to remove surface organics and oxide scales.

Several procedural steps require ultrasonic cleaning (fig. 38) with various solutions, some of them being highly corrosive. To protect the ultrasonic cleaners, they are filled with deionized water and components are placed within glass or low-density polyethylene (LDPE) vials containing the required cleaning solutions. Vials are then immersed in the ultrasonic cleaner.

Figure 37. Fume hood and associated pickling equipment.

Figure 38. Branson ultrasonic cleaners.

Bellows Sealed Stainless Steel Valves

High-density polyethylene (HDPE) containers should be used, due to the caustic nature of the chemicals used to pickle the SS valves. Clean SS forceps should be used to manipulate the components. To prevent contamination, rinse forceps in distilled water after immersion in any substance before reusing them to manipulate the components.

(1) Wrap the valve handle in plastic and secure with a zip tie to prevent infiltration of liquid or vapor into the valve handle that can react with valve lubricant (fig. 39).

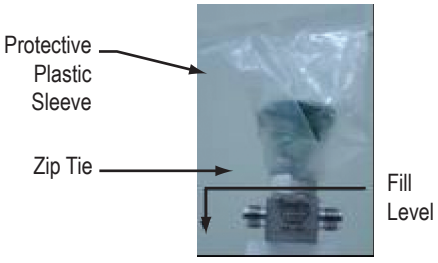

Figure 39. Valve prepared for pickling.

(2) Immerse in Freon and ultrasonically clean for 5 min.

(3) Immerse in caustic solution consisting of 11 parts (by volume) deionized water, 1 part sodium hydroxide (NaOH), and 1 part hydrogen peroxide (H_2O_2) and ultrasonically clean for 5 min.

(4) Immerse in hot deionized water and ultrasonically clean for 5 min.

(5) Repeat steps (2) and (3) three times.

(6) Rinse in hot deionized water.

(7) Immerse in ethanol (CH_3CH_2OH) and ultrasonically clean for 5 min.

(8) Place in plastic bag and seal.

(9) Transport plastic bag for vacuum bakeout.

(10) Vacuum bakeout at a pressure of 10^{-6} torr and a temperature of 200 °C for 2 to 4 hr.

201 Nickel Tubes

Due to the acidic nature of the chemicals used to pickle the Ni tubes, use glass containers and clean PTFE Teflon®-coated forceps to manipulate the components. Rinse forceps in distilled water after substance immersion before reuse to prevent contamination.

(1) Immerse in hot water bath for 5 min to heat the components.

(2) Immerse in solution consisting of sulfuric acid (H_2SO_4) (148 mL, 35 wt%), nitric acid (HNO_3) (229 mL, 30 wt%), sodium chloride (NaCl) (3.7 g), and deionized water (H_2O) (123 mL) and ultrasonically clean for 2 min (room temperature).

(3) Rinse components in distilled (deionized) water.

(4) Immerse in ammonia (NH_3) for 10 s to neutralize the part.

(5) Rinse in distilled water and allow to dry.

(6) Place in plastic bag, seal, and transport for vacuum bakeout.

(7) Vacuum bakeout at a pressure of 10^{-6} torr and a temperature of 800 °C for 4 hr in a vacuum baking chamber. The tubes will have a clean, lustrous finish (fig. 40).

Figure 40. Ni tubes postprocessing.

Electropolishing of Molybdenum and Vanadium Wire

This process is in part based on ASTM C997–83, sections 65 to 74. The electrolysis cell consists of a 1,000-mL beaker with a platinum cathode (figs. 41 and 42). The lead from this electrode is insulated with shrink-fit tetrafluoroethylene (TFE)-fluorocarbon or polyethylene. Anode contact is made through spring-loaded forceps. Direct current is supplied from a power supply providing up to 4 A at 4 to 25 V. A magnetic TFE-fluorocarbon-coated stirring bar was used. Use clean PTFE Teflon-coated forceps to manipulate components. Rinse forceps in distilled water after substance immersion.

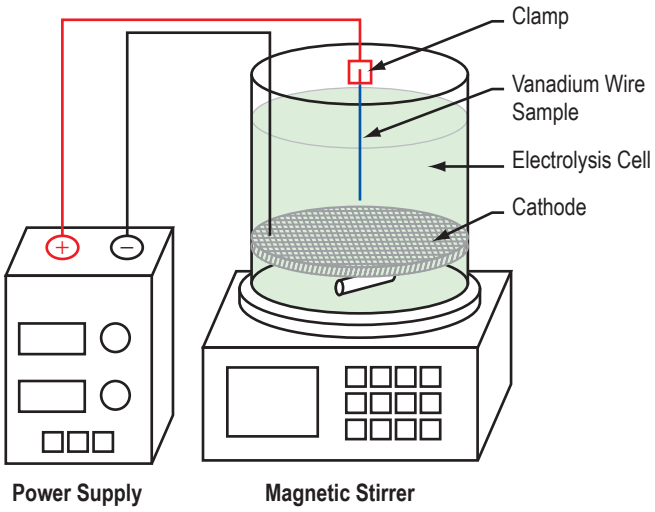

Figure 41. Typical electropolishing apparatus.

Figure 42. Buehler® Electromet III electropolisher/etcher.

(1) Obtain several control lengths (L=110 mm) and several test lengths (L=130 mm) of as-received V wire.

(2) Create a small bend in the last 3 mm using forceps (fig. 43).

(3) Store one control wire in a vial.

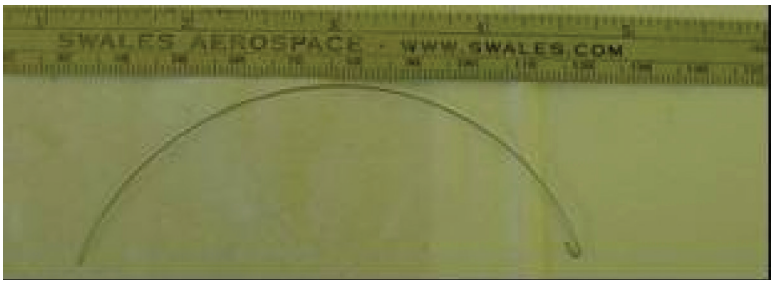

Figure 43. Typical as-received V wire sample.

(4) Create electropolishing solution by cautiously adding 200 mL of concentrated sulfuric acid (H_2SO_4) to 800 mL of chilled methanol (CH_3OH) while stirring. The reaction is exothermic, therefore it is important to keep the methanol chilled and slowly mix the two to prevent boiling and splattering. Figure 44 shows a beaker of methanol chilled in an ice-water bath.

Figure 44. Methanol-filled beaker in ice bath.

(5) Create a loop from V wire that will be clamped in the spring-loaded anode forceps, from which the sample V wire can hang, as shown in figure 45. This loop allows for the full immersion of the sample V wire in the electrolytic solution, significantly reducing the possibility of contamination.

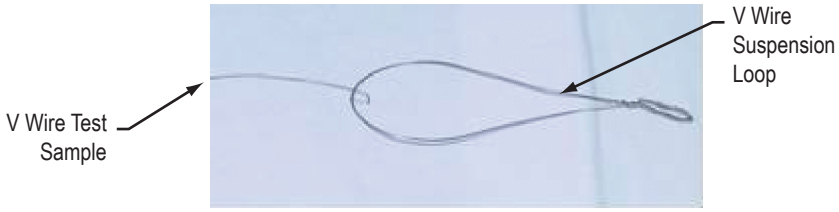

Figure 45. Vanadium wire suspension loop and sample wire.

(6) Fill the glass electrolytic cell with electropolishing solution.

(7) Immerse each wire (four control, three test) in acetone ($[CH_3]_2CO$) (PTFE tray) and ultrasonically clean for 5 min.

(8) Remove from acetone bath and allow drying to degas.

(9) Store a second control sample in a vial.

(10) Grasp the loop with the clamp and adjust the anode position so that the loop tip is just in contact with the liquid and the wire is centered in the cell (fig. 46).

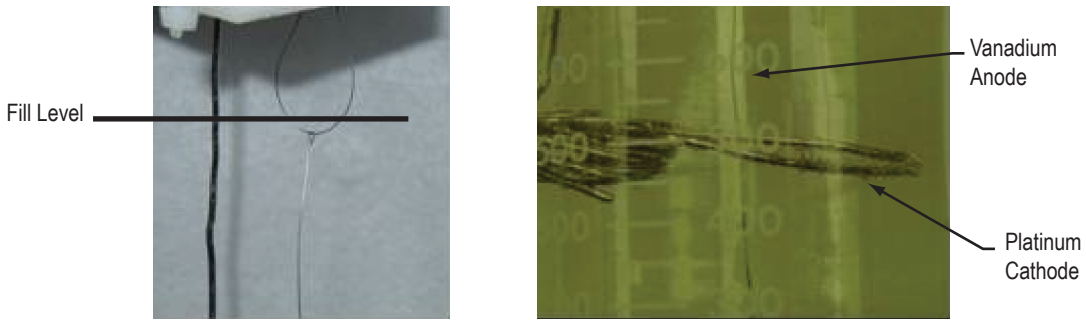

Figure 46. Anode and cathode positioning.

(11) With the stirrer at a low speed, apply current and adjust the voltage to provide a current of 5 to 10 mA/mm for 0.25-mm wire. Avoid electrical sparks when electropolishing to prevent ignition of the polishing solution.

(12) Electropolish each wire for 3 min, 30 s to reduce the diameter from 0.25 to 0.22 mm.

(13) Remove wire from electropolish solution and allow to dry.

(14) Measure the diameter of the wire after etching using calipers, shown in figure 47.

Figure 47. Mitutoyo CD 12-in digital calipers.

(15) Store a third control wire in a vial.

(16) Immerse wire in deionized water beaker and ultrasonically clean for 30 s.

(17) Remove wire from deionized water bath and allow to dry.

(18) Store a fourth control wire in a vial.

(19) Immerse in methanol and ultrasonic cleaner for 30 s.

(20) Remove wire from methanol bath and allow to dry.

(21) Store a fifth control wire in a vial.

(22) Place each test wire in a vial and backfill each vial with Ar.

(23) Measure the weight of each control and test wire using an analytical balance, shown in figure 48.

Figure 48. Denver Instruments M–220D analytical balance.

(24) Transport test vials purge bag for vacuum degas, at room temperature.

(25) Establish a pressure of 10^{-6} torr for 24 hr to degas at room temperature.

(26) Repeat the complete procedure to prepare the Mo wires.

Vacuum Bakeout Procedures

The vacuum bakeout system is shown in figure 49.

Ni tubes and Mo wires are placed inside the vacuum tube (fig. 50). The process to bakeout the SS valves is described later.

Vacuum is achieved by linking a Varian TriScroll 300 rough vacuum pump (fig. 51) in series with a Varian V70 turbomolecular vacuum pump (fig. 52), an oil-free vacuum system.

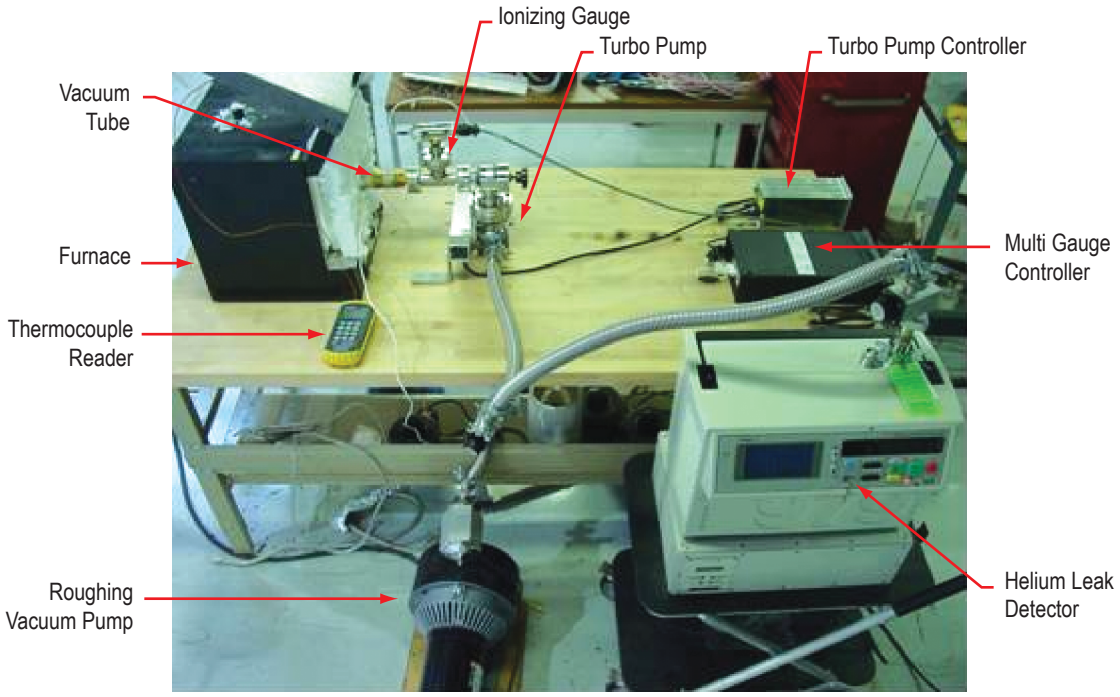

Figure 49. Vacuum bakeout system.

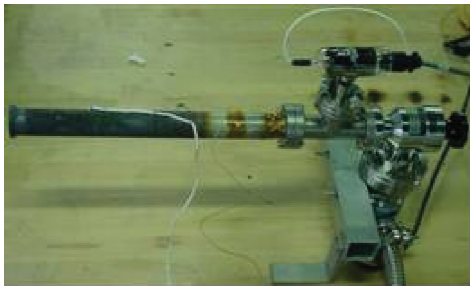

Figure 50. Vacuum tube assembly.

Figure 51. Roughing pump.

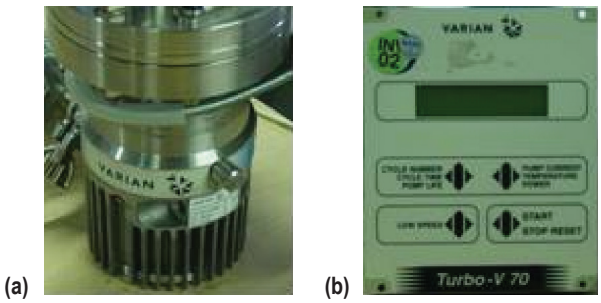

Figure 52. Turbopump (a) and with controller (b).

Vacuum level is monitored with a Varian 564 BA ionizing vacuum gauge (fig. 53) used in conjunction with a Varian multigauge reader (fig. 54).

Figure 53. Ion gauge.

Figure 54. Multigauge reader.

A Varian 979 He leak detector (fig. 55) and helium source (fig. 56) were used to verify a leak-tight seal at all connection points.

Figure 55. Leak detector.

Figure 56. He source.

After components of the same material are placed in the bakeout system vacuum tube and all connections leak checked, the vacuum tube was inserted in an Omegalux® LMF–A550 furnace, as shown in figure 57. Since the door has to be open to accept the vacuum tube, an insulating wall was fabricated of Insulfrax fibrous alumina blanket material and held in place with SS wire. Vacuum tube temperature is monitored using two type-K thermocouples connected to an Omega HH509 hand-held thermocouple reader (fig. 58).

After the components have been baked, the vacuum tube isolation valve is closed and the tube is disconnected from the rest of the vacuum system. The tube is then transported into a glove box backfilled with Ar from a standard-K bottle, as shown in figure 59, to minimize oxidation and moisture absorption when parts are removed.

Figure 57. Vacuum tube in furnace.

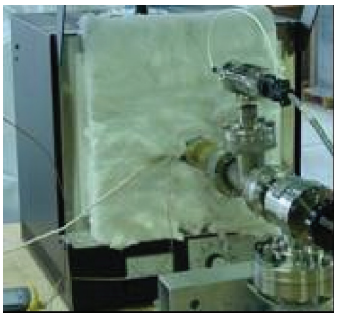

Figure 58. Thermocouple reader.

Figure 59. Ar glove box.

Using a temporary inert environment glove box, the vacuum baked components were removed from the tube assembly and placed in a purge bag. The bag was then transferred from the glove box to the sodium fill machine, a Vacuum Atmospheres Company (VAC) controlled atmosphere glove box.

Prior to vacuum baking, the SS valves are connected in series using 1/4 in (0.035-in wall) 304 SS tube stubs. One end is plugged while the other is connected to a 2.75-in ConFlat® flange with a compression-fitting adapter. The bakeout approach uses the same vacuum, thermal monitoring, and leak check system previously described.

The assembly is wrapped in heater tape and several layers of aluminum foil insulation, and then vacuum baked. Once the vacuum baking is completed, they are closed and disconnected from the flange and placed in a bag backfilled with Ar, as shown in figure 60. The valves are then transferred to the sodium fill machine VAC glovebox for assembly.

Figure 60. SS valves after vacuum bake.

Vanadium Wire Sample Assembly

(1) Weigh each component separately.

(2) Carefully bend the Mo wire so that it has a slight curve.

(3) Add two notches, 90 mm apart, by scratching the Mo wire.

(4) Wrap the V wire around the Mo wire at the notches, forming a bow, as shown in figure 61.

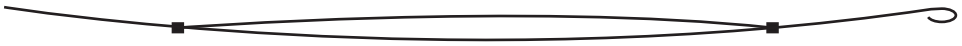

Figure 61. Wire bow.

(5) Ultrasonically clean in methanol for 5 min.

(6) Remove from bath and allow to dry.

(7) Place in vacuum chamber and degas at $\approx 5 \times 10^{-8}$ torr for 24 hr at room temperature.

(8) Place assembled bow in inert sodium fill machine VAC glovebox.

(9) Inside the glovebox, insert the wire bow into the Ni tube, as shown in figure 62.

Figure 62. Bow with tube.

Sodium Vessel Sample Tube Assembly (conducted in the sodium fill machine VAC glovebox)

(1) Assemble sample tubes, charging vessels, valves, and thermocouples as shown in figure 63.

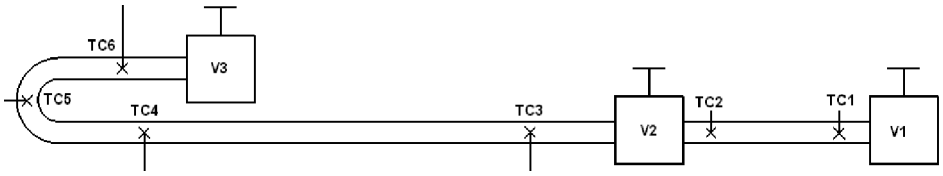

Figure 63. Assembled sample tube.

(2) Weigh the completed assembly.

(3) Close all valves.

(4) Connect the assembly to the glove box high vacuum system at V1.

(5) Open V1 and V2 to evacuate the system into the 10^{-5} torr range.

(6) Heat assembly to 200 °C, and then allow to cool to ambient temperature.

(7) Close V1 and V2 and disconnect from vacuum system.

(8) Connect V1 to the glove box Na fill stem.

(9) Connect V3 to the glove box vacuum source.

(10) Wrap the assembly in two heater tapes (H1 and H2), as shown in figure 64.

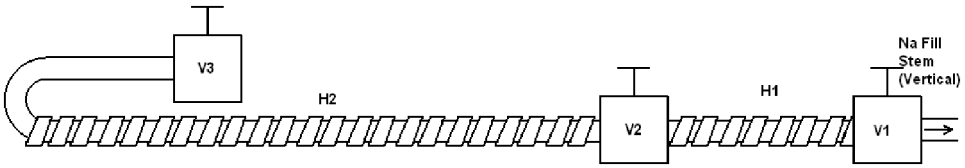

Figure 64. Tube test configuration.

Sample Tube Charging With Sodium

(1) Heat Na supply system to 150 °C in preparation of sample tube charging.

(2) Open all valves to evacuate the system to 10^{-5} torr range.

(3) Close V1.

(4) Note temperature: TC1_____ TC2_____.

(5) Heat H1 to 140 °C and H2 to 125 °C.

(6) Close all valves.

(7) Open Na fill machine isolation valve.

(8) Open valve V1.

(9) Check TC1 and TC2. If TC1 and TC2 read 150 °C, the vessel is charged.

(10) Close V1.

(11) Close Na fill machine isolation valve.

(12) Open V2.

(13) Check TC3, TC4, and TC5. If TC3, TC4, and possibly TC5 read 140 to 150 °C, the wire tube is charged. If not, the tube should be tapped to help transfer the Na.

(14) After tapping, the Na should flow toward the end of the tube near TC6, and TC3 should cool, indicating that the section from TC3 to V2 is clear for crimping.

(15) Close V2.

(16) Turn off H1 and H2.

(17) Allow the sample tube to cool to ambient temperature.

(18) Disconnect the sample tube from the Na fill stem and replace fill stem plug.

(19) Weigh assembly. If additional Na is required, repeat from step (2).

(20) Remove from glove box.

(21) Using a hydraulic press, crimp both ends of the tube as shown in figure 65. (The crimp should allow for 0.002 in of plastic deformation.)

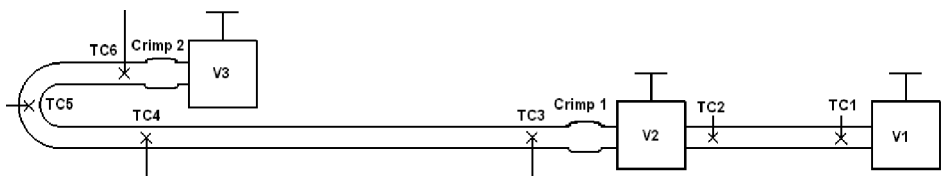

Figure 65. Tube processing—crimp.

(22) Place assembly within the EB welder, create two fusion zones on the crimps, as shown in figure 66 (adjust the current to achieve near-full penetration: Setting_____).

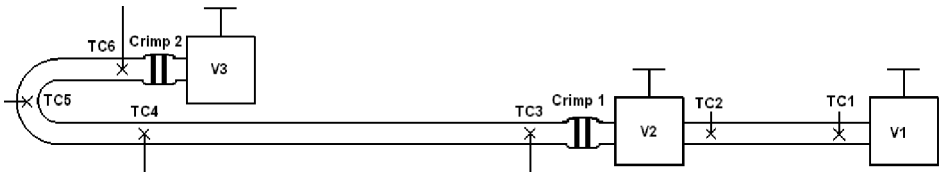

Figure 66. Tube processing—EB weld.

(23) Use the EB welder to make a third pass, cutting off the excess as shown in figure 67 (adjust the current to fully penetrate: Setting_____).

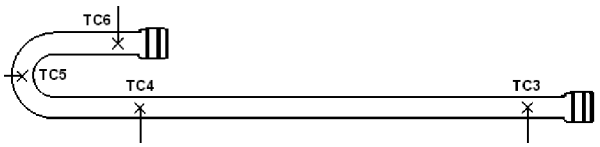

Figure 67. Tube processing—cutoff.

(24) Weigh the sample tube, charge vessel, and cut off V3 end.

(25) Using a TIG welder, trace over the cut-off crimped ends created by the EB welder, building up the weld creating a nugget (should be performed in the VAC glove box).

(26) Weigh the sample tube.

(27) Place the sample tube into a purge bag.

(28) Transfer container to the tube furnace.

Sample Tube Heating to Equilibration Temperature

(1) Transfer the sample tube from the bag and place in the tube furnace, as shown in figure 68.

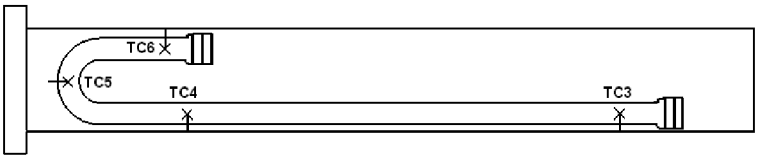

Figure 68. Tube processing—furnace heating.

(2) Evacuate the tube furnace to 10^{-6} torr.

(3) Heat the tube furnace to 750 °C for 4 hr to reach chemical equilibrium.

(4) Allow the furnace to cool to ambient temperature.

(5) Remove the sample tube from tube furnace and place in a bag.

(6) Transport to VAC glove box.

Wire Bow and Sodium Separation

(1) Inside the glove box, remove the sample tube from the bag.

(2) Cut both ends off the sample tube just past TC3 and TC4, using tube cutters.

(3) Attach the charge vessel and V3 at either end of the tube, as shown in figure 69.

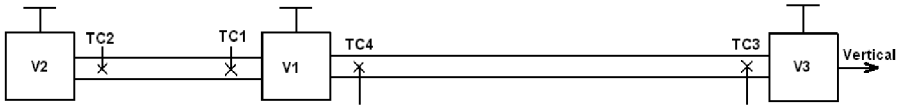

Figure 69. Tube processing—wire removal.

(4) Wrap the assembly in heater tape.

(5) Close all valves.

(6) Connect V2 to the glove box vacuum source.

(7) Heat the system to 150 °C.

(8) Open V2 to evacuate the system.

(9) Close V2 once a vacuum level of 10^{-4} torr is established.

(10) Open V1 followed by V3 to transfer Na from tube to vessel.

(11) Vibrate/tap the surface of the sample tube to agitate the Na, causing it to flow from the bow and tube.

(12) Monitor thermocouple readings (TC3 and TC4 should drop, while TC1 and TC2 should increase, indicating that the Na has transferred from the sample tube to the charge vessel).

(13) Close V1 and V3.

(14) Allow system to cool to ambient temperature.

(15) Remove V3 from the tube.

(16) Remove bow from the tube using forceps. If the wire bow does not pull free easily, reheat it to about 150 °C and attempt again.

(17) Separate V wire from Mo wire by unraveling the V wire.

(18) Weigh each component separately.

(19) Dissolve the residual Na adhering to the V wires in about 1,000 mL of technical-grade ethanol. The large volume of ethanol prevents excessive heating of the wires.

(20) Rinse wires with water and allow the wires to dry.

Note: For the rest of the procedure, wires must be handled with clean ceramic forceps.

(21) Make cuts at least 3 mm from each bend (only straight portions are used for analysis).

(22) Weigh each V wire piece separately.

(23) Separate wires for archival storage from those for immediate analysis.

(24) Store the archival and test wires in capped vials that are properly identified.

(25) V wires can be submitted for LECO gas-fusion analysis to determine oxygen content.

APPENDIX S—VANADIUM AND MOLYBDENUM WIRE SAMPLE PREPARATION RESULTS

Sample of V and Mo wires were processed to evaluate the operational procedures with results, as listed in tables 26–28.

Table 26. Data sheet for V wire samples.

Vanadium Wire Sample Preparation Data Sheet							
Name	L_i (mm)	L_f (mm)	W_i (g)	W_f (g)	D_i (mm)	D_f (mm)	Notes
Control 1	111	111	0.0341	0.0341	0.25	0.25	As received
							Stored in vial backfilled w/ Argon
Control 2	113	113	0.0345	0.0345	0.25	0.25	Ultrasonically cleaned in Acetone for 5 min
							Stored in vial backfilled w/ Argon
Control 3	110	110	N/A	0.0258	0.25	0.22	Ultrasonically cleaned in Acetone for 5 min
							Electro-etched 3.5 min***
							Stored in vial backfilled w/ Argon
Control 4	110	102	N/A	0.0253	0.25	0.22	Ultrasonically cleaned in Acetone for 5 min
							Electro-etched 3.5 min***
							Ultrasonically cleaned in water for 5 min
							Stored in vial backfilled w/ Argon
Control 5	110	102	N/A	0.0248	0.25	0.22	Ultrasonically cleaned in Acetone for 5 min
							Electro-etched 3.5 min***
							Ultrasonically cleaned in water for 5 min
							Ultrasonically cleaned in methanol for 5 min
							Stored in vial backfilled w/ Argon
Control 6	110	110	0.0336	0.0233	0.25	0.21	Ultrasonically cleaned in Acetone for 5 min
							Electro-etched 3.5 min***
							Ultrasonically cleaned in water for 5 min
							Ultrasonically cleaned in methanol for 5 min
							Vacuumed out at 10-8 Torr for over 1 week
							Stored in vial backfilled w/ Argon
Control 7	110	110	0.0336	0.0266	0.25	0.22	Ultrasonically cleaned in Acetone for 5 min
							Electro-etched 3.5 min***
							Ultrasonically cleaned in water for 5 min
							Ultrasonically cleaned in methanol for 5 min
							Vacuumed out at 10-8 Torr for over 1 week
							Stored in vial backfilled w/ Argon
*** Electro-etch process utilizes a methanol/sulfuric acid bath, Platinum Cathode, and V~8V and i~2A							
*All chemical containers and storage vials were cleaned w/ ethanol prior to use.							

Table 27. Data sheet for V wire test segments.

Vanadium Wire Test Sample Data Sheet											
Name	L_1 (*mm*)	L_2 (*mm*)	L_3 (*mm*)	L_4 (*mm*)	D_1 (*mm*)	D_2 (*mm*)	D_3 (*mm*)	W_1 (*g*)	W_2 (*g*)	W_3 (*g*)	W_4 (*g*)
Test 1	130	125	119		0.25	0.22		~0.0405	0.0313	0.03	
Test 2	130	121	114		0.25	0.22		~0.0405	0.0305	0.0292	
Test 3	130	120	117		0.25	0.22		~0.0405	0.0302	0.0293	
L_1 = Initial length				D_1 = Initial diameter				W_1 = Initial weight			
L_2 = Post etching length				D_2 = Post-etching diameter				W_2 = Post etch weight			
L_3 = Pre-equilibration length (bow)				D_3 = Post-equilibration diameter				W_3 = Pre equilibration weight			
L_4 = Post equilibration length								W_4 = Post equilibration weight			
All three Vanadium wire test samples received the following pre-equilibration treatment:											
1. Ultrasonically cleaned in acetone for 5 minutes											
2. Electro-etched 3.5 minutes*											
3. Ultrasonically cleaned in water for 5 minutes											
4. Ultrasonically cleaned in methanol for 5 minutes											
5. Stored in vial backfilled with argon**											
6. Wrapped with Mo wire, inserted into Ni tube, subjected to vacuum of ~4×10^{-8} Torr for over 7 days											
Steps for equilibration:											
1. Tube charged with sodium at 150°C											
2. Heated to T_{equil} = 800°C for 4 hours											
3. Removed from sodium, surface rinsed with ___ to remove residual sodium											
4. Stored in sample vial back filled with argon											
* Electro-etched in methanol/sulfuric acid bath, Platinum Cathode, V~8V and i~2A											
**All chemical containers and storage vials were cleaned w/ ethanol prior to use.											
*** V wire Test 1 was matched with Mo Wire Test 1, V Test 2 with Mo Test 2, V Test 3 with Mo Test 3											

Table 28. Data sheet for Mo wire test holders.

Molybdenum Wire Sample Preparation Data Sheet							
Name	L_i (mm)	L_f (mm)	W_i (g)	W_f (g)	D_i (mm)	D_f (mm)	Notes
Test 1	151	151	0.6563	0.6235	0.73	0.67-0.72	Ultrasonically cleaned in Acetone for 5 min
							Electro-etched 3.5 min***
							Ultrasonically cleaned in water for 5 min
							Ultrasonically cleaned in methanol for 5 min
							Vacuumed out at 10^{-8} Torr for over 1 week
							Stored in vial backfilled w/ Argon
Test 2	153	153	0.6844	0.6398	0.73-0.74	0.72	Ultrasonically cleaned in Acetone for 5 min
							Electro-etched 3.5 min***
							Ultrasonically cleaned in water for 5 min
							Ultrasonically cleaned in methanol for 5 min
							Vacuumed out at 10^{-8} Torr for over 1 week
							Stored in vial backfilled w/ Argon
Test 3	153	153	0.6923	0.6132	0.74	0.72	Ultrasonically cleaned in Acetone for 5 min
							Electro-etched 3.5 min***
							Ultrasonically cleaned in water for 5 min
							Ultrasonically cleaned in methanol for 5 min
							Vacuumed out at 10^{-8} Torr for over 1 week
							Stored in vial backfilled w/ Argon
Control	146	146	0.6742	0.643	0.75	0.71-0.72	Ultrasonically cleaned in Acetone for 5 min
							Electro-etched 3.5 min***
							Ultrasonically cleaned in water for 5 min
							Ultrasonically cleaned in methanol for 5 min
							Vacuumed out at 10^{-8} Torr for over 1 week
							Stored in vial backfilled w/ Argon
*** Electro-etch process utilizes a methanol/sulfuric acid bath, Platinum Cathode, and V~8V and i~2A							
*All chemical containers and storage vials were cleaned w/ ethanol prior to use.							
Test 1 was etched previously as as test from 0.74 to 0.73 mm diameter							
Test 2 was half etched previously to illustrate the results							
Test 3 was etched from an as received sample							
Contol was etched from an as received sample							

REFERENCES

1. "Standard Practice for Liquid Sodium Corrosion Testing of Metals and Alloys," *ASTM G68–80*, ASTM International, West Conshohocken, PA, 1980.

2. Martin, J.J.; Reid, R.S.; and Bragg-Sitton, S.M.: "Design of Refractory Metal Life Test Heat Pipe and Calorimeter," *NASA/TP—2010–216435*, Marshall Space Flight Center, AL, August 2010.

3. Martin, J.J.; and Reid, R.S.: "Refractory Metal Heat Pipe Life Test—Test Plan and Standard Operating Procedures," *NASA/TP—2010–216452*, Marshall Space Flight Center, AL, December 2010.

4. Martin, J.J.; Bragg-Sitton, S.M.; Reid, R.S.; et al.: "Design of Refractory Metal Heat Pipe Life Test Environmental Chambers, Cooling System, and Radio Frequency Heating System," *NASA/TP—2011–216456*, Marshall Space Flight Center, AL, February 2011.

5. Verma, M.P.: "Steam Tables for Pure Water as an ActiveX Component in Visual Basic 6.0," *Computers & Geosciences*, Vol. 29, pp. 1155–1163, 2003.

6. Incoropera, F.P.; and De Witt, D.P.: *Fundamentals of Heat and Mass Transfer*, 2d Edition, John Wiley & Sons, 1985.

7. Wadsworth, J.; Nieh, T.G.; and Stephens, J.J.: "Dilute Mo-Re Alloys—A Critical Evaluation of Their Comparative Mechanical Properties," *Scripta Metallurgica*, Vol. 20, No. 5, Pergamon Press Ltd, pp. 637–642, 1986.

8. Ammon, R.L.; and Buckman, Jr., R.W.: "Observations on the As-Welded (GTAW) Bend Ductility of Mo-13% Rhenium Alloy," *Space Nuclear Power Systems 1986*, M.S. El-Genk and M.D. Hoover (eds.), Orbit Book Company, Inc., Malabar, FL, pp. 283–289, 1987.

9. Morito, F.: "Structures and Properties of Molybdenum-Rhenium Alloys," *Rhenium and Rhenium Alloys*, The Minerals, Metals, & Materials Society, B.D. Bryskin (ed.), pp. 559–568, 1997.

10. Kramer, D.P.; Ruhkamp, J.D.; McNeil, D.C.; et al.: "Investigation of Mo-44.5%Re as Cell Wall Material in an AMTEC Based Space Power System," *Space Technology and Applications International Forum* (*STAIF–2000*), M.S. El-Genk (ed.), American Institute of Physics, New York, NY, AIP Conference Proceedings No. 504, Vol. 2, pp. 1402–1407, 2000.

11. Moore, J.P.; King, J.F.; DiStefano, J.R.; and Ohriner, E.K.: "Production and Properties of Mo-41%Re for AMTEC Cell Construction," *Space Technology and Applications International Forum* (*STAIF–2002*), M.S. El-Genk (ed.), American Institute of Physics, New York, NY, pp. 963–971, 2002.

12. Hooper, A.J.; and Trevillion E.A.: "Oxygen Analysis of Sodium by Equilibration with Vanadium: An Assessment," *Journal of Nuclear Materials*, Vol. 48, pp. 216–222, 1973.

13. Keough, R.F.: "Evaluation of the Vanadium Wire Equilibration Method for Determining Oxygen in Sodium," *Journal of Nuclear Materials*, Vol. 75, pp. 294–296, 1978.

14. Smith, D.L.; and Lee, R.H.: "Characterization of the Vanadium-Wire Equilibration Method for Measurement of Oxygen Activity in Liquid Sodium," *ANL–7891*, Argonne National Lab, IL, 16 pp.,1972.

15. "Standard Test Methods for Chemical and Instrumental Analysis of Nuclear-Grade Sodium and Cover Gas," *ASTM C 997–83* (Reapproved 1993), ASTM International, West Conshohocken, PA, 1993.

REPORT DOCUMENTATION PAGE

Form Approved
OMB No. 0704-0188

PLEASE DO NOT RETURN YOUR FORM TO THE ABOVE ADDRESS.

1. REPORT DATE *(DD-MM-YYYY)*	2. REPORT TYPE	3. DATES COVERED *(From - To)*
01–01–2013	Technical Publication	

4. TITLE AND SUBTITLE

Closeout Report for the Refractory Metal Accelerated Heat Pipe Life Test Activity

5a. CONTRACT NUMBER

5b. GRANT NUMBER

5c. PROGRAM ELEMENT NUMBER

6. AUTHOR(S)

J. Martin, R. Reid, E. Stewart, R. Hickman, and O. Mireles

5d. PROJECT NUMBER

5e. TASK NUMBER

5f. WORK UNIT NUMBER

7. PERFORMING ORGANIZATION NAME(S) AND ADDRESS(ES)

George C. Marshall Space Flight Center
Huntsville, AL 35812

8. PERFORMING ORGANIZATION REPORT NUMBER

M–1353

9. SPONSORING/MONITORING AGENCY NAME(S) AND ADDRESS(ES)

National Aeronautics and Space Administration
Washington, DC 20546–0001

10. SPONSORING/MONITOR'S ACRONYM(S)

NASA

11. SPONSORING/MONITORING REPORT NUMBER

NASA/TP—2013–217477

12. DISTRIBUTION/AVAILABILITY STATEMENT

Unclassified-Unlimited
Subject Category 20
Availability: NASA CASI (443–757–5802)

13. SUPPLEMENTARY NOTES

Prepared by the Propulsion Research and Technology Branch, Engineering Directorate

14. ABSTRACT With the selection of a gas-cooled reactor, this heat pipe accelerated life test activity was closed out and its resources redirected. The scope of this project was to establish the long-term aging effects on Mo-44.5%Re sodium heat pipes when subjected to space reactor temperature and mass fluences. To date, investigators have demonstrated heat pipe life tests of alkali metal systems up to ≈50,000 hours. Unfortunately, resources have not been available to examine the effect of temperature, mass fluence, or impurity level on corrosion or to conduct posttest forensic examination of heat pipes. The key objective of this effort was to establish a cost/time effective method to systematically test alkali metal heat pipes with both practical and theoretical benefits. During execution of the project, a heat pipe design was established, a majority of the laboratory test equipment systems specified, and operating and test procedures developed. Procurements for the heat pipe units and all major test components were underway at the time the stop work order was issued. An extremely important outcome was the successful fabrication of an annular wick from Mo-5%Re screen (the single, most difficult component to manufacture) using a hot isostatic pressing technique. This Technical Publication (TP) includes specifics regarding the heat pipe calorimeter water-cooling system, vendor design for the radio frequency heating system, possible alternative calorimeter designs, and progress on the vanadium equilibration technique. The methods provided in this TP and preceding project documentation would serve as a good starting point to rapidly implement an accelerated life test. Relevant test data can become available within months, not years, and destructive examination of the first life test heat pipe might begin within 6 months of test initiation. Final conclusions could be drawn in less than a quarter of the mission duration for a long-lived, fission-powered, deep space probe.

15. SUBJECT TERMS

alkali metal, sodium, heat pipe, refractory metal, molybdenum, rhenium, radio frequency heating, fission power system, nuclear, life testing

16. SECURITY CLASSIFICATION OF:			17. LIMITATION OF ABSTRACT	18. NUMBER OF PAGES	19a. NAME OF RESPONSIBLE PERSON
a. REPORT	b. ABSTRACT	c. THIS PAGE			STI Help Desk at email: help@sti.nasa.gov
U	U	U	UU	154	19b. TELEPHONE NUMBER *(Include area code)* STI Help Desk at: 443-757-5802

National Aeronautics and
Space Administration
IS20
George C. Marshall Space Flight Center
Huntsville, Alabama 35812